Contents

Preface 1
Intramolecular Hydrogen Bond (IMHB) in Medicinal Chemistry 4
Nitrogen-Walk in Medicinal Chemistry 6
Polarized C-H as Nonconventional Hygen Bond Donor 8
Halogen Bond in Medicinal Chemistry 11
Dihedral Angle in Medicinal Chemistry 14
Aliphatic Rings as Bioisosteres of Phenyl Ring 17
Noncovalent Sulfur Interactions in Medicinal Chemistry 24
Fluorine in Medicinal Chemistry 28
Scaffold Hopping in Medicinal Chemistry 36
Magic Methyl Group in Medicinal Chemistry 43
Acetylene Group in Medicinal Chemistry 51
Spirocyclic Rings in Medicinal Chemistry 55
Fused Cyclic Rings in Medicinal Chemistry 66
Bridged Cyclic Rings in Medicinal Chemistry 75
Cyclopropane in Medicinal Chemistry 85
Nitrile in Medicinal Chemistry 91
Sulfone in Medicinal Chemistry 99

About Author

Jin Li

Senior Director

10+ years' experience in organic chemistry
3+ years' experience in medicinal chemistry
10+ patents and papers published
Inventor of 2 clinical candidates
Email: li_jin@pharmablock.com

Contact Us

PharmaBlock Sciences (Nanjing), Inc.
Tel: +86-400 025 5188
Email: sales@pharmablock.com

PharmaBlock (USA), Inc.
Tel(PA): +1(877)878-5226 Tel(CA): +1(267) 649-7271
Email: salesusa@pharmablock.com

Find out more at www.pharmablock.com

Official Website | Product Search | Wechat | LinkedIn

Preface

A typical small-molecule drug molecule consists of 2-4 motifs, which is synthesized from corresponding building blocks bearing desired functional groups for linking reactions. Quick access of a high-quality, novel and diverse building block collection is critical for accelerating drug discovery processes. [1,2] Wildly employed functional groups include amine, carboxylic acid, boronic acid pinacol ester, halogen, aldehyde, etc. Besides, diverse substitutions are also important components of building blocks, which consequently make synthetic chemistry of building blocks much more challenging (**Figure A**).

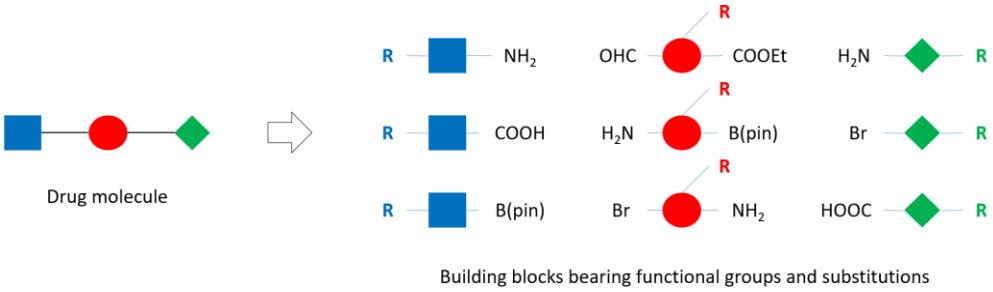

Figure A. A typical drug molecule and corresponding building blocks.

Functional groups are mainly used to link motifs and are engaged in critical interactions between molecule and protein. Substitutions are also engaged in critical interactions between molecule and protein, and more importantly they modify properties of the whole molecule, because of which chemists spend much cost to develop robust synthetic routes for incorporation of substitutions. For instance, Tofacinitib, a pan-JAK inhibitor, was approved for the treatment of autoimmune and inflammatory diseases (**Figure B**). The chemical structure is featured with a chiral methyl group, which makes synthetic chemistry of SM much challenging. So, we would question: can the chiral methyl group be removed? In other words, what is the critical difference between Tofacitinib and Demethyl-Tofacitinib? [3] The answer is obviously No. Otherwise, Demethyl-Tofacinitib would be selected as clinical candidate preferentially, due to cheap and commercially available SM.

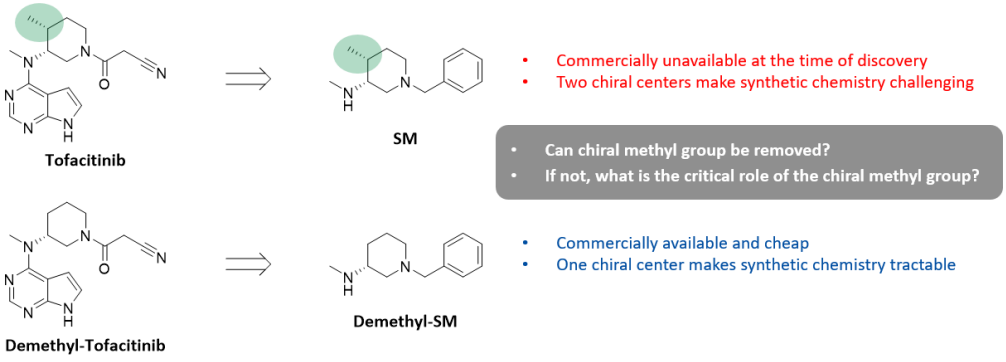

Figure B. Tofacitinib and building blocks involved in its synthesis.

This is exactly the beauty of building blocks, which attracts much interest of medicinal chemists in developing diverse and robust synthetic routes for building blocks they need to solve critical issues in drug discovery process, even though the synthetic chemistry is extremely challenging. In this book, we emphasized the critical role of building block in modification of physicochemical properties of molecule, such as solubility, permeability, metabolic stability, etc. and *in vitro* toxicity

of molecule, such as CYP inhibition, hERG inhibition etc. In several case studies cited in the book, a small change of molecule, such as a nitrogen addition or elimination, a methyl group, a fluorine, etc. can impact significantly.

All case studies in this book were cited from literature, including Journal of Medicinal Chemistry, ACS Medicinal Chemistry, Bioorganic Medicinal & Chemistry Letter, etc.

References

[1] Ying Wang; *et al.* What is in our kit? An analysis of building blocks used in medicinal chemistry parallel libraries. *J. Med. Chem.* **2021**, *64*, 17115-17122.
[2] Mark Seierstad; *et al.* Novel reagent space: identifying unorderable but readily synthesizable building blocks. *ACS Med. Chem. Lett.* **2021**, *12*, 1853-1860.
[3] Mark E. Flanagan; et al. Discovery of CP-690,550: a potent and selective Janus kinase (JAK) inhibitor for the treatment of autoimmune diseases and organ transplant rejuection. *J. Med. Chem.* **2010**, *53*, 8468-8484.

Jin Li
PharmaBlock Sciences (Nanjing)
March 2023

Intramolecular Hydrogen Bond (IMHB) in Medicinal Chemistry

The formation of intramolecular hydrogen bonds has a very pronounced effect on molecular structure and properties. [1] Medicinal chemists widely employ IMHB strategy to modify molecules with respect to locking conformation, increasing permeability, aqueous solubility, scaffold hopping, etc. In the circumstances, building blocks bearing HBD or HBA to form IMHB are of great value in drug discovery.

As shown in **Figure 1**, scaffolds 1,5-naphthyridine in compound **3** and pyrazolo[1,5-a]pyrimidine in compound **4**, which have nitrogen atoms highlighted in red color forming IMHB with adjacent hydrogen atoms highlighted in blue color, decreased efflux ratio significantly comparing with compound **1** and compound **2**. [2] Quick access of dichloro building blocks listed in the right of **Figure 1** as starting material for paralleled medicinal chemistry, enabled the structure-property relationship (SPR) study efficiently.

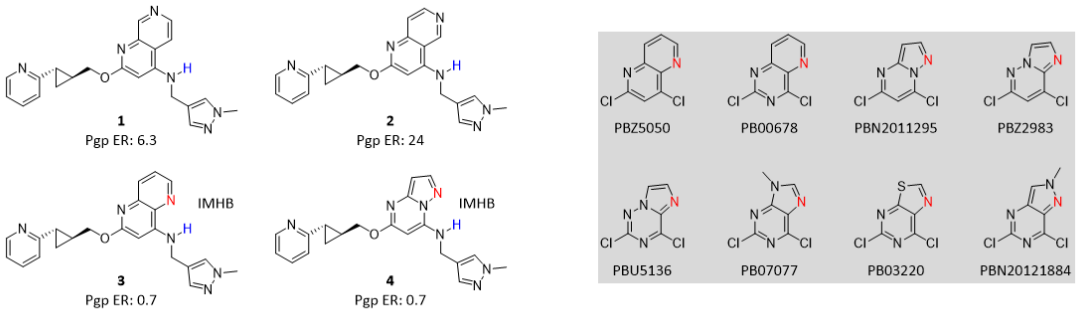

Figure 1. 1,5-Naphthyridine in compound **3** and pyrazolo[1,5-a]pyrimidine in compound **4** decreased efflux ratio.

A fluorine atom ortho- to the NH of an anilide can influence conformation. Biological evaluation of isomers **5** and **6** demonstrated a 10-fold difference in CGPR affinity, with F-HN interaction favoring desired binding conformation (**Figure 2**). [3]

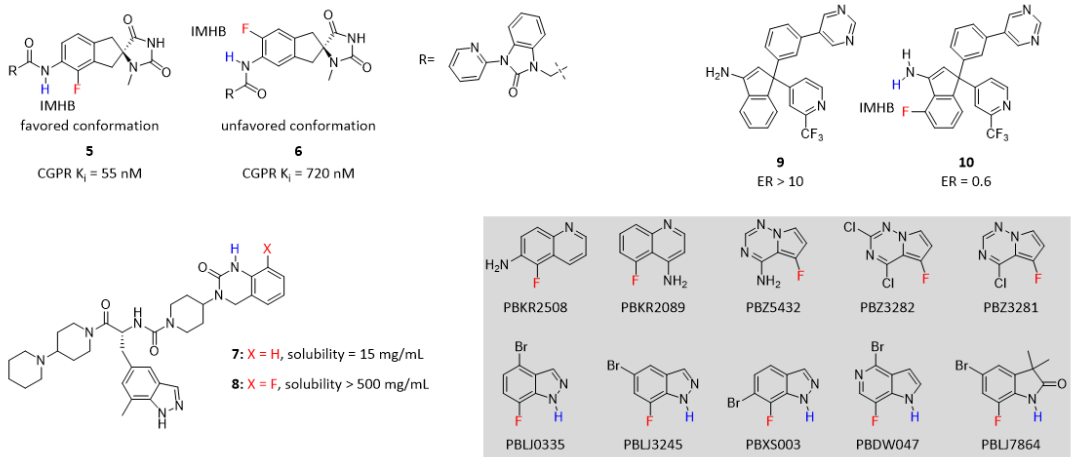

Figure 2. IMHB between F and N-H can influence many properties of molecule.

Replacing a hydrogen atom ortho- to an anilide N-H in compound **7** by a fluorine atom in compound **8** increased water solubility by 30-fold, probably due to “mask effect” of F on N-H. A positive effect on permeability was observed when comparing compound **9** and **10**, attributed to a weak interaction between F and one of N-H that reduces the number of HBD available to the

environment. Building blocks with F able to form IMHB with adjacent N-H as exemplified in **Figure 2**, are extremely useful and have been widely utilized in medicinal chemistry to improve molecular properties. [3]

Compound **11** was discovered as a potent GSK-3β inhibitor. However, cleavage of the cyclopropyl carboxamide group was observed in mouse serum. In co-crystal structure of **11** complexed with GSK-3β, a water-bridging hydrogen bond between the carbonyl of amide and the upper amide NH was observed, which may help to predispose the molecule to energetically favor the bioactive conformation (**Figure 3**). [4] With this in mind, the imidazo[1,2-b]pyridazine ring system appeared to be an attractive heterocyclic scaffold, with an interaction between amide NH (blue) and imidazole nitrogen atom (red) locking molecule in the desired bioactive conformation. When carboxylic acid building blocks, which have adjacent HBA to –COOH group, are converted to amide, IMHB are formed.

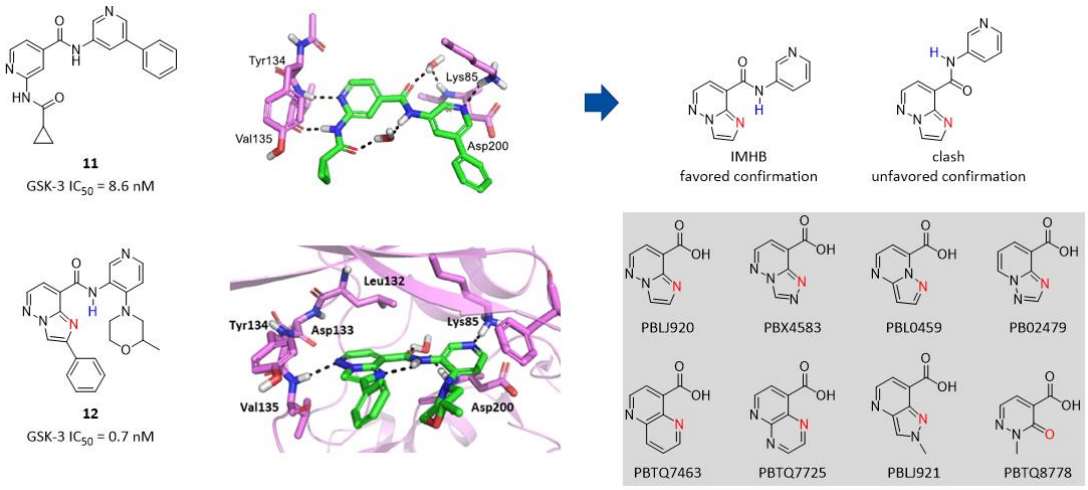

Figure 3. An interaction between amide N-H and imidazole N locks the molecule in the bioactive conformation.

References

[1] Bernd Kuhn; *et al.* Intramolecular hydrogen bond in medicinal chemistry. *J. Med. Chem.* **2010**, *53*, 2601-2611.
[2] Mark E. Layton; *et al.* Discovery of MK-8189, a highly potent and selective PDE10A inhibitor for the treatment of schizophrenia. *J. Med. Chem.* **2023**, *66*, 1157-1171.
[3] Nicholas A. Meanwell; Fluorine and fluorinated motifs in the design and application of bioisosteres of drug design. *J. Med. Chem.* **2018**, *61*, 5822-5880.
[4] Richard A. Hartz; *et al.* Design, structure-activity relationships, and in vivo evaluation of potent and brain-penetrant imidazo[1,2-b]pyridazines as glycogen synthase kinase-3beta inhibitors. *J. Med. Chem.* **2023**, doi:10.1021/acs.jmedchem.3c00133.

Nitrogen-Walk in Medicinal Chemistry

The replacement of a CH group with a N atom in aromatic and heteroaromatic ring systems can have many important effects on molecular and physicochemical properties and intra- and intermolecular interactions that can translate to improved pharmacological profiles. [1] Therefore, nitrogen-walk approach has been reported as a successful strategy to optimize biological activity, metabolic stability, and overall physicochemical properties. [2]

Nitrogen-walk on azaindole rings in compound **13**, **14**, **15** and **16** significantly impacted both potency and water solubility. Nitrogen at 7-postion of compound **16** afforded balance between potency and water solubility (Figure 4). [2] In the right of **Figure 4** are systematically designed azaindole building blocks bearing various functional groups for coupling reactions, supporting quick SAR and SPR explorations in medicinal chemistry campaign.

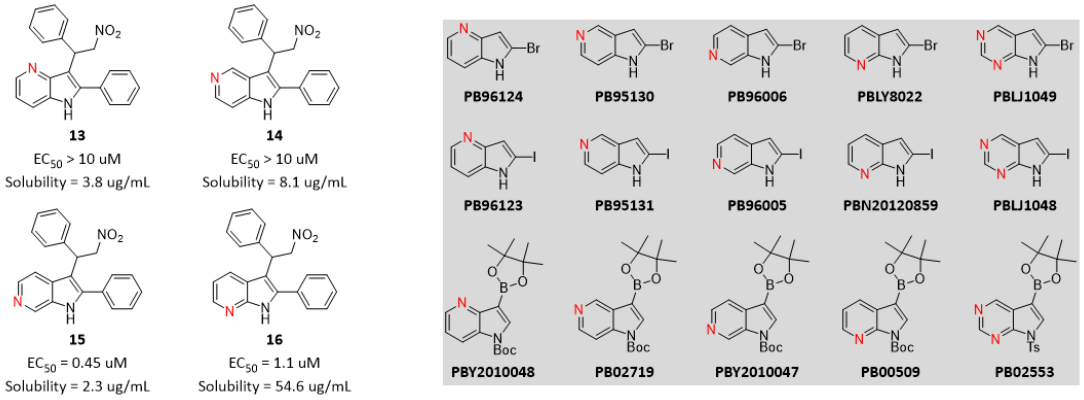

Figure 4. Nitrogen-walk on azaindole rings significantly impacted potency and solubility.

Nitrogen-walk from pyrazolo[4,3-b]pyridine **17** to pyrazolo[3,4-c]pyridine **18** yielded no significant increase in ALK2 inhibition. It was interesting additional nitrogen atom provided compound **19** with > 10-fold improved potency (**Figure 5**). [3] Dihalo- building blocks are the key starting materials for quick synthesis and evaluation of designed molecules.

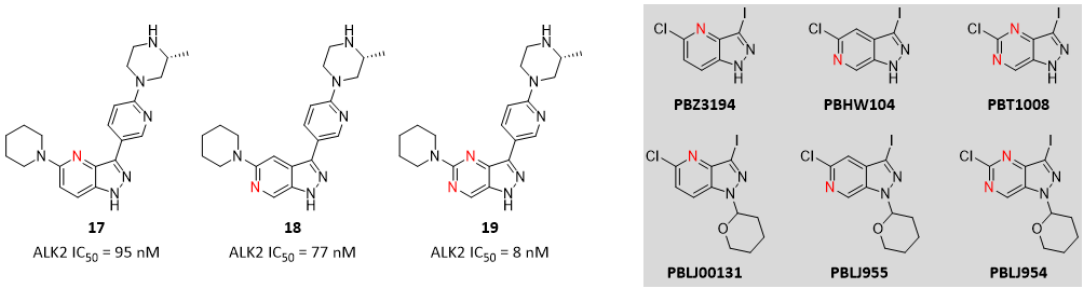

Figure 5. Nitrogen-walk on azaindazole rings impacted ALK2 inhibition.

Nitrogen-walk on pyridine rings in compound **20**, **21**, **22** and **23** gave extremely interesting results. Two nitrogen atoms in compound **20** and **23** are both ortho- to pyrazole ring, but **23** was proved inactive while **20** demonstrated high potency. Compound **21** with a meta- nitrogen and compound **22** with a para- nitrogen increased solubility dramatically while keeping high potency comparing to compound **20**. It was suggested that the polarity of ortho- nitrogen atom in compound **20** is somehow masked, possibly by an interaction with the lactam ring protons (**Figure 6**). [4]

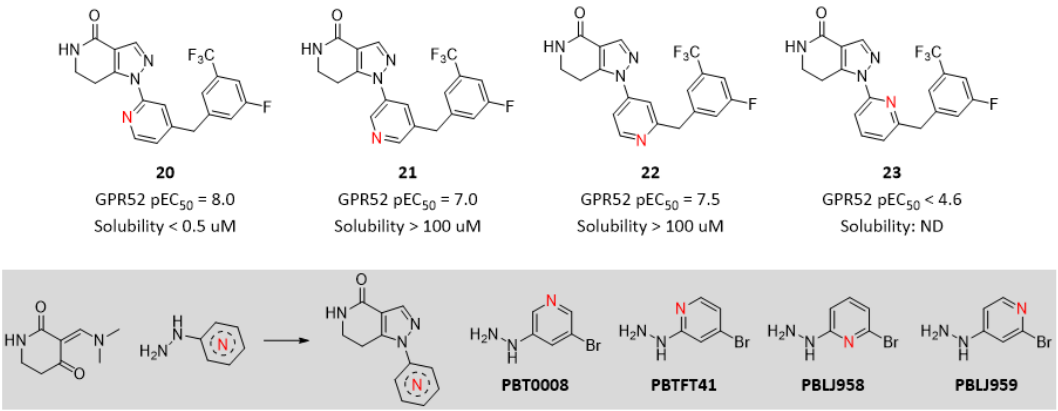

Figure 6. Nitrogen-walk on pyridine ring dramatically impacted potency and solubility.

References

[1] Lewis D. Pennington; *et al.* The necessary nitrogen atom: a versatile high-impact design element for multiparameter optimization. *J. Med. Chem.* **2017**, *60*, 3552-3579.

[2] Sumanta Garai; *et al.* Application of fluorine- and nitrogen-walk approaches: defining the structural and functional diversity of 2-phenylindole class of Cannabinoid 1 receptor positive allosteric modulators. *J. Med. Chem.* **2020**, *63*, 542-568.

[3] Minh H. Nguyen; et al. Discovery of novel pyrazolopyrimidines as potent, selective, and orally bioavailable inhibitors of ALK2. *ACS Med. Chem. Lett.* **2022**, *13*, 1159-1164.

[4] Simon Poulter; et al. The identification of GPR52 agonist HTL0041178, a potential therapy for schizophrenia and related psychiatric disorder. *J. Med. Chem.* **2023**, doi:10.1021/acsmedchemlett.3c00052.

Polarized C-H as Nonconventional Hydrogen Bond Donor

Canonical hydrogen bond donors, N-H and O-H, play key roles in interactions between molecules and proteins and exist in substantial drug and clinical candidate molecules, especially in kinase inhibitors which have a N-H forming a hydrogen bond with hinge region. Issues associated with canonical hydrogen bond donors are their potentially negative influences in aqueous solubility, permeability, glucosidation metabolism, etc. In order to circumvent this, C-H in heteroaromatic rings containing nitrogen is often used as nonconventional hydrogen bond donors due to the increased acidity of the involved C-H hydrogen. For example, C-H in pyrazine was found to form nonconventional hydrogen bonds with protein backbone and –COOH residues (**Figure 7**). [1]

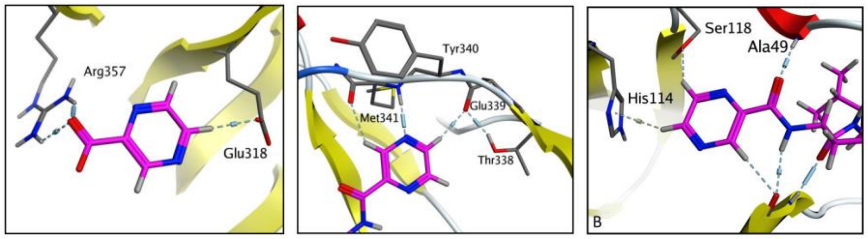

Figure 7. C-H in pyrazine ring as nonconventional hydrogen bond donors (PDB code: 4NNI, 3U4W respectively)

In order to discover BBB-penetrant LRRK2 inhibitors, replacement of indazole N1-H in compound **24** with imidazo[1,5-a]pyridine core C-H in compound **25** and "reverse indazole" C3-H in compound **26** was explored. [2] Despite the anticipated loss in potency, significantly reduced P-gp efflux was observed for compound **26**, positively differentiating this core. Further optimization of compound **26** afforded highly potent, selective and BBB-penetrant LRRK2 inhibitors. A nonconventional hydrogen bond between C3-H in indazole with backbone C=O of LRRK2 Glu85 was demonstrated in an X-ray structure of one of LRRK2 inhibitors bound to LRRK2 (**Figure 8**).

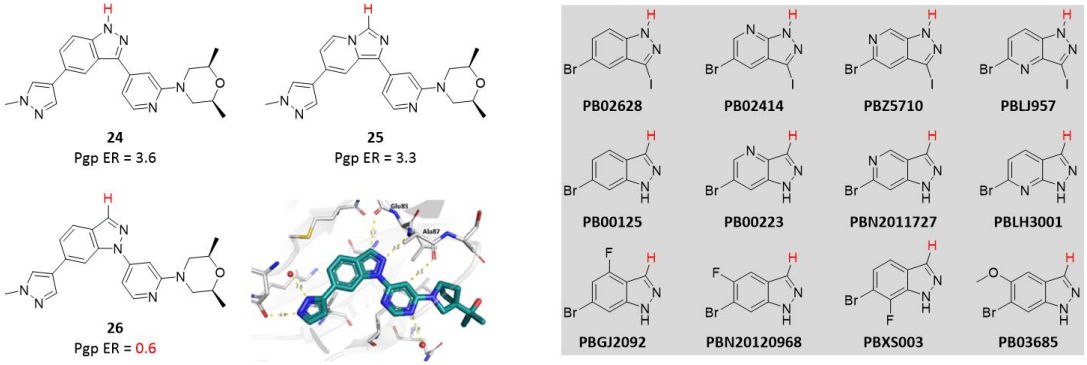

Figure 8. C3-H in "reverse indazole" was used as a nonconventional hydrogen bond donor. (PDB code: 8E80)

Polarization of the aryl C-H to increase the hydrogen bonding potential was believed to be necessary to bring about sufficient TYK2 activity and two point binding. With this strategy in mind, several [5,6]-fused heteroaromatic systems, including imidazopyrdine scaffold in compound **27**, [1,2,4]triazole[1,5]pyridine scaffold in compound **28**, [1,2,4]triazole[4,3]pyridine scaffold in compound **29** and pyrazole[1,5]pyrazine scaffold in compound **30**, were designed and evaluated (**Figure 9**). [3] Among of the above scaffolds, pyrazole[1,5]pyrazine scaffold was of particular interest due to the calculated increased polarization of the C-H for hydrogen bond donor properties. Consistent with calculation result, pyrazole[1,5]pyrazine analog **30** was found to be a potent TYK2 enzyme inhibitor at 10 nM. An X-ray crystal structure of compound **30** bound to TYK2 confirmed the

expected binding mode with polarized C7-H engaged in an interaction with the backbone C=O of TYK2 Val981. As proved by this case study, pyrazole[1,5]pyrazine scaffold could be potentially used as kinase hinge binding motif for discovery of kinase inhibitors, especially for that requiring BBB-penetration.

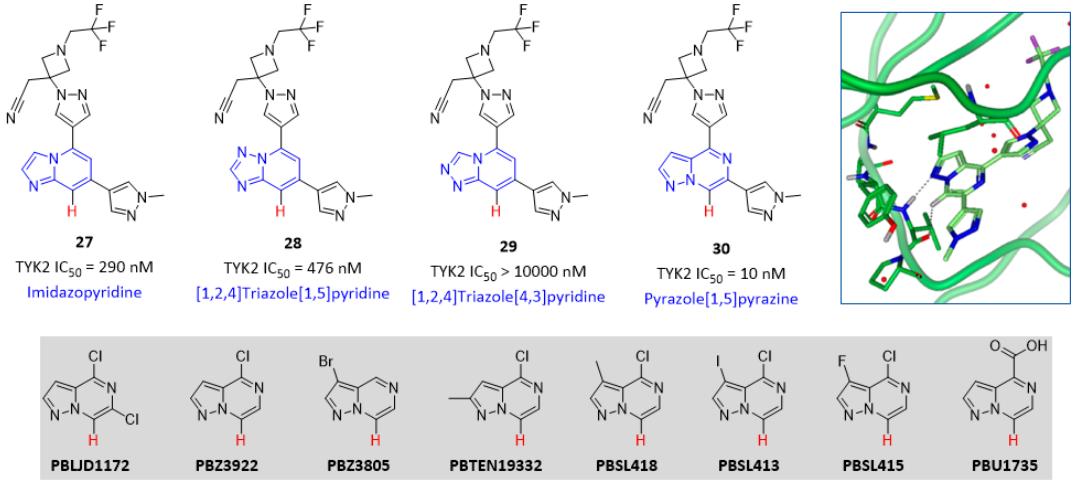

Figure 9. C7-H of pyrazole[1,5]pyrazine was used as a nonconventional hydrogen bond donor. (PDB code: 6X8F)

To better understand the origin of the increased potency and subtype selectivity of CK1δ inhibitor **31**, an X-ray structure of compound **31** bound to CK1δ was obtained. It was found that polarized C-H of lactam motif formed a nonconventional hydrogen bond with the backbone C=O of Leu85. Meanwhile, polarized C-H of pyridine formed an additional nonconventional hydrogen bond with the backbone C=O of Glu83 (**Figure 10**). [4] Scaffold 6,7-dihydropyrrolo[3,4-b]pyridine-5-one could be utilized in the discovery of inhibitors of more kinases, since it potentially affords three hydrogen bonds with kinase hinge region.

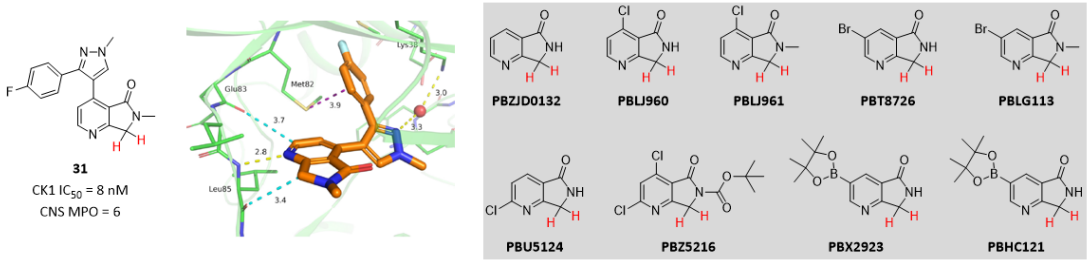

Figure 10. 6,7-Dihydropyrrolo[3,4-b]pyridine-5-one scaffold formed two nonconventional hydrogen bonds with CK1δ hinge region. (PDB code: 5W4W)

References

[1] Martin Juhas; *et al.* Molecular interactions of pyrazine-based compounds to proteins. *J. Med. Chem.* **2020**, *63*, 8901-8916.

[2] David A. Candito; *et al.* Discovery and optimization of potent, selective, and brain-penetrant 1-heteroaryl-1H-indazole LRRK2 kinase inhibitors for the treatment of Parkinson's disease. *J. Med. Chem.* **2022**, *65*, 16801-16817.

[3] Brian S. Gerstenberger; *et al.* Discovery of tyrosine kinase 2 (TYK2) inhibitor (PF-06826647) for the treatment of autoimmune diseases. *J. Med. Chem.* **2020**, *63*, 13561-13577.

[4] Travis T. Wager; *et al.* Identification and profiling of a selective and brain penetrant radioligand for in vivo target occupancy measurement of Casein kinase (CK1) inhibitors. *ACS Chem. Neurosci.* **2017**, *8*, 1995-2004.

Halogen Bond in Medicinal Chemistry

Halogen bond is driven by the σ-hole, a positively charged region on the hind side of chlorine (Cl), bromine (Br) and iodine (I) along the axis of R-Cl, R-Br and R-I bond that is caused by an anisotropy of electron density on the halogen. [1-2] Because of its presence in every amino acid, the backbone C=O is the most prominent acceptor involved in halogen bonds as found from an analysis of PDB. Additionally, halogen bonds can be formed involving protein residues, such as –OH in serine, threonine and tyrosine, -COOH in aspartate and glutamate, -SH in cysteine, -SMe in methionine, N in histidine, and pi-surface of phenylalanine, tyrosine and tryptophan (**Figure 11**). Therefore, this multitude of different interactions possibilities in ligand-protein interactions makes halogen bond a very useful tool to enhance affinity and selectivity.

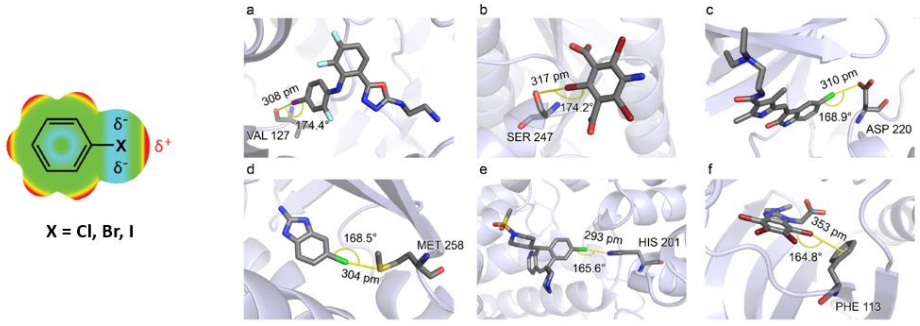

Figure 11. σ-Hole of Cl, Br and I; Different types of halogen bonds in ligand-protein interactions.

It was interesting to observe that a single chlorine in compound **33** increased potency by > 5-fold comparing with analog compound **32**. The same trend was also observed when comparing compound **34** and compound **35** with 20-fold difference in potency caused by a single chlorine. [3] To better understand this observation and further optimize, an X-ray crystal structure of compound **33** bound to HPK1 was obtained. The chlorine atom at the C2 position on compound **33** forms a halogen bond with the gatekeeper Met91, well explaining the reason for potency difference caused by chlorine atoms in compound **33** and compound **35**.

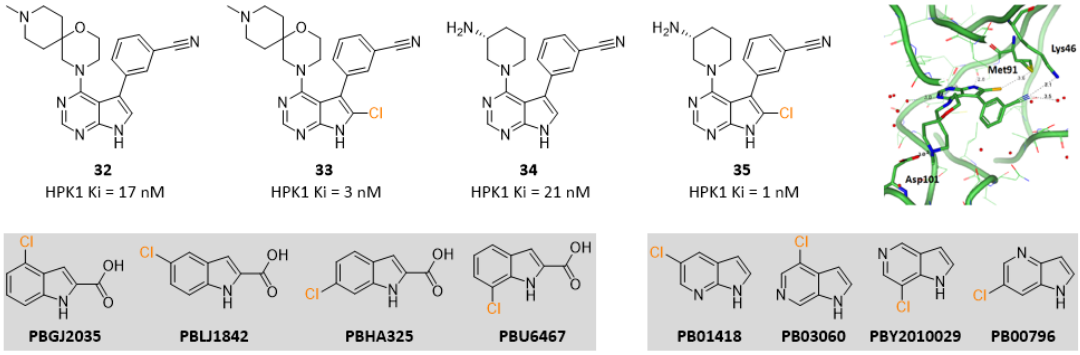

Figure 12. Halogen bond between chlorine and sulfur of Met91 increased potency. (PDB code: 8FH4)

Fragment-based drug discovery (FBDD) has become a standard asset in the search for structurally novel small-molecule therapeutics. Incorporation of halogens into fragments could change their interaction profile significantly based on halogen bond, leading to previously overlooked binding modes to known targets, which could have intrinsic advantages in selectivity. [4] Screening DYRK1a against a halogen-enriched fragment library using an STD-NMR protocol generated fragment hit **36**,

with Kd = 533 uM and a high LE = 0.45. The crystal structure of DYRK1a in complex with fragment **36** was solved. The binding mode in the ATP pocket is dominated by a halogen bond between Br and the backbone C=O of E239 (**Figure 13**). Structure-activity relationship (SAR) insights gained from analogues demonstrated that: 1) removing a nitrogen from triazole increased affinity by > 10-fold (**36** *vs* **37**); 2) the pyridine nitrogen seems to have no significant effect (**37** *vs* **38**). A new fragment-growth vector was established, and incorporation of an acetamide increased the affinity to single-digit 4 uM.

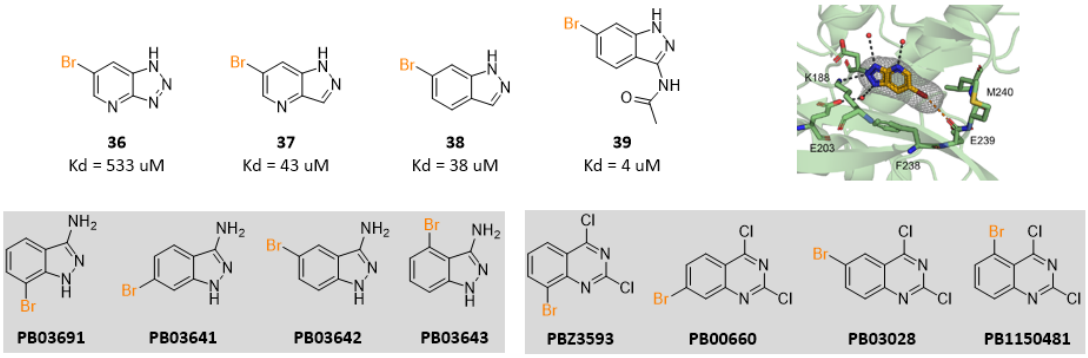

Figure 13. Br of compound **36** forms a halogen bond with the backbone C=O of E239. (PDB code: 7ZH8)

The general trend for the strength order of halogen bond is Cl < Br < I. As exemplified in **Figure 14**, halogen bond between chlorine in compound **41** and the backbone C=O of Phe217 brought 25-fold increased affinity (**40** *vs* **41**). The affinity trend from compound **41** to **43** is consistent with the strength order of halogen bond, although the difference is within 4-fold. [5]

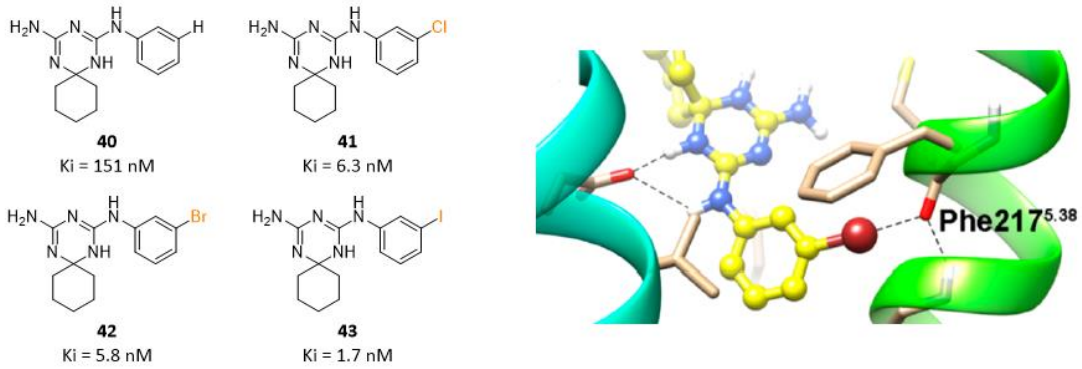

Figure 14. Br of compound 42 forms a halogen bond with the backbone C=O of Phe217.

With possibility of improving the bioactivity by halogen bond in mind, hydrogen atom in compound **44** was replaced by halogen atoms: Cl in compound **45**, Br in compound **46** and I in compound **47** (**Figure 15**). [6] The affinity trend from compound **45** to **47** is also consistent with the strength order of halogen bond. X-ray crystal structures of compound **45** and compound **46** bound to PDE5 were obtained. Both Cl in compound **45** and Br in compound **46** form halogen bonds with O of PDE5 residue Y612, which agrees with observation in affinity increasing.

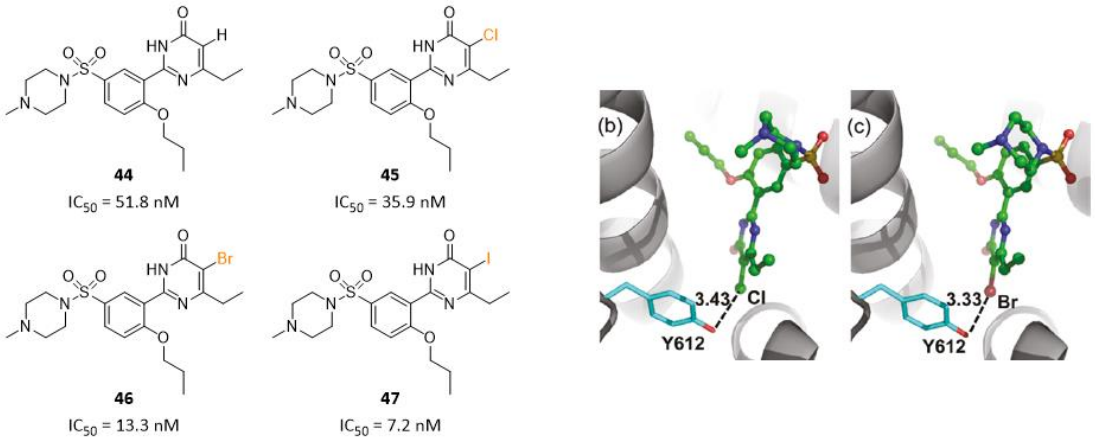

Figure 15. Halogen bonds between Cl or Br and O of PDE5 residue Y612.

References

[1] Rainer Wilcken; *et al.* Principles and applications of halogen bonding in medicinal chemistry and chemical biology. *J. Med. Chem.* **2013**, *56*, 1363-1388.
[2] Nicolas K. Shinada; *et al.* Halogens in protein-ligand binding mechanism: a structural perspectivel. *J. Med. Chem.* **2019**, *62*, 9341-9356.
[3] Rebecca A. Gallego; *et al.* Design and synthesis of functionally active 5-amino-6-aryl pyrrolopyrimidine inhibitors of hematopoietic progenitor kinase 1. *J. Med. Chem.* **2019**, *62*, doi:10.1021/acs.jmedchem.2c02038.
[4] Marcel Dammann; *et al.* Screening of a halogen-enriched fragment library leads to unconventional binding modes. *J. Med. Chem.* **2022**, *65*, 14539-14552.
[5] Yu Zhou; *et al.* Exploring halogen bonds in 5-hydroxytryptamine 2B receptor-ligand interactions. *ACS Med. Chem. Lett.* **2018**, *9*, 1019-1024.
[6] Zhijian Xu; *et al.* Utilization of halogen bond in lead optimization: a case study of rational design of potent phosphodiesterase type 5 (PDE5) inhibitors. *J. Med. Chem.* **2011**, *54*, 5607-5611.

Dihedral Angle in Medicinal Chemistry

Dihedral angle-based drug design has been a commonly used approach for improving both activity or selectivity of molecules and conformation or orientation of molecules. For instance, small-molecule crystal data from the Cambridge Structural Database (CSD) revealed a dependence of the dihedral angle between the C=O and the phenyl ring on the size and polarity of R1 substituents (**Figure 16**). [1]

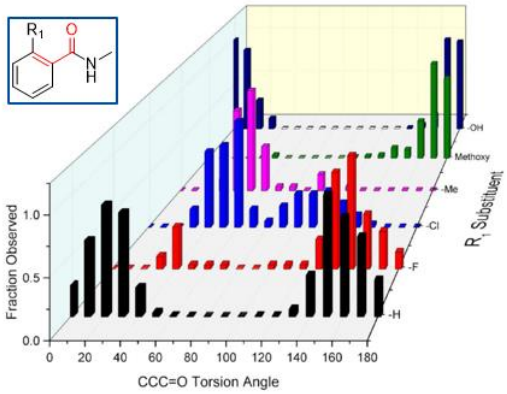

Figure 16. Distribution of relative fractions of C=C-C=O dihedral angle for various R1-substituted benzamides.

In the course of discovering a novel class of EZH2 inhibitors, there were two critical hypotheses: 1) the carbonyl oxygen makes an important hydrogen bond with the backbone NH of Tyr111 that is located approximately 50° above or below the plan of the phenyl ring; 2) the linker orients the dimethylpyridone and phenyl rings into an optimal binding geometry. [1,2] With this in mind, dihedral angle-based drug design strategy was used by introducing a Me or a Cl at the ortho-position of benzamide in compound **49** and **50** with activity increased by > 20-fold comparing to compound **48**. In conformation restricted six-membered lactam compounds **51**, **52** and **53**, the same trend was observed. An X-ray crystal structure of compound **54** bound to EZH2 revealed that carbonyl oxygen forms a hydrogen bond with the backbone NH of Tyr111 as expected (**Figure 17**).

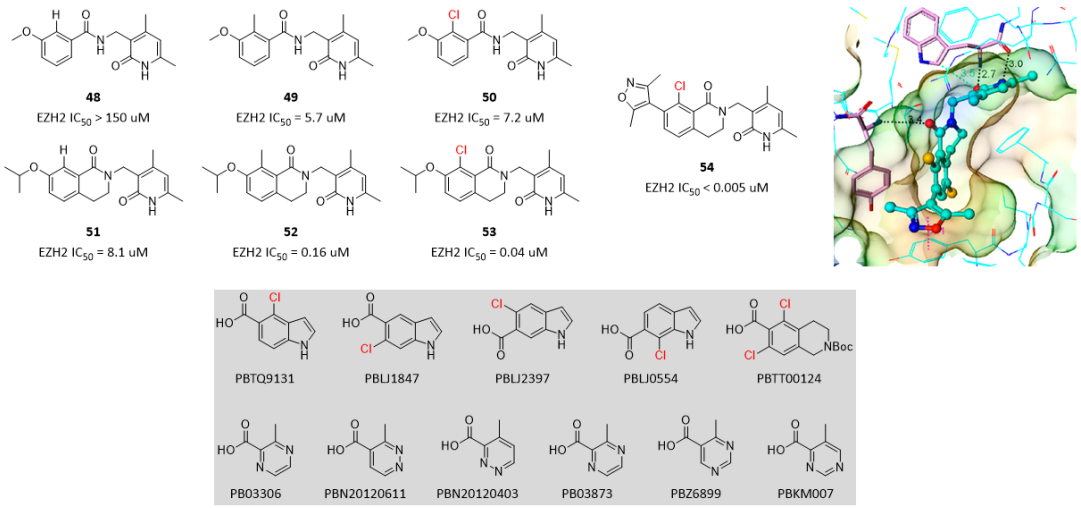

Figure 17. Impact of dihedral angle between amide and phenyl ring on EZH2 inhibition (PDB code: 6B3W).

Docking compound **55** into AKT protein revealed that a critical hydrogen bond interaction between Glu278 and the nitrogen on the piperidine ring was missing. It was assumed that hydrogen bond interaction might be formed through deflecting the piperidine by a certain angle. A fluorine atom

was incorporated at the ortho- position of amide in compound **56**, and docking revealed that a 43.2° dihedral angle was observed between the phenyl flat and amide flat, leading to the nitrogen on piperidine ring close to Glu278 and forming a stable hydrogen bond (**Figure 18**). [3] Consistent with docking result, compound **56** had 5-fold more potent AKT1 activity than compound **55**. It was also interesting that compound **56** had 16-fold less potent AKT2 activity than compound **55**, inhibition of which contributes to cutaneous toxicity.

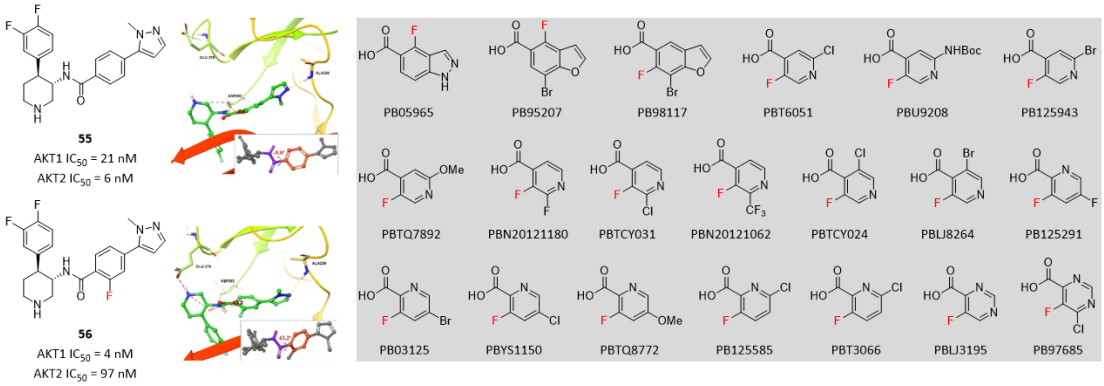

Figure 18. Impact of dihedral angle on AKT1 activity and selectivity against AKT2.

Besides impact on activity or selectivity, dihedral angle can also play influences on physicochemical properties of molecules significantly. [4] Molecular planarity and symmetry are known to influence crystal packing, and disruption of molecular planarity would be expected to decrease efficiency of crystal packing, consequently changing physicochemical properties such as solubility etc.

It was noteworthy that disruption of molecular planarity of compound **57** by incorporating two steric methyl groups in compound **58** had greatly improved solubility by 350-fold (**Figure 19**). [5] The similar strategy has been widely used to disrupt dihedral angle between two aromatic rings.

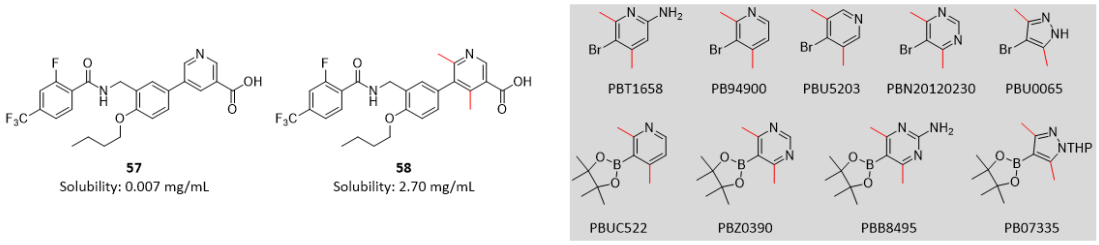

Figure 19. Two methyl groups disrupt molecular planarity and increase solubility significantly.

Besides biaryl structures as demonstrated in **Figure 19**, increase of dihedral angle by steric hinder was also useful for benzamide, anilide and phenylurea structures.

Transformation from compound **59** to compound **60** by adding chlorine caused an increase in solubility by at least 10-fold. The calculated LogP value of these two compounds are comparable which can't explain the solubility difference. This can be understood in terms of a conformational effect constraining the urea group to be orthogonal to the aromatic ring in compound **60**, whereas more planar conformations that may stack better in the solid state are permitted in the case of compound **59** (**Figure 20**). [6]

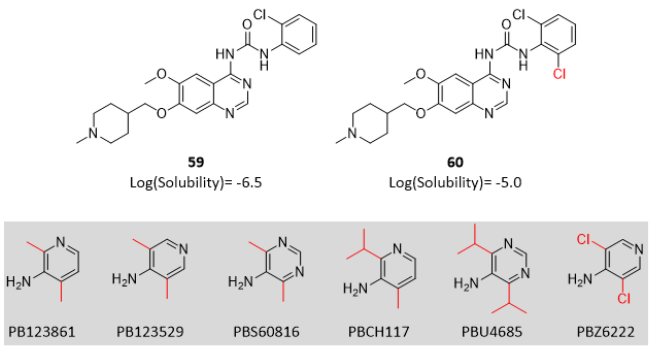

Figure 20. Improvement of solubility by ortho-substitution of a phenylurea.

In the course of discovering CDK inhibitors, it was found that introduction of a methyl group in compound **62** at the ortho-position of dimethylbenzamide compound **61** led to a 230-fold increase of aqueous solubility (**Figure 21**). [7]

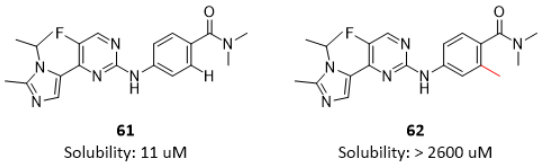

Figure 21. Improvement of aqueous solubility by ortho-substitution of benzamide.

References

[1] Pei-pei Kung; *et al.* Design and synthesis of pyridine-containing 3,4-dihydroisoquinoline-1(2H)-ones as a novel class of enhancer of zeste homolog 2 (EZH2) inhibitors. *J. Med. Chem.* **2016**, *59*, 8306-8325.
[2] Pei-pei Kung; *et al.* Optimization of orally bioavailable enhancer of zeste homolog 2 (EZH2) inhibitors using ligand and property-based design strategies: identification of development candidate (R)-5,8-dichloro-7-(methoxy(oxetan-3-yl)methyl)-2-((4-methoxy-6-methyl-2-oxo-1,2-dihydropyridin-3-yl)methyl)-3,4-dihydroisoquinolin-1(2H)-one (PF-06821497). *J. Med. Chem.* **2018**, *61*, 650-665.
[3] Jinxin Che; *et al.* Discovery of N-((3S,4S)-4-(3,4-difluorophenyl)piperidin-3-yl)-2-fluoro-4-(1-methyl-1H-pyrazol-5-yl)benzamide (Hu7691), a potent and selective Akt inhibitor that enables decrease of cutaneous toxicity. *J. Med. Chem.* **2021**, *64*, 12163-12180.
[4] Minoru Ishikawa; *et al.* Improvement in aqueous solubility in small molecule drug discovery programs by disruption of molecular planarity and symmetry. *J. Med. Chem.* **2011**, *54*, 1539-1554.
[5] Sauerberg P.; *et al.* Identification and synthesis of a novel selective partial PPARdelta agonist with full efficacy on lipid metabolism in vitro and in vivo. *J. Med. Chem.* **2007**, *50*, 1495-1503.
[6] Leach A. G.; *et al.* Matched molecular pairs as a guide in the optimization of pharmaceutical properties: a study of aqueous solubility, plasma protein binding and oral exposure. *J. Med. Chem.* **2006**, *49*, 6672-6682.
[7] Jones C. D.; *et al.* Imidazole pyrimidine amides as potent, orally bioavailable cyclin-dependent kinase inhibitors. *Bioorg. Med. Chem. Lett.* **2008**, *18*, 6486-6489.

Aliphatic Rings as Bioisosteres of Phenyl Ring

The high prevalence of benzene rings in marketed drugs reflects its fundamental importance as both a structural and pharmacophoric element in drug design. Meanwhile, its versatility qualifies it as the preeminent privileged scaffold. [1] However, there are several issues associated with phenyl ring, including low aqueous solubility, poor metabolic stability, membrane permeability, etc. To circumvent these drawbacks, significant effort has been dedicated to exploring the design of bioisosteric replacements for phenyl rings that would offer advantageous properties. [2] Among of them, sp^3-riched aliphatic rings, including monocyclic and bicyclic, have emerged as frequently used bioisosteres of the phenyl ring (**Figure 22**).

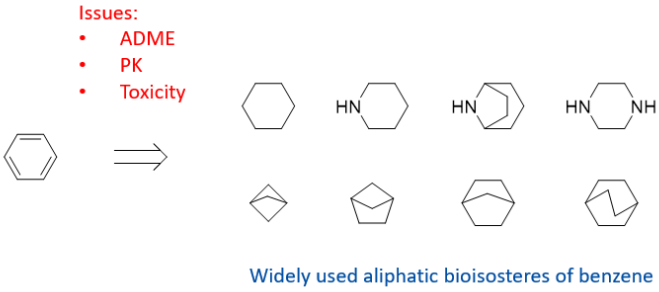

Figure 22. Sp^3-riched aliphatic rings as bioisosteres of the phenyl ring to circumvent critical issues.

Compound **63** (AMG-517) is Amgen's first-generation TRPV1 antagonist which was evaluated in clinical trials. However, it was found to have low aqueous solubility (< 1 ug/mL). The goal to identify a novel second-generation clinical candidate with increased aqueous solubility was achieved by replacing the phenyl ring with sp^3-riched aliphatic rings (**Figure 23**). [3] Cyclohexene in compound **64**, cyclohexane in compound **65** and piperidine in compound **66** were used as bioisosteres of the phenyl ring in compound **63**, and all of them increased aqueous solubility significantly. In studies of structure-solubility relationship, diverse cyclohexenyl boronic acid pinacol ester building blocks played crucial roles in quick synthesis of designed molecules.

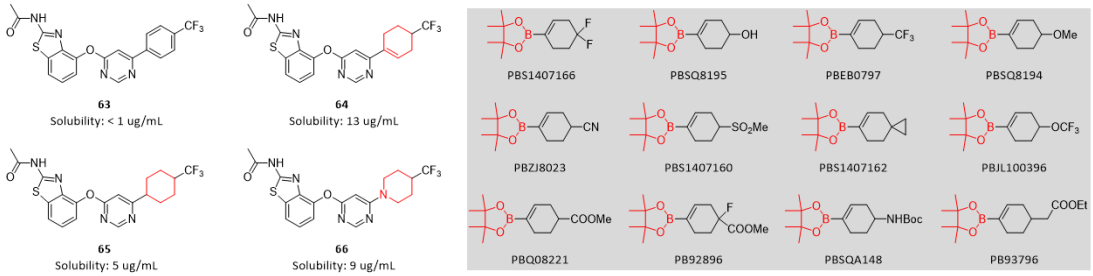

Figure 23. Cyclohexene, cyclohexane and piperidine increased aqueous solubility.

In the course of discovering a novel selective PDE9A inhibitor, compound **67** was identified as an early lead compound with excellent PDE9A inhibition and good selectivities against PDE family members (**Figure 24**). [4] However, in studies of PK profile of compound **67** in rats, high clearance and low bioavailability were observed, which was attributed to extensive phase 2 metabolism. Replacement of the 4-methylphenyl group in compound **67** with 4-dimethylpiperidine afforded compound **68**, which interestingly showed no phase 2 glucuronidation metabolism after incubation in rat hepatocytes. Although without phase 2 metabolism, oral bioavailability of compound **68** was slightly improved. It was found that the main clearance pathway of compound **68** was driven by

oxidative metabolism. It was hypothesized that cyclopropane can be metabolically more stable than the corresponding gem-dimethyl analogue. With this hypothesis in mind, compound **69** which has a spiro-piperidine motif was identified. It was extremely exciting that compound **69** (**BAY-7081**) improved bioavailability significantly. In the discovery campaign, diverse spiro-piperidine building blocks played crucial roles in quick synthesis of designed molecules.

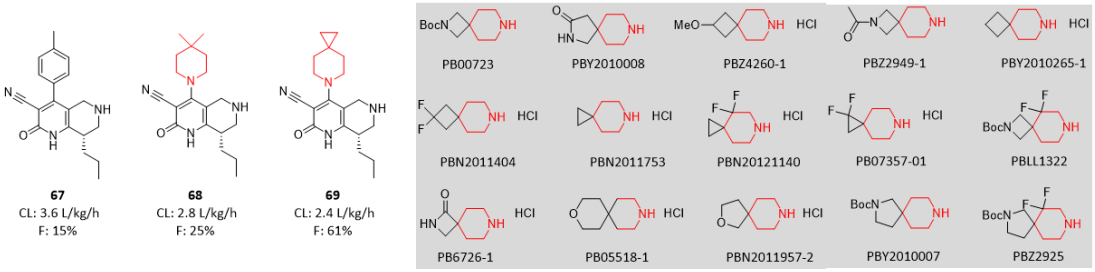

Figure 24. Piperidines as bioisosteres of the phenyl ring improved PK profiles.

Compound **70** was originally discovered as a novel potent SETD2 inhibitor (**Figure 25**). [5] The structure contains an aniline motif which impacts less-than-ideal pharmacokinetic properties and potential metabolism-derived toxicities. The team has experience before that saturating of the phenyl ring significantly improved the physicochemical properties of the series and avoided the potential AMES toxicity. With this in mind, replacement of the phenyl ring in compound **70** with cis-cyclohexane in compound **71** improved clearance and oral bioavailability significantly. There are two chiral centers on 1,3-disubstituted cyclohexane ring, and chirally pure bifunctional cyclohexane building blocks played crucial roles in quick SAR and SPR studies.

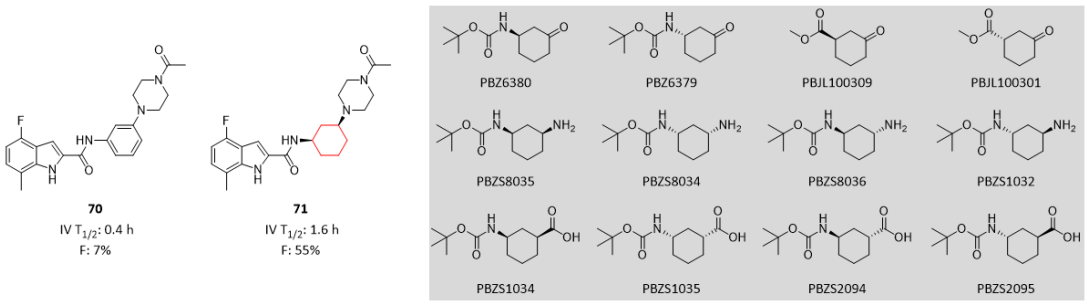

Figure 25. Cyclohexanes as bioisosteres of the phenyl ring improved PK profile.

Although bicylco[1.1.1]pentane (BCP) has a different stereoelectronic property compared to the 1,4-disubstituted phenyl ring, it shares comparable dihedral angle and similar distance and coplanar linear disposition of the substituents (**Figure 26**). [1] BCP system significantly increase aqueous solubility and noticeably decreases nonspecific binding. Consequently, the sp^3-riched BCP system serves as a nonclassical phenyl bioisostere to escape from flatland imposed by high aromatic ring count and modulate physicochemical properties during lead optimization. For instance, isosteric replacement of the 1,4-disubstituted phenyl ring with BCP has been shown to confer significant improved passive permeability and aqueous solubility. however, it should be noted that such bioisosteric replacement strategy will not be effective in lead compounds where a 1,4-disubstituted phenyl ring plays a pharmacophore role such as pi-pi stacking or pi-cation interactions with the aromatic or positively charged residue of the target protein. [6]

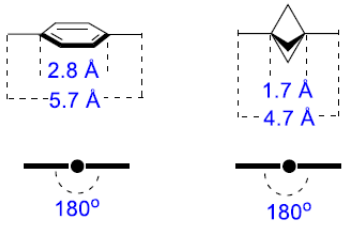

Figure 26. Geometrical parameters of phenyl ring and BCP ring

The significant advantage of the BCP moiety in compound **73** over the phenyl ring in compound **72** was manifested in physicochemical properties, with aqueous solubility increased by 360-fold and clearance decreased by at least 4-fold (**Figure 27**). It is noteworthy that this case story is one of the earliest examples using BCP as bioisostere of the phenyl ring. [7]

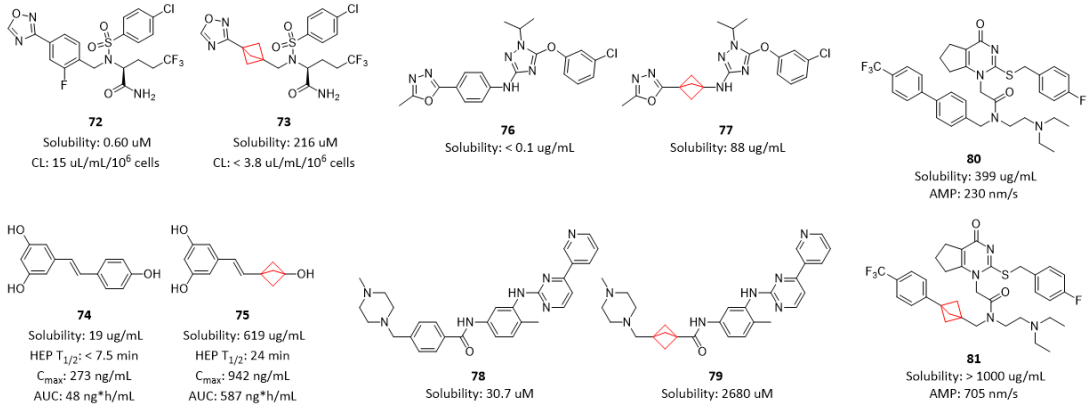

Figure 27. Representative examples where BCP improved ADME and PK profiles over the phenyl ring

The natural product **74** is associated with a wide range of biological activities. However, the poor bioavailability in preclinical species and humans has hampered its clinical progression, which can be attributed, in part, to metabolic modification of the phenolic hydroxyl moieties which are subjected to rapid first-pass glucuronidation or sulfation. An interesting approach to improve the pharmacokinetic profile of compound **74** conceived of replacing the phenol ring with a hydroxyl-substituted BCP moiety, explored in the context of compound **75** (**Figure 27**). [8] The BCP moiety dramatically increased aqueous solubility by 32-fold, and improved hepatocyte half-time by at least 3-fold which translated into 12-fold higher expousure.

The compound **76** exhibited a poor physicochemical profile, with an aqueous solubility of less than 1 ug/mL that was reflective of the overall planar nature of the structure (**Figure 27**). [9] The strategy adopted to address this deficiency was to replace the phenyl ring with a range of sp^3-riched bioisosteres. Among of them, BCP in compound **77** increased aqueous solubility significantly by at least 880-fold.

Despite the presence of the piperazine heterocycle, a basic element introduced to support salt formation as a means of enhancing aqueous solubility, the solubility of compound **78** is low at 0.01 mg/mL (**Figure 27**). [10] It was anticipated that reducing the aryl ring count by introducing the sp^3-riched, nonaromatic structural motifs would productively modulate physicochemical properties by lowering lipophilicity and enhancing aqueous solubility. This hypothesis was proved to be correct, with aqueous solubility increased by 87-fold in compound **79** in which BCP was used as bioisostere of the phenyl ring.

Compound **80** showed high membrane permeability and low aqueous solubility (BCS II). Based on assumption that reducing aromatic ring count and disrupting the planarity associated with the biaryl system would led to improved physicochemical profiles, the effect of replacing the central phenyl ring with a BCP isostere was examined in the compound **81** (**Figure 27**). [11] Compound **81** has both improved aqueous solubility and membrane permeability (BCS I).

With great success achieved in application of BCP as bioisostere of the phenyl ring, efficient access of diverse BCP building blocks is of substantial need, including monofunctional BCP building blocks (amines, carboxylic acids, etc.) and difunctional BCP building blocks (**Figure 28**).

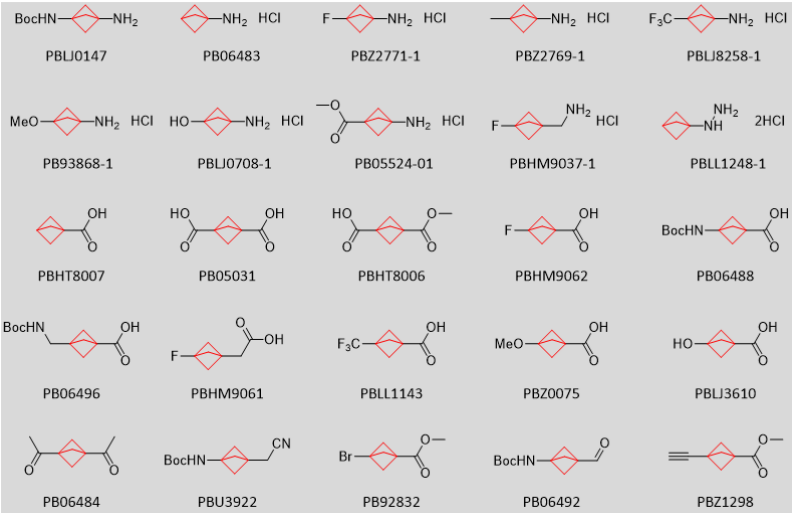

Figure 28. BCP building blocks have been widely used in medicinal chemistry.

Besides bicyclo[1.1.1]pentane (BCP) ring system, bicyclo[2.2.2]octane (BCO) ring system is another commonly used bioisostere of the phenyl ring by medicinal chemists. As part of a study of structurally novel HCV NS5A inhibitors, replacement of the biphenyl scaffold of compound **82** with alternative conformationally constrained spacers offering improved physicochemical properties was explored in a survey that included BCO-phenyl motif in compound **83**. The aqueous solubility was increased by 6-fold which was translated into high oral bioavailability (**Figure 29**). [12]

As described previously, compound **76** exhibited a poor physicochemical profile, with an aqueous solubility of less than 1 ug/mL that was reflective of the overall planar nature of the structure. The team also used BCO in compound **84** to replace the phenyl ring to improve aqueous solubility by at least 150-fold (**Figure 29**). [9]
Compound **85** caused only partial tumor regression in a mouse model attributed to low *in vivo* exposure. To address the PK deficiency, the benzoic acid was replaced with the conformationally rigid, sp^3-riched BCO ring system in compound **86**. C_{max} and AUC were improved dramatically by 5-fold and 11-fold respectively (**Figure 29**). [13]

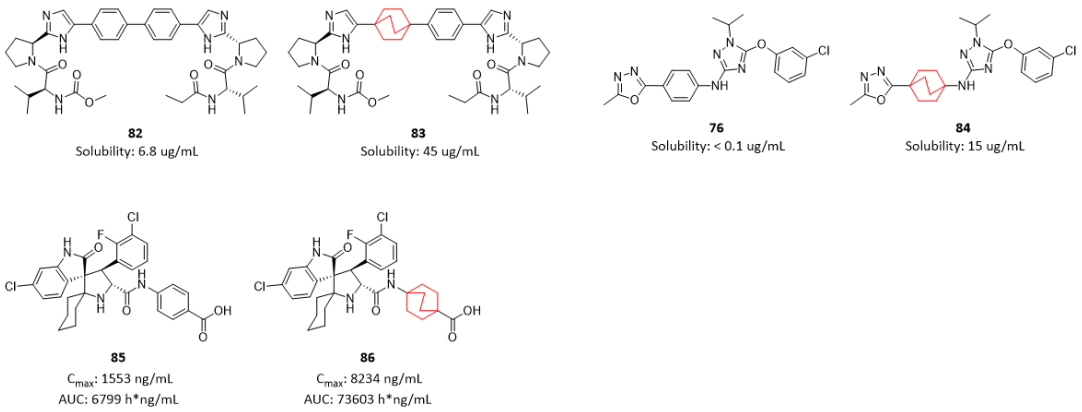

Figure 29. Representative examples where BCO improved ADME and PK profiles over the phenyl ring

Like BCP, great success was also achieved in application of BCO as bioisostere of the phenyl ring. Therefore, an efficient access of diverse BCO building blocks is of substantial need for medicinal chemists, including monofunctional BCO building blocks (amines, carboxylic acids) and difunctional BCO building blocks (**Figure 30**).

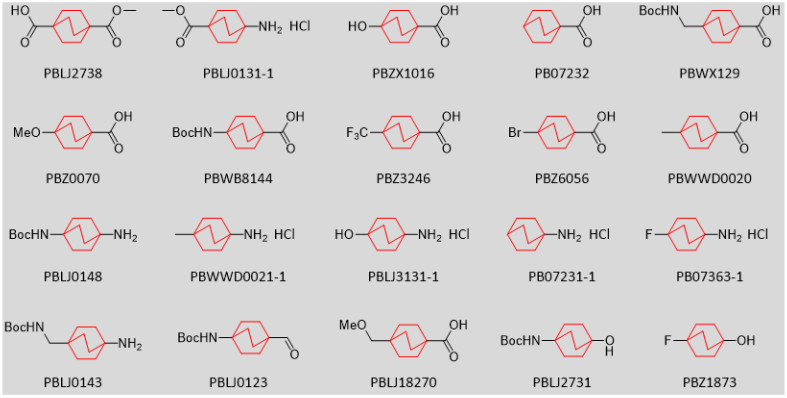

Figure 30. Like BCP, BCO building blocks have also been widely used in medicinal chemistry.

The altered geometries associated with the introduction of an oxygen atom into the skeleton of a BCP moiety confers plausible mimicry between 2-oxabicyclo[2.1.1]hexanes and *meta*-disubstituted benzene as depicted in **Figure 31**. [1]

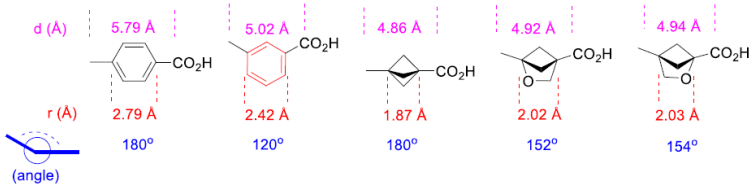

Figure 31. Geometric parameters of the phenyl ring and oxabicyclo[2.1.1]hexane ring system

Replacement of the phenyl ring of compound **87** with a 2-oxabicyclo[2.1.1]hexane ring system resulted in at least 6-fold improvement in aqueous solubility in both compound **89** and **90** (**Figure 32**). [14] Besides, there is a potentially IMHB between the ring oxygen atom and the amide N-H in compound **90**, which would reduce both the exposed polarity and solvation.

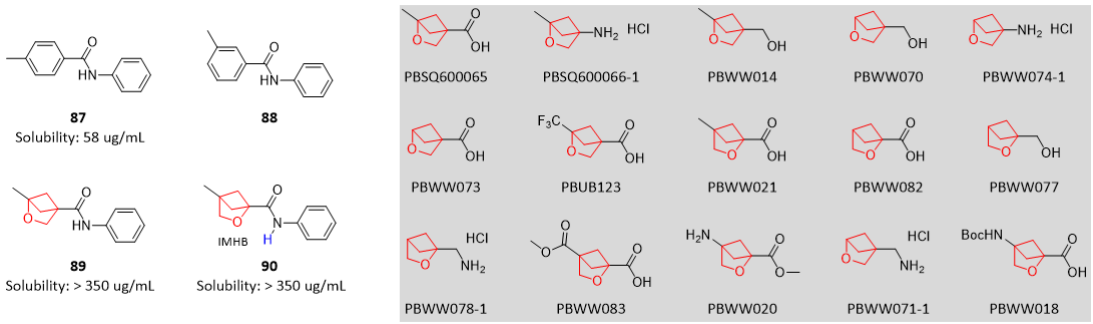

Figure 32. 2-Oxabicyclo[2.1.1]hexane moiety increased aqueous solubility.

As described previously, compound **76** exhibited a poor physicochemical profile, with an aqueous solubility of less than 1 ug/mL that was reflective of the overall planar nature of the structure. The team also used bridged piperidine in compound **91** to replace the phenyl ring to improve aqueous solubility by at least 1040-fold (**Figure 33**). [9] Besides, compound **91** exhibited improved potency by almost 10-fold.

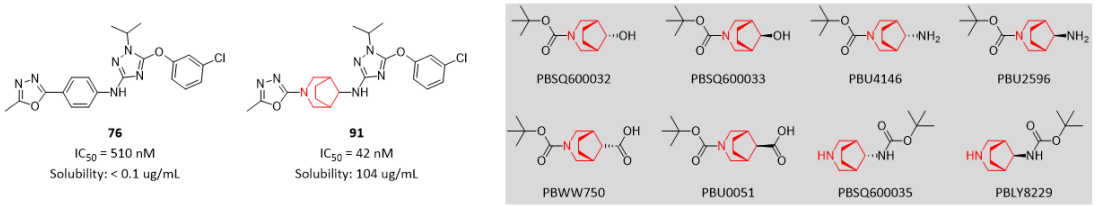

Figure 33. Bridged piperidine increased both aqueous solubility and potency.

References

[1] Murugaiah A. M. Subbaiah; *et al.* Bioisosteres of the phenyl ring: recent strategic applications in lead optimization and drug design. *J. Med. Chem.* **2021**, *64*, 14046-14128.
[2] Mykhailiuk P. K. Saturated bioisosteres of benzene: where to go next? *Org. Biomol. Chem.* **2019**, *17*, 2839-2849.
[3] Hui-ling Wang; *et al.* Novel vanilloid receptor-1 antagonists: 3. The identification of a second-generation clinical candidate with improved physicochemical and pharmacokinetic properties. *J. Med. Chem.* **2007**, *50*, 3528-3539.
[4] Daniel Meibom; *et al.* BAY-7081: a potent, selective, and orally bioavailable cyanopyridone-based PDE9A inhibitor. *J. Med. Chem.* **2022**, *65*, 16420-16431.
[5] Joshua S. Alford; *et al.* Conformational-design-driven discovery of EZM0414: a selective, potent SETD2 inhibitor for clinical studies. *ACS Med. Chem. Lett.* **2022**, *13*, 1137-1143.
[6] Tanaji T. Talele Opportunities for tapping into three-dimensional chemical space through a quaternary carbon. *J. Med. Chem.* **2020**, *63*, 13291-13315.
[7] Stepan A. F.; *et al.* Application of the bicycle[1.1.1]pentane motif as a nonclassical phenyl ring bioisostere in the design of a potent and orally active r-secretase inhibitor. *J. Med. Chem.* **2012**, *55*, 3414-3424.
[8] Goh Y. L.; *et al.* Toward resolving the resveratrol conundrum: synthesis and *in vivo* pharmacokinetic evaluation of BCP-resveratrol. *ACS Med. Chem. Lett.* **2017**, *8*, 516-520.
[9] Ratni H.; *et al.* Phenyl bioisosteres in medicinal chemistry: discovery of novel r-secretase modulators as a potential treatment for Alzheimer's disease. *RSC Med. Chem.* **2012**, *12*, 758-766.

[10] Nicolaou K. C.; *et al.* Synthesis and biopharmaceutical evaluation of Imatinib analogues featuring unusual structural motifs. *ChemMedChem* **2016**, *11*, 31-37.
[11] Measom N. D.; *et al.* Investigation of a bicyclo[1.1.1]pentane as a phenyl replacement within an LpPLA2 inhibitor. *ACS Med. Chem. Lett.* **2017**, *8*, 43-48.
[12] Zhong M.; *et al.* Discovery of functionalized bisimidazoles bearing cyclic aliphatic-phenyl motifs as HCV NS5A inhibitors. *Bioorg. Med. Chem. Lett.* **2014**, *24*, 5731-5737.
[13] Aguilar A.; *et al.* Discovery of 4-((3'R,4'S,5'R)-6'-chloro-4'-(3-chloro-2-fluorophenyl)-1'-ethyl-2'-oxodispiro[cyclohexane-1,2'-pyrrolidine-3',3'-indoline]-5'-carboxamido)bicyclo[2.2.2]octane-1-carboxylic acid (AA-115/APG-115): a potent and orally active murine double minute 2 (MDM2) inhibitor in clinical development. *J. Med. Chem.* **2017**, *60*, 2819-2839.
[14] Levterov V. V.; *et al.* Water-soluble non-classical benzene mimetics. *Angew. Chem. Int. Ed.* **2020**, *59*, 7161-7167.

Noncovalent Sulfur Interactions in Medicinal Chemistry

Like halogen bond, there can be seen from the front and side view of thiophene ring that a region of positive, σ-hole-like potential exists near the sulfur atom (**Figure 34**). [1] The presence of σ-hole on sulfur atom is available for interaction with electron donating atoms, particularly nitrogen and oxygen. For instance, most commonly sulfur-containing heterocycles can participate in attractive nonbonding interactions that are proving to be useful in the control of molecular conformation. As illustrated in **Figure 34**, there is a sulfur-long pair interaction in 2-(2'-thienyl)pyridine which causes "s-*cis*-locked" conformational preference. One of the earliest examples of an intramolecular N-S interaction that stabilized a specific conformation was reported in 1976. The small molecule single X-ray structure of compound **92** revealed a *syn*, coplanar arrangement of the electron-donating guanidine N atom and the acceptor S atom of the thiadiazole ring. [2]

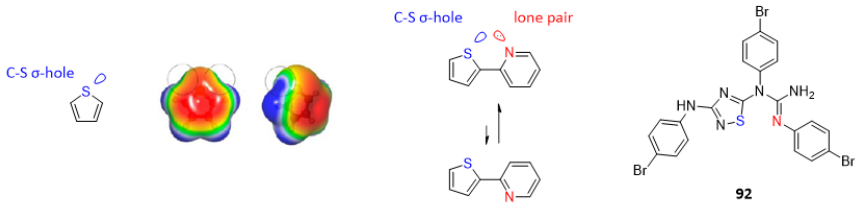

Figure 34. Illustration of σ-hole on sulfur atom and associated intramolecular interaction

Single replacement of oxygen atom in compound **93** with sulfur atom in compound **94** increased both Aurora A and Aurora B inhibition by at least 300-fold (**Figure 35**). Modeling of the heterocyclic core of compound **94** suggested that the two heterocyclic rings adopted a coplanar conformation in which the thiazole sulfur atom and the quinazoline N-3 atom were oriented proximal to each other. [3]

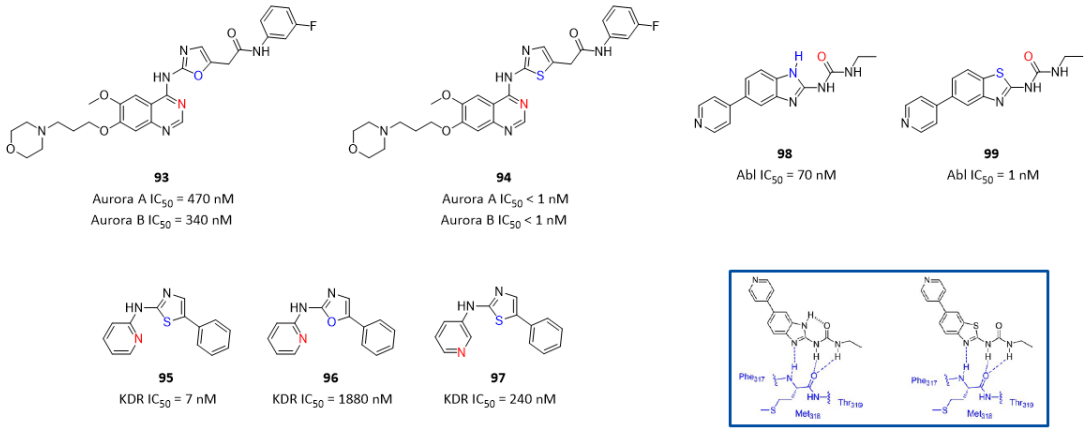

Figure 35. Intramolecular interaction between sulfur atom and nitrogen atom increased inhibition.

It was interesting to observe that a basic nitrogen atom in heteroaryl rings *ortho*- to the 2-amino group in compound **95** increased KDR inhibition by at least 30-fold, compared to isomer **97** with a *meta*- nitrogen. Single replacement of sulfur atom in compound **95** with oxygen atom in compound **96** decreased inhibition by at least 260-fold. Both two observations indicated that there was a key intramolecular interaction between sulfur atom and nitrogen atom in compound **95**, constraining binding favored conformation (**Figure 35**). [4]

There was 70-fold difference in potency between compound **98** and **99**, although both compounds had binding favored conformation resulted from intramolecular hydrogen bond and S-N interaction respectively. Calculations suggested that the difference in potency was more a function of desolvation costs, which are higher for the more basic compound **98** (**Figure 35**). [5]

In order to discover highly selective PI3K inhibitors based on primary hit compound **100**, replacing amide moiety in compound **100** with pyridine moiety in compound **101** maintained same desired conformation. Co-crystal structure of compound **101** in PI3K revealed that the pyridine ring was coplanar with the thiazole and with the nitrogen of the pyridine pointing inward. It was interpreted that long pair-sulfur interaction stabilized this conformation (**Figure 36**). [6]

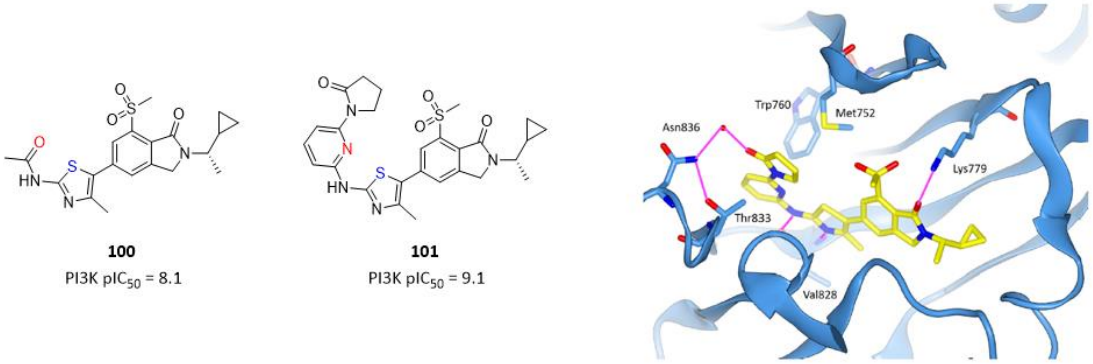

Figure 36. Co-crystal structure of compound **101** in PI3K revealed intramolecular interaction between S-N locked binding desired conformation. (PDB code: 7OIL)

As revealed above, intramolecular interaction between the sulfur atom in thiazole or fused-thiazole rings and adjacent nitrogen or oxygen plays a critical role in locking favored conformation. Thiazole or fused-thiazole building blocks are of great value (**Figure 37**).

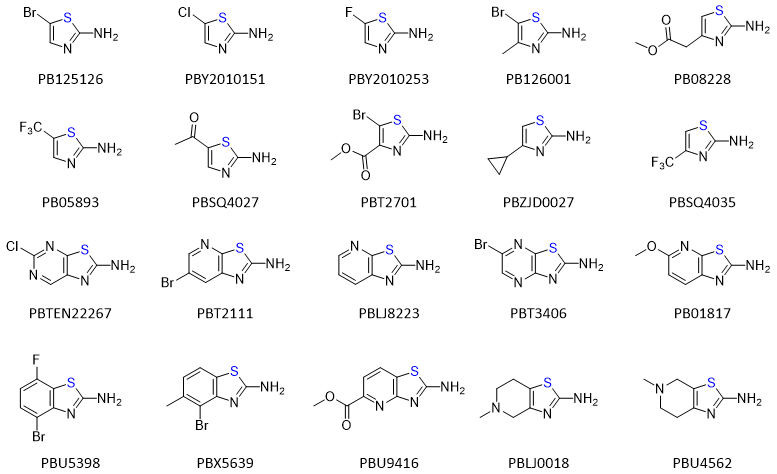

Figure 37. Thiazole and fused-thiazole building blocks

An intramolecular O-S interaction plays a role in orienting the thiazolopyridine heterocycle of the factor Xa inhibitor Edoxaben (**102**), which was approved for the prevention of venous thromboembolism following lower-limb surgery. In the crystal structure of the structurally related factor Xa inhibitor **103**, the close contact between the thiazole S and adjacent amide carbonyl O atom was considered to contribute to the correct alignment of the whole molecule (**Figure 38**). [7]

Thiazole-2-carboxylic acid building blocks are of great value for incorporation of O-S interaction into molecule.

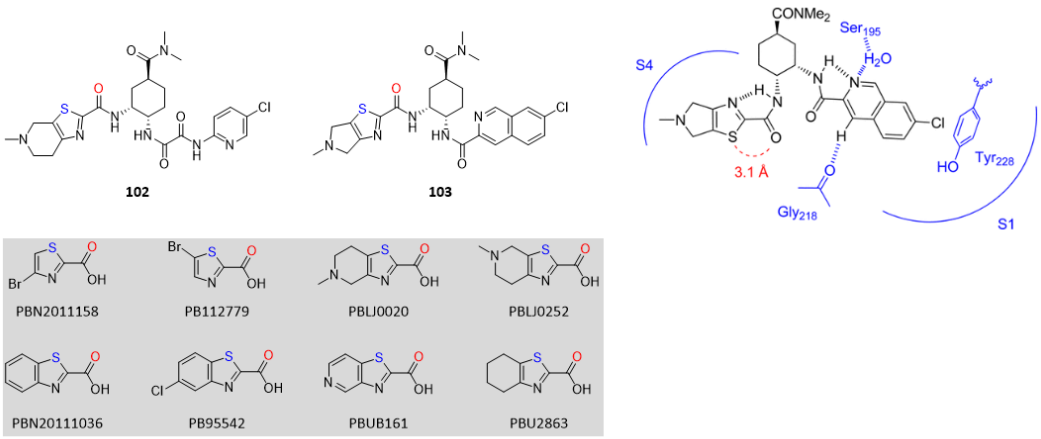

Figure 38. Intramolecular O-S interaction in Edoxaben and its analogues.

Compound **105** is a potent inhibitor of SIRT family members with IC_{50} values of 15 nM, 10 nM and 33 nM respectively, while the analogous compound **104** is about 10-fold weaker. These data are consistent with the co-crystal structure of SIRT3 with an analogue. The orientation of the 2-carboxamide is coplanar with the thienyl ring such that the oxygen atom lies proximal to the sulfur atom to facilitate a 1,4-electrostatic interaction. This topology facilitates four hydrogen bond interactions between the amide moiety and elements of the protein and a structural bridging water molecule (**Figure 39**). [8]

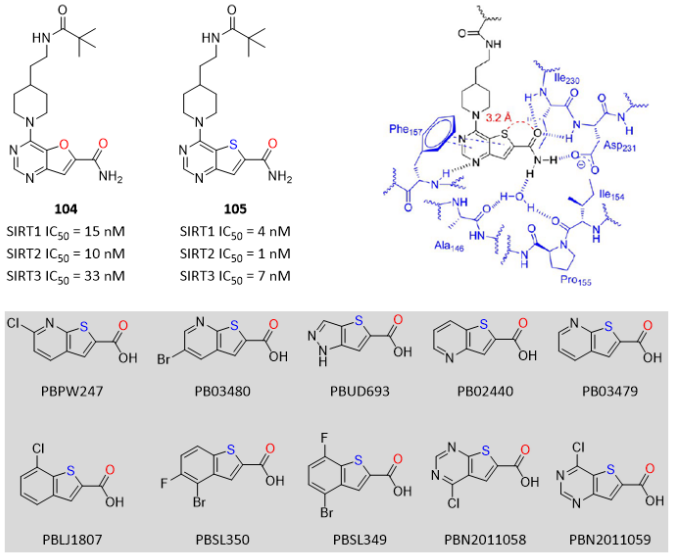

Figure 39. Key O-S contact was revealed in co-crystal structure in SIRT3 protein.

An X-ray co-crystal structure of compound **107** confirmed that the key enzyme-inhibitor interaction was preserved as the topology of the carboxamide moiety favored by close O-S interaction. The importance of this interaction on biological activity was understood by the dramatic difference in potency that was observed between compound **107** and close isomer compound **106**, with the latter 1500-fold weaker than the former. This was attributed to distortion of the carboxamide moiety of compound **106** from planarity, which resulted in a poor alignment for the important hydrogen bond with the protein (**Figure 40**). [9]

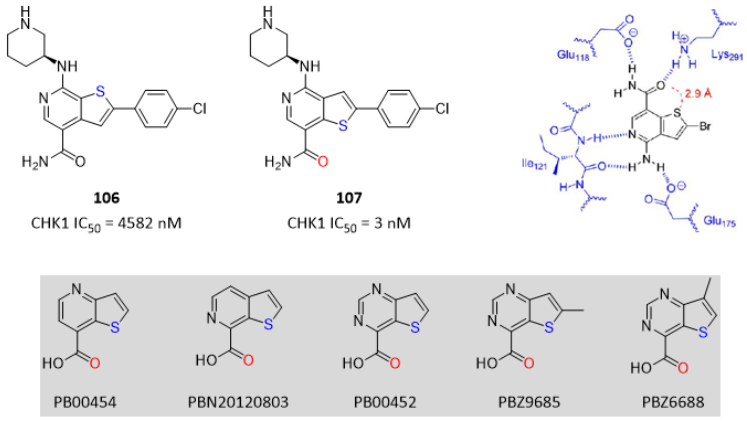

Figure 40. Key O-S contact was revealed in co-crystal structure in CHK1 protein.

References

[1] Brett R. Beno; *et al.* A survey of the role of noncovalent sulfur interactions in drug design. *J. Med. Chem.* **2015**, *58*, 4383-4438.
[2] Akiba K.; *et al.* Chemistry of hypervalent sulfur. V. A ^{13}C-NMR study of the 1:1 adduct of "Hector's base" with arylcyanamides. Evidence for intramolecular S-N interaction. *Tetrahedron Lett.* **1976**, *17*, 3819-3820.
[3] Jung F. H.; *et al.* Discovery of novel and potent thiazoloquinazolines as selective Aurora A and B kinase inhibitors. *J. Med. Chem.* **2006**, *49*, 955-970.
[4] Bilodeau M. T.; *et al.* The discovery of N-(1,3-thiazol-2-yl)pyridine-2-amines as potent inhibitors of KDR kinase. *Bioorg. Med. Chem. Lett.* **2004**, *14*, 2941-2945.
[5] Park H.; *et al.* Discovery of picomolar ABL kinase inhibitors equipotent for wild type and T315I mutant via structure-based de novo design. *J. Am. Chem. Soc.* **2013**, *135*, 8227-8237.
[6] Matthew W. D. Perry; *et al.* Discovery of AZD8154, a dual PI3K inhibitor for the treatment of asthma. *J. Med. Chem.* **2021**, *64*, 8053-8075.
[7] Yoshikawa K.; *et al.* Design, synthesis, and SAR of cis-1,2-diaminocyclohexane derivatives as potent factor Xa inhibitors. Part II: exploration of 6-6 fused rings as alternative S1 moieties. *Bioorg. Med. Chem.* **2009**, *17*, 8221-8233.
[8] Disch J. S.; *et al.* Discovery of thieno[3,2-d]pyrimidine-6-carboxamides as potent inhibitors of SIRT1, SIRT2 and SIRT3. *J. Med. Chem.* **2013**, *56*, 3666-3679.
[9] Zhao L.; *et al.* Design, synthesis and SAR of thienopyridines as potent CHK1 inhibitors. *Bioorg. Med. Chem. Lett.* **2010**, *20*, 7216-8221.

Fluorine in Medicinal Chemistry

Fluorine atom has been playing a prominent role in drug discovery, and the applications of fluorine atom in the design of drug and agricultural chemicals are continuing to grow as our knowledge and understanding of how to take full advantage of the unique properties. This has been facilitated by the development of innovative synthetic methodology which providing access to new **fluorinated building blocks**. While early applications of fluorine as a bioisostere focused on the relatively simple replacement of hydrogen atoms in drug molecules, often as a means of influencing metabolism, the last 30 years has been broader deployment of fluorine and fluorinated building blocks in the construction of more sophisticated structural arrangements that are able to emulate and influence a number of more traditional functionalities (**Figure 41**). [1-2]

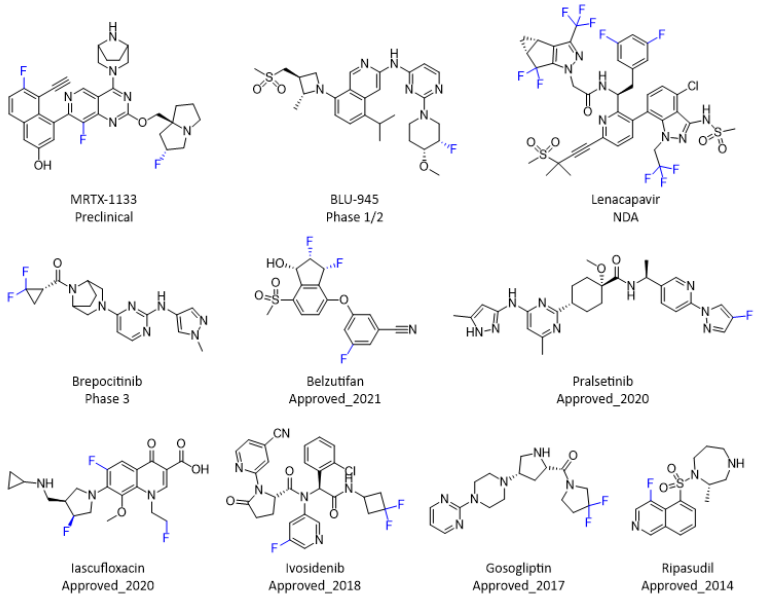

Figure 41. Representative fluorine-containing drug and clinical candidate molecules

Fluorine atom can exert plenty of positive influences on molecules, including increasing potency by forming a critical interaction with the protein, increasing solubility by forming an intramolecular hydrogen bond, reducing hERG inhibition by modulating basicity of nitrogen atom, and reducing metabolism by blocking metabolic sites.

In a series of potent inhibitors of BTK, a fluorine scan identified a site for substitution that led to a 400-fold enhancement of potency by comparison of the matched pair of BTK inhibitors **108** and **109** where the introduction of a single fluorine atom increased potency by two orders of magnitude (**Figure 42**). [3] An X-ray co-crystal structure of compound **109** provided some understanding of the SAR observation. The fluorine atom of compound **109** was observed to be close to the protonated amine of Lys, the ortho C-H of Phe and a conserved water molecule. Like nitrogen-walking described previously, fluorine-walking is also an important tactic for medicinal chemists to explore potential interactions with protein. Therefore, a quick access of diverse fluorine-containing building blocks is of great value for drug discovery campaign to understand structure-activity and structure-property relationship.

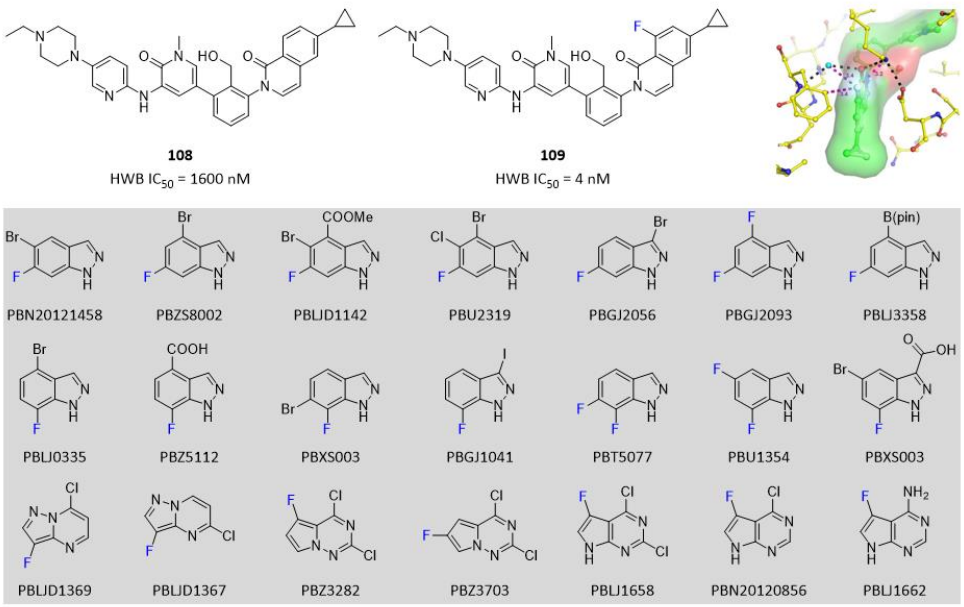

Figure 42. Key interactions between fluorine atom and BTK

A dramatic fluorine effect was observed by comparison of compound **110** and **111**, with the latter 30-fold more potent than the former. With regard to the remarkable fluorine phenomenon, an X-ray structure of compound **111** revealed that the fluorine of compound **111** was located close to the terminal carboxamide in Gln530 with a F-N distance of 2.97 A and functioned as a hydrogen bond acceptor (**Figure 43**). [4] Additionally, the introduction of fluorine also strengthened the hydrogen bond interaction between the amidecarbonyl group of compound **111** and Ser555. Therefore, carboxylic acid building blocks with a fluorine atom at alpha-position are of great interest for medicinal chemists in this kind of context.

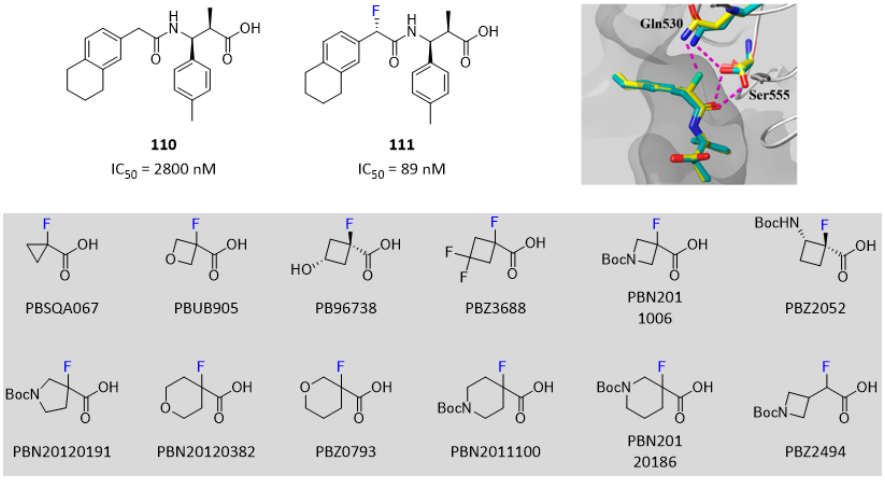

Figure 43. Introduction of fluorine increased potency by 40-fold.

Introduction of two fluorine atoms in compound **113** on methyl group of compound **112** displayed improved biochemical potency by 10-fold. An X-ray co-crystal structure of an analogue compound revealed a critical interaction between one fluorine atom with Ser774, explaining the observation (**Figure 44**). [5]

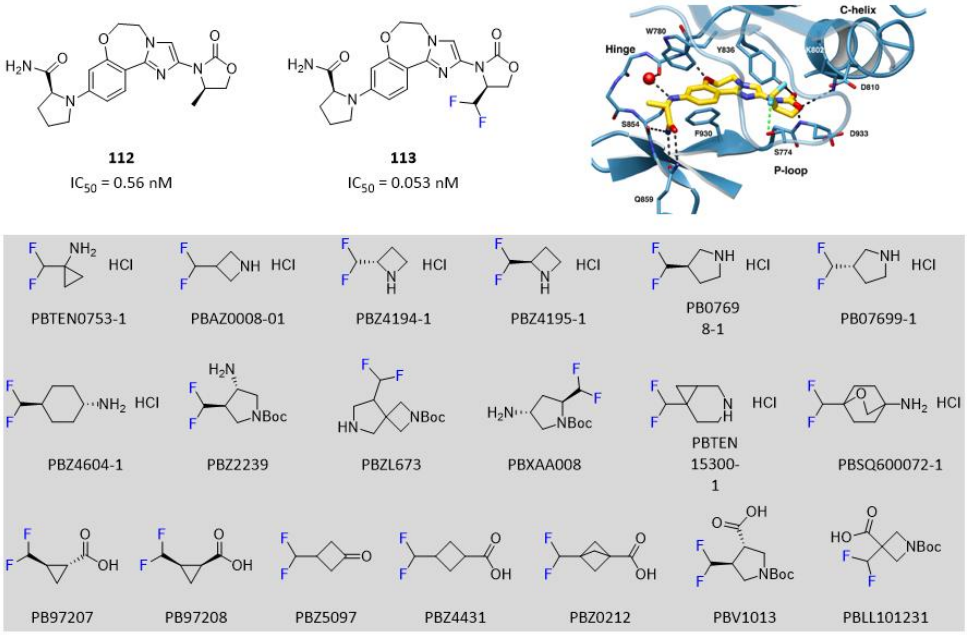

Figure 44. Difluoromethyl increased potency by forming an interaction with Ser774 (PDB code: 8EXU).

Difluoro- compound **115** demonstrated a 4-fold increase in CBP inhibitory potency, compared to methyl compound **114**. To further understand the increased CBP potency of compound **115**, an X-ray co-crystal structure of compound **115** in CBP bromodomain was obtained. The crystal structure revealed that additional favorable dipolar interaction between the partial negative charge on the fluorines of the difluoromethyl and the positively charged guanidine on Arg1173 was observed (**Figure 45**). [6]

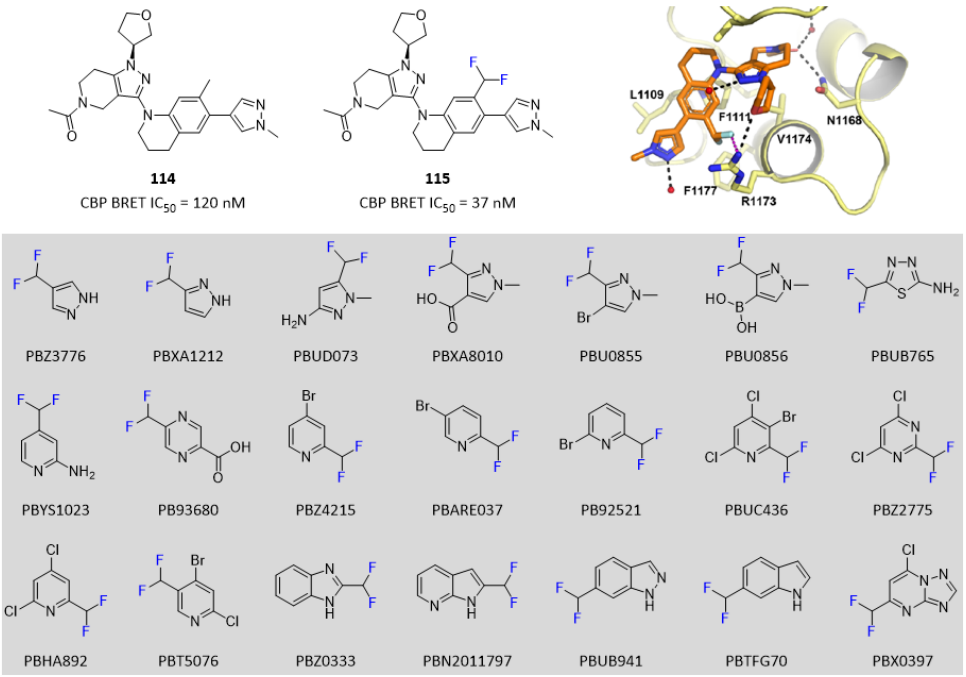

Figure 45. Interaction between negatively charged fluorine and positively charged Arg1173 (PDB code: 5W0I)

A weak but nevertheless interesting interaction between the CF_3 moiety and electron rich centers of protein, such as COOH, amide carbonyl and oxygens of serine, threonine and tyrosine, that involves tetrel CF_3-O bonding has recently been reported. [7] The geometry of the interaction of

electron rich species with the sigma-hole associated with the CF_3 substituent is highly directional in nature, optimal at an angle of 180° to the Ar-sp^3 carbon bond (**Figure 46**).

Two examples were depicted in **Figure 46**: in the first case, the side chain carboxylate of Asp312 interacted with the CF_3 of the inhibitor, while in the second case, the oxygen atom of Tyr246 was the partnering element.

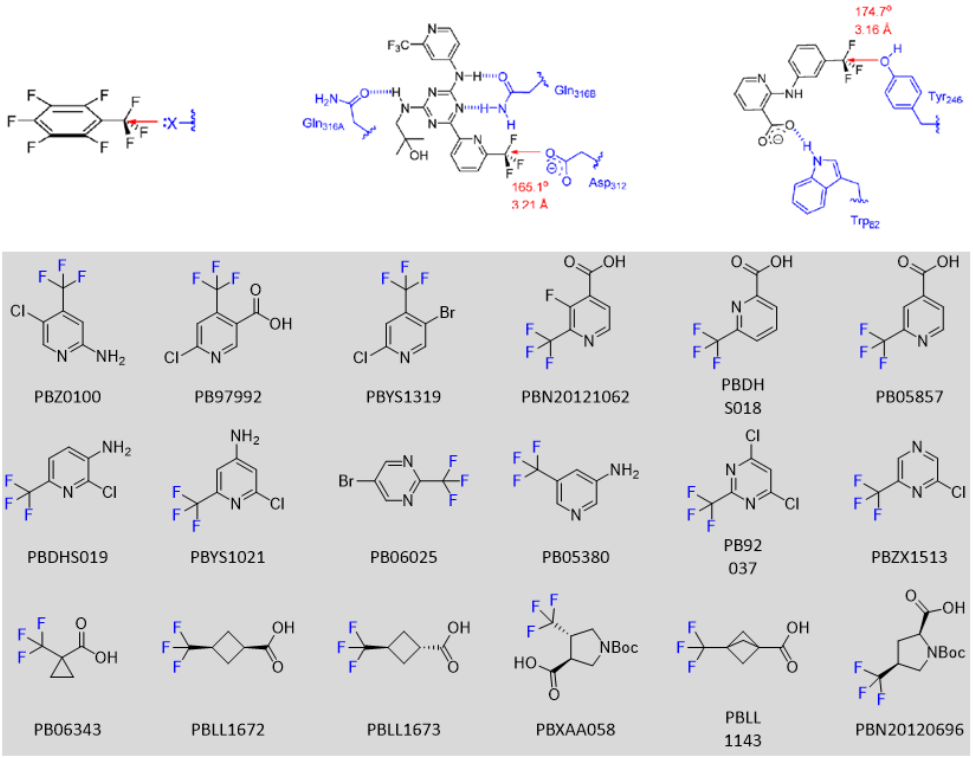

Figure 46. Key interactions between CF_3 and electron rich centers of the protein

Compound **116** exhibited a weak hERG inhibition at 44 uM. Estimate for effective therapeutic plasma concentration for compound **116** was typically in the range of 2 to 10 uM free concentration. The resulting ratio for hERG IC_{50}/free drug concentration < 22 reflected a high risk for QT prolongation signals in man. A recent analysis of human thorough QT studies at Pfizer demonstrated that a hERG IC_{50} within 60-fold of the effective therapeutic plasma concentration results in an 82% chance of causing a significant signal in a human thorough QT study. [8] Therefore, the team aimed to further reduce hERG inhibition of compound **116**. To reduce the risk of a positive signal in the human thorough QT study, the team aimed for a > 100 ratio of hERG IC_{50}/free drug concentration, which translated approximately into a hERG IC_{50} target of > 200 uM.

It is well-established that pKa has an impact on hERG inhibition. [9] The team explored reduction of pKa through substitution at the 3-position of the piperidine moiety with electron-withdrawing substituents, specifically both cis- and trans-substitution with hydroxyl, methoxy and fluoro groups (**Figure 47**). [10] All of these strategies worked, with cis-fluoro substitution in compound **117** decreasing hERG inhibition to 233 uM which meet criteria of target product profile and advanced into phase 1 clinical studies. Addition of a substituent adjacent to -NH_2 results in two chiral centers making molecule more complexed, so an efficient access of chirally pure building blocks is of great value for medicinal chemists.

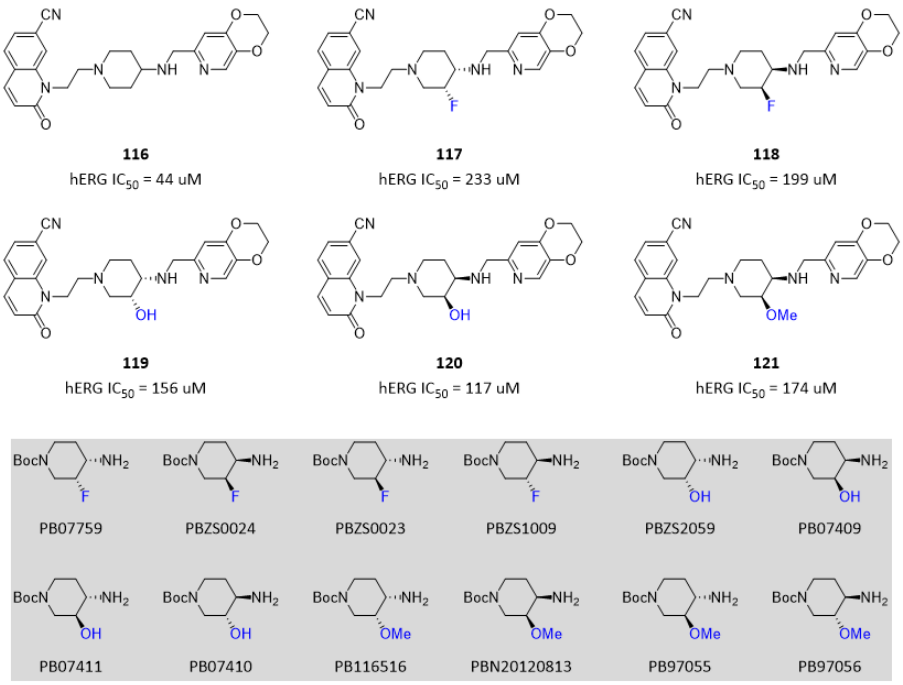

Figure 47. Impact of F-, -OH and –OMe on hERG inhibition

Another example is that reduction in the electron density of the pyridine heterocycle of JAK3 inhibitor **122** was examined as an approach to reduce the affinity of this compound for the hERG channel. As captured in **Figure 48**, the installation of a fluorine atom in the piperidine ring reduced hERG binding by an order of magnitude in both cis- compound **123** and trans- compound **124**. [11]

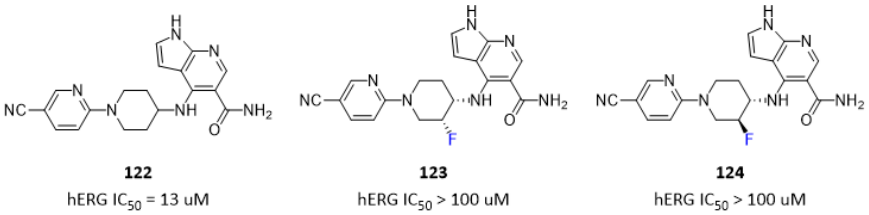

Figure 48. Fluorine substitutions impact hERG inhibition.

In part because of the strength of the C-F bond, fluorine is often used to overcome issues associated with poor metabolic stability, where it may be deployed as the direct replacement for a metabolically liable H atom in both aromatic and aliphatic settings. In the course of discovering oral EP300/CBP inhibitors, compound **125** was found to be metabolically unstable. Two fluorine atoms were introduced on cyclohexane ring to block the metabolic site. As expected, the *in vitro* microsome stability of compound **126** was increased by about 16-fold compared to compound **125**, which translated into *in vivo* PK with AUC improved by about 8-fold and oral bioavailability improved by 3-fold compared to compound **125**. As discussed in this example, difluoro-aliphatic building blocks have been widely used by medicinal chemists to circumvent the metabolism issue (**Figure 49**). [12]

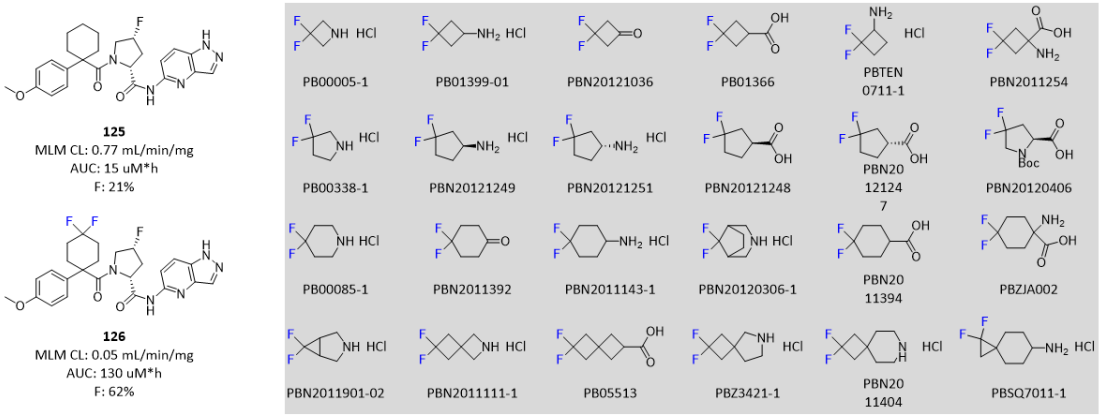

Figure 49. Two fluorine atoms block the metabolic site and improve PK profile.

Compound **127** exhibited good potency, but suffered from poor metabolic stability with just 8% remaining after incubation in mouse microsome. Introduction of two fluorine atoms on cyclopetane ring in compound **128** exhibited improved microsome stability (**Figure 50**). [13] Hydroxylation process of compound **129** caused rapid in vivo clearance from mouse plasma. Compared to compound **129**, the anti-fluoro on cyclobutane ring of compound **130** exhibited lower clearance and increased oral bioavailability. [14]

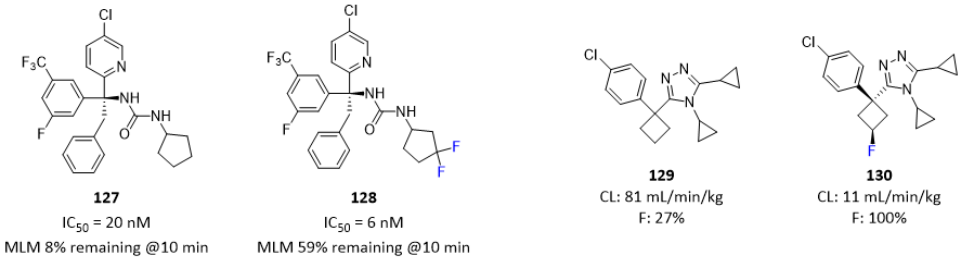

Figure 50. Fluorine atom improved microsome stability and oral bioavailability.

The 1,3-benzodioxole moiety is a structural element in prevalent natural products and in small-molecule candidates or drugs. However, this moiety is susceptible to metabolism by CYP450 enzymes following a pathway that leads to the formation of a carbine intermediate that binds to the Fe atom of the enzyme tightly (**Figure 51**). This carbine-bound intermediate is referred to as a metabolite intermediate complex that inactivates the enzyme until the complex degrades, which relieves the inhibition, with the methylenedioxy carbon atom released as carbon monoxide. However, this step generates a catechol than can be subject to bioactivation by oxidizing enzymes, including CYP450, to afford quinone derivatives that are highly reactive toward both soft and hard nucleophiles. Consequently, the moiety is considered to be a structural alert because it can be associated with drug-drug interaction, metabolic activation, and toxicities that includes hepatotoxicity. For example, despite its relatively low clinical dose of 10-50 mg, the antidepressant drug Paroxetine (**111**) is metabolized by CYP2D6 in a fashion that leads to inhibition of the enzyme, inhibiting both its own metabolism and that of other drugs that are cleared by CYP2D6.
An appreciation of these problems has prompted the design of 1,3-benzodioxole replacements that would abrogate this metabolic pathway while preserving the physicochemical properties. Deuteration of the methylene moiety represents the most conservative isosteric substitution that can slow this metabolic process while preserving biological activity and has been successful in the context of compound **132**, a deuterated derivative of compound **131** (**Figure 51**). [15]

Fluorination offers a more definitive solution, although the effects on biological potency are less predictable with increases, decreases and minimal changes described that show dependence on the specific target or chemotype within a target. Lumacaftor (**133**) has been approved by FDA for the treatment of cystic fibrosis (**Figure 51**). [16] Compound **134** is a clinically evaluated, mechanism-based inhibitor of FAAH for which the 2,2-difluorobenzo[d][1,3]dioxole heterocycle was observed to be metabolically stable (**Figure 51**). [17]

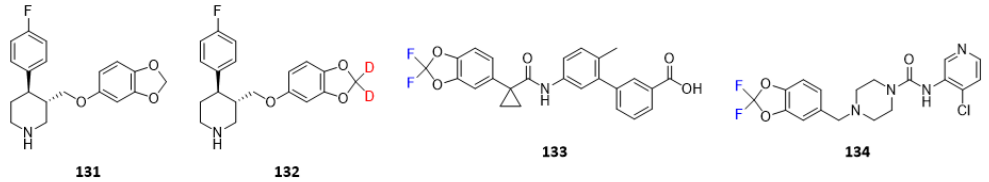

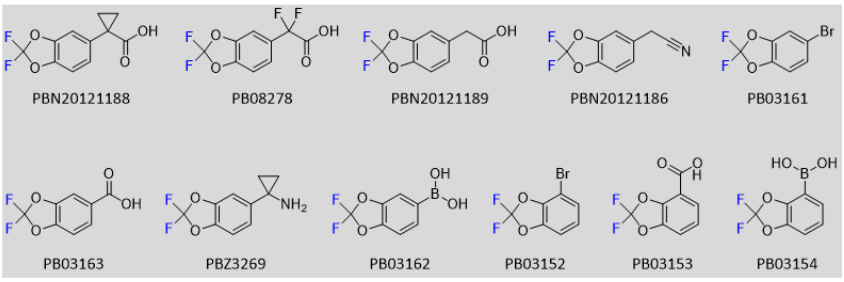

Figure 51. 2,2-Difluorobenzo[d][1,3]dioxole heterocycle is more metabolically stable.

References

[1] Eric P. Gillis; *et al.* Applications of fluorine in medicinal chemistry. *J. Med. Chem.* **2015**, *58*, 8315-8359.
[2] Nicholas A. Meanwell. Fluorine and fluorinated motifs in the design and application of bioisosteres for drug design. *J. Med. Chem.* **2018**, *61*, 5822-5880.
[3] Lou Y.; *et al.* Finding the perfect spot for fluorine: improving potency up to 40-fold during a rational fluorine scan of a Bruton's tyrosine kinase (BTK) inhibitor scaffold. *Bioorg. Med. Chem. Lett.* **2015**, *25*, 367-371.
[4] Kazuki Otake; *et al.* Methyl and fluorine effects in novel orally bioavailable Keap1-Nrf2 PPI inhibitor. *ACS Med. Chem. Lett.* **2023**, doi:10.1021/acsmedchemlett.3c00067.
[5] Emily J. Hanan; *et al.* Discovery of GDC-0077 (Inavolisib), a highly selective inhibitor and degrader of mutant PI3Kalpha. *J. Med. Chem.* **2022**, *65*, 16589-16621.
[6] F. Anthony Romero; *et al.* GNE-781, a highly advanced potent and selective bromodomain inhibitor of cyclic adenosine monophosphate response element binding protein, binding protein (CBP). *J. Med. Chem.* **2017**, *60*, 9162-9183.
[7] Garcia-LLinas X.; *et al.* Importance of R-CF_3-O tetrel bonding interactions in biological system. *J. Phys. Chem. A* **2017**, *121*, 5371-5376.
[8] Wallis R. M. Themed section: QT safety review-integrated risk assessment and predictive value to humans of non-clinical repolarization assays. *Br. J. Pharmacol.* **2010**, *159*, 115-121.
[9] Aronov A. M. Ligand structural aspects of hERG channel blockade. *Curr. Top. Med. Chem.* **2008**, *8*, 1113-1127.
[10] Folkert Reck; *et al.* Novel N-linked aminopiperidine inhibitors of bacterial topoisomerase type II with reduced pKa: antibacterial agents with an improved safety profile. *J. Med. Chem.* **2012**, *55*, 6916-6933.

[11] Nakajima Y.; *et al.* Synthesis and evaluation of novel 1H-pyrrolo[2,3-b]pyridine-5-carboxamide derivatives as potent and orally efficacious immunomodulators targeting JAK3. *Bioorg. Med. Chem.* **2015**, *23*, 4871-4883.
[12] Ryutaro Kanada; *et al.* Discovery of DS-9300: a highly potent, selective, and once-daily oral EP300/CBP histone acetyltransferase inhibitor. *J. Med. Chem.* **2023**, *66*, 695-715.
[13] van Niel M. B.; *et al.* Fluorination of 3-(3-(piperidin-1-yl)propyl)indoles and 3-(3-(piperazin-1-yl)propyl)indoles gives selective human 5-HT1D receptor ligands with improved pharmacokinetic profiles. *J. Med. Chem.* **1999**, *42*, 2087-2104.
[14] Paulini R.; *et al.* Orthogonal multipolar interactions in structural chemistry and biology. *Angew. Chem. Int. Ed.* **2005**, *44*, 1788-1805.
[15] Uttamsingh V.; *et al.* Altering metabolic profiles of drugs by precision deuteration: reducing mechanism-based inhibition of CYP2D6 by paroxetine. *J. Pharmacol. Exp. Ther.* **2015**, *354*, 43-54.
[16] Van Goor F.; *et al.* Correction of the F508del-CFTR protein processing defect in vitro by the investigational drug VX-809. *Pro. Natl. Acad. Sci. U. S. A.* **2011**, *108*, 18843-18848.
[17] Keith J. M.; *et al.* Preclinical characterization of the FAAH inhibitor JNJ-42165279. *ACS Med. Chem. Lett.* **2015**, *6*, 1204-1208.

Scaffold Hopping in Medicinal Chemistry

In medicinal chemistry, scaffold hopping is a strategy for designing new drug molecules by replacing the core structure or scaffold of an existing drug molecule with a structurally different one while still retaining the key biological activity. This can be done by identifying common features or pharmacophores of the original scaffold and the desired scaffold, and then using computational or medicinal methods to design and optimize new molecules with similar activity. In the practice, scaffold hopping is carried out for different purposes. For example, one might be interested in circumventing an intellectual property position by identifying novel chemical entities having a desired activity, improving ADMET profile, or decreasing toxicity. [1]

The past 10 years witnessed great success in discovery and development of BTK inhibitors. **Ibrutinib** (**135**) was the first BTK inhibitor approved for the treatment of several B cell malignancies. [2] However, due to its binding to BTK in its active conformation, **Ibrutinib** not only potently inhibits BTK, but also inhibits all kinases which carry a Cys at the same position as BTK. Consequently, it is associated with several side effects, such as skin rash and diarrhea which are well associated with EGFR inhibition, and platelet disfunction which is resulted from TEC and SRC inhibition. Second generation of BTK inhibitors, **Acalabrutinib** [3] and **Tirabrutinib** [4], were discovered by employing scaffold hopping strategy based on **Ibrutinib**. Althought both of them retain a similar binding mode to BTK as **Ibrutinib**, they offer an overall improved selectivity profile against other kinases and therefore reduce side effects observed in treatment with **Ibrutinib** (**Figure 52**).

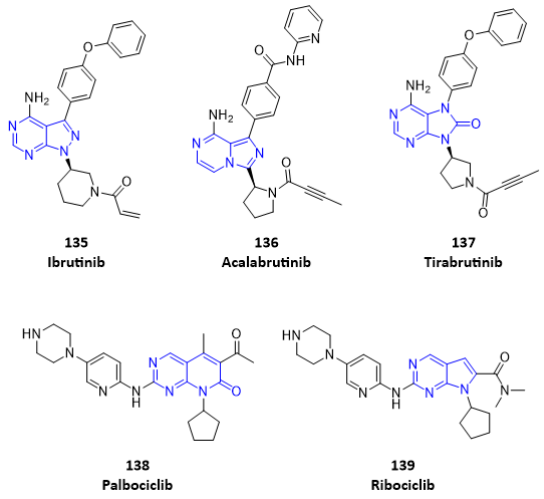

Figure 52. BTK inhibitors and CDK4/6 inhibitors approved by FDA

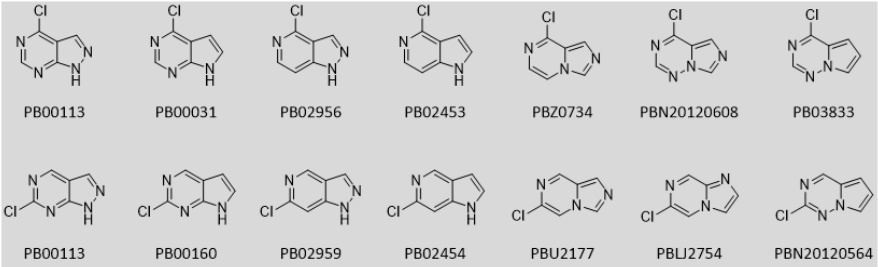

Figure 53. Building blocks for systematic scaffold hopping studies

Discovery of CDK4/6 inhibitors is another well-known example, representing the high value of scaffold hopping. CDK4/6 inhibitors brought as remarkable influence as BTK inhibitors for the

treatment of cancers and became a new standard of care of patients with advanced hormone receptor-positive breast cancer. [5] **Palbociclib** (**138**) and **Ribociclib** (**139**) were the first two drugs approved by FDA. [6] Obviously, there are several common features in structures of **Palbociclib** and **Ribociclib**, and the most distinct difference is the two scaffolds used (**Figure 52**). An efficient access of a set of diverse building blocks is considered of great value for medicinal chemists to conduct SAR/SPR studies by scaffold hopping (**Figure 53**).

In order to discover selective oral inhibitors of ERK1/2, previous scaffold hopping efforts based on compound **140** with a pyrrolo-pyrazinone scaffold generated compound **141** with an imidazo-pyrazinone scaffold. It was remarkable than a nitrogen atom in the scaffold of compound **141** increased aqueous solubility significantly by 55-fold and reduced metabolism in human microsome. The same trend was observed in paired compounds **142** and **143**. In addition, compounds **141** and **143** also demonstrated improved kinase selectivity to compounds **140** and **142** respectively (data not shown, **Figure 54**). Further lead optimization based on compound **143** generated a clinical candidate **AZD0364** for the treatment of NSCLC. [7]

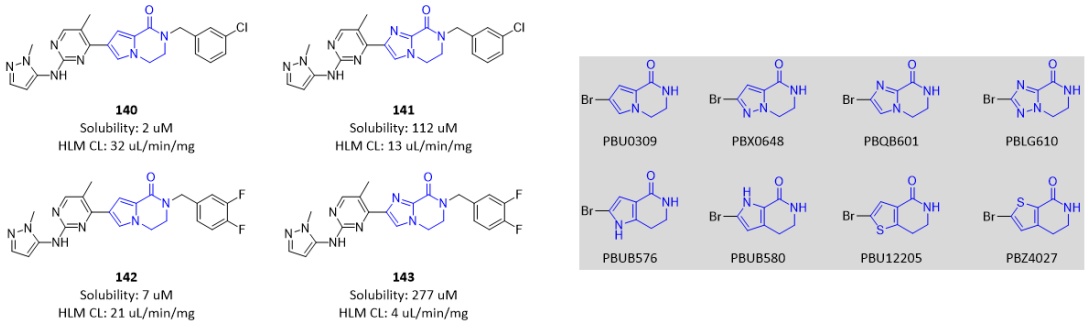

Figure 54. Scaffold hopping increased aqueous solubility and reduced metabolism.

Filgotinib (**144**) is one of second-generation JAK inhibitors with high JAK1 selectivity against other JAK family members, which was approved for the treatment of autoimmune and inflammatory diseases, such as rheumatoid arthritis (RA) and inflammatory bowel diseases (IBD). [8] The amide hydrolysis reaction and the corresponding metabolite **AMF** (**145**) of **Filgotinib** (**144**) is primarily mediated by CES2. Notably, its amide hydrolysis metabolite **AMF** (**145**) show much higher exposure, longer half-life but 10-fold lower potency than those of **Filgotinib** (**144**) in human. Besides, both **Filgotinib** (**144**) and **AMF** (**145**) are substrates of PgP, and potential inhibitors of organic anion transporting polypeptides. Hereby further investigations of drug-drug interactions based on these transporters in clinic is still ongoing. In order to circumvent amide hydrolysis, scaffold hopping studies based on **Filgotinib** (**144**) generated a novel clinical candidate **FZJ-003** (**146**) where a nitrogen atom was removed from core structure. It was extremely interesting that amide hydrolysis of **FZJ-003** (**146**) was not observed, which was reflected by higher exposure of **FZJ-003** (**146**) than **Filgotinib** (**144**) and almost no metabolite **FZJ-004** (**147**) of **FZJ-003** (**146**) was detected in PK studies (**Figure 55**). It was hypothesized that electron density of nitrogen of amide of **FZJ-003** (**146**) is higher than that of **Filgotinib** (**144**), which is resulted from the lower electron-withdrawing ability of imidazole ring of **FZJ-003** (**146**) than that of triazole ring of **Filgotinib** (**144**). In addition, compared to **Filgotinib** (**144**), **FZJ-003** (**146**) displayed 5-fold higher potency for JAK1 while maintaining similar selectivity against other JAK family members. [9]

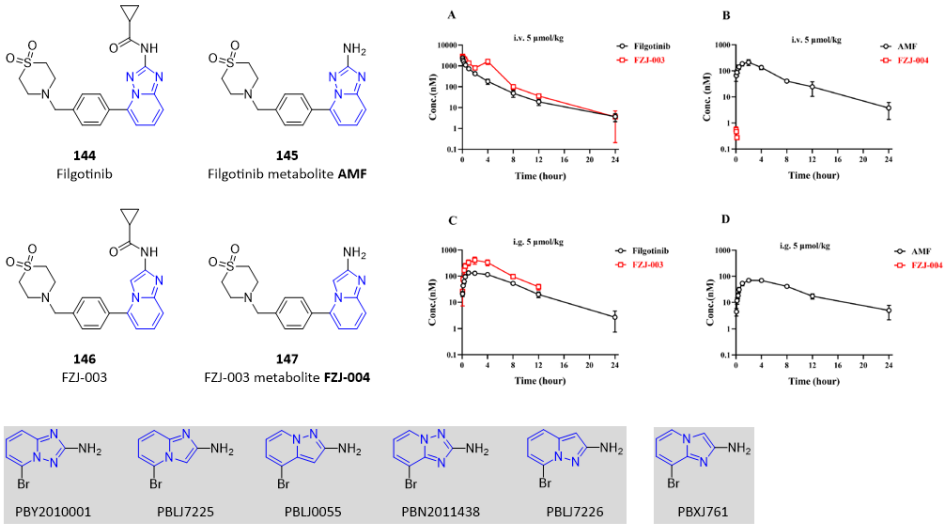

Figure 55. Novel scaffold in FZJ-003 resolved amide hydrolysis issue of Filgotinib.

Compound **148** was selected as a starting point for medicinal chemistry to discover novel CAMKK2 inhibitors. The team employed scaffold hopping by replacing 7-azaindole ring in compound **148** with a variety of diverse scaffolds. In summary, most of scaffolds exhibited robust CAMKK2 enzyme inhibition, such as furopyridine ring in compound **149**, thienopyridine ring in compound **150**, pyrazolopyridine ring in compound **151** and pyrazolopyrimidine in compound **152**. Among of them, compound **150** demonstrated comparable potency to compound **148**. [10] Dihalo- scaffolds are critical starting materials for quick access of these compound for evaluation. (**Figure 56**)

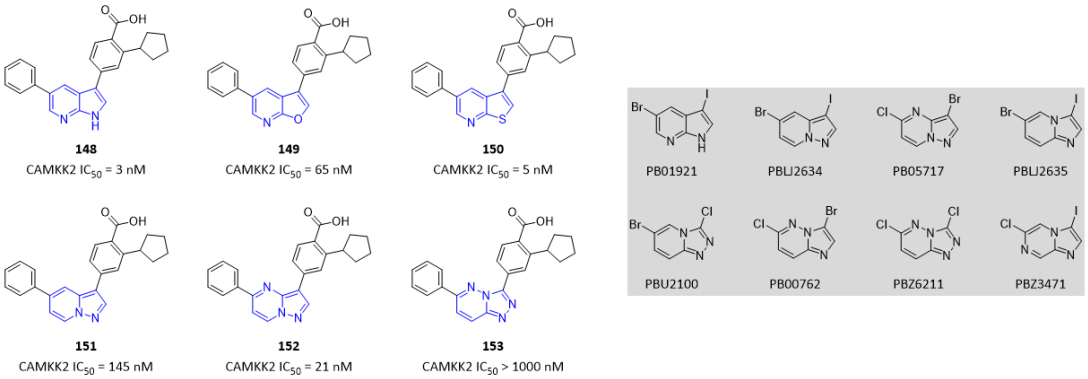

Figure 56. Scaffold hopping identified novel CAMKK2 inhibitors.

To further evaluate fused 5,6-ring structures as CAMKK2 inhibitors, the team switched from 3,5-ring substitutions as depicted in **Figure 56** to 2,4-ring substitutions as depicted in **Figure 57**. All of these compounds, compound **154** with an imidazopyridine core structure, compound **155** with a thienopyrimidine core structure and compound **156** with a reverse thienopyrimidine core structure, exhibited high CAMKK2 inhibition. Besides three scaffold used by the team in **Figure 57**, there are several other novel scaffolds which could potentially be employed by the team to further explore SAR and SPR.

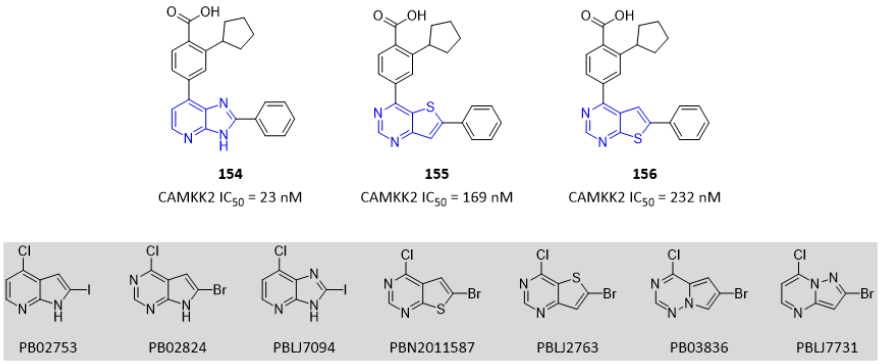

Figure 57. Scaffold hopping identified novel CAMKK2 inhibitors.

In order to discover a novel NIK inhibitor which is sufficient for robust *in vivo* evaluation of NIK pharmacology, the team tried several scaffolds with some of them represented in **Figure 58**. Comparing compound **157** and compound **158**, it was found that an additional nitrogen atom in the scaffold of compound **158** increased NIK binding affinity by at least 1500-fold. This observation can be explained by a potential intramolecular hydrogen bond between hydrogen of amide and the nitrogen atom, which lock the molecule in a binding favorable conformation as shown in the X-ray structure of an analogue. [11] Elimination of nitrogen from pyridine ring of compound **158** generated compound **159** with NIK binding affinity kept. It can be concluded that the nitrogen atom has no interaction with NIK protein, and this why compound **160** and **161** also displayed high NIK binding affinity.

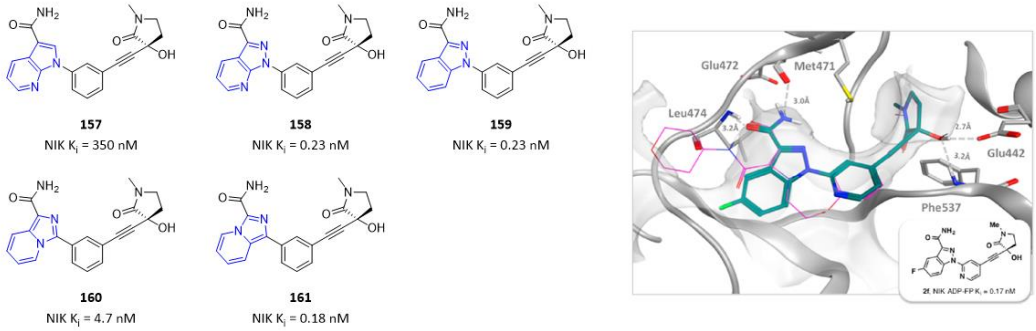

Figure 58. Scaffold hopping identified novel highly potent NIK inhibitors. (PDB code: 6G4Z)

Ester scaffold building blocks listed in **Figure 59** are essential starting materials for quick access of designed molecules in above medicinal campaign. Furthermore, building blocks which can offer C-C linking are of great value for medicinal chemists.

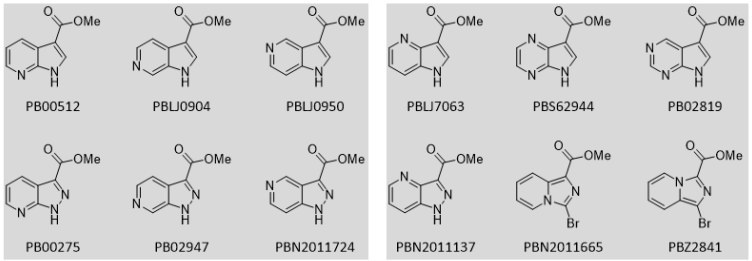

Figure 59. Ester building blocks used in scaffold hopping in above discovery campaign

In order to discover GCS inhibitors with a novel scaffold, the team screened internal library and identified a hit compound **163** which was structurally distinct from previously reported GCS inhibitors. Hit-to lead optimization was started by scaffold hopping. Isoindolinone core in compound **162** displayed improved potency, but reduced significantly solubility due to enhanced

lipophilicity. In order to circumvent solubility issue, a nitrogen atom was introduced at another position on the core to reduce lipophilicity. The introduction of a nitrogen atom in compound **164** and in compound **165** was well tolerated in terms of GCS inhibitory potency, and compound **165** demonstrated significantly improved solubility. Further optimization based on compound **165** by exploration of substitutions on two phenyl rings generated lead compound **166**. Although compound **166** showed encouraging *in vivo* activity, oral administration of compound **166** at 30 or 100 mg/kg daily for 3 days reduced body weight. The team hypothesized that the observed body weight reduction was due to off-target inhibition of SERT with IC_{50} = 310 nM. SERT inhibition was reportedly induces hypophagia and reduces body weight in rats. With this in mind, the team continued to optimize by scaffold hopping, and found that pyridazin-3-one core in compound **167** exhibited comparable potency while decreasing efflux ratio which potentially benefit BBB-penetration. Removing fluorine from compound **167** generated compound **168** which exhibited 3-fold increased GCS potency (**Figure 60**). Compound **168** has no SERT inhibitory activity with IC_{50} > 10 uM, and showed no reduction in body weight at any dose examined, indicating that compound **168** has a safer off-target toxicology profile than compound **166**. [12]

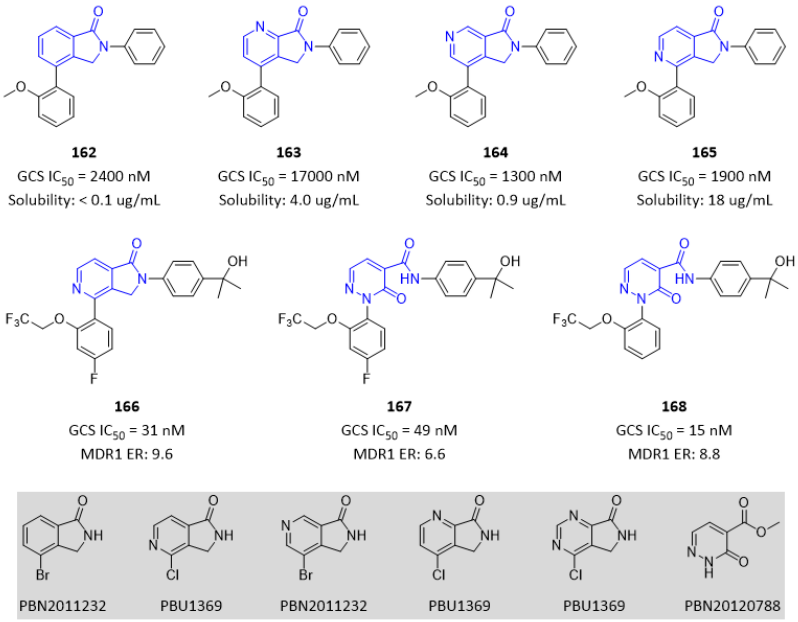

Figure 60. Scaffold hopping resolved toxicity issue.

A new chemical series, triazolo[4,5-b]pyridine, has been identified as an inhibitor of PIM-1 by scaffold hopping strategy. Comparing compound **169** with an imidazolo[1,2-b]pyridazine core and compound **170** with a triazolo[4,5-b]pyridine core, it was extremely interesting that FLT-3 selective compound **169** was changed to PIM-1/2/3 selective compound **170** by a simple scaffold hopping. The same trend was also observed in pair compound **171** and **172**. [13] It was notable that compound **171** was discontinued from phase 1 clinical trials, because it failed to demonstrate a safe therapeutic window (**Figure 61**).

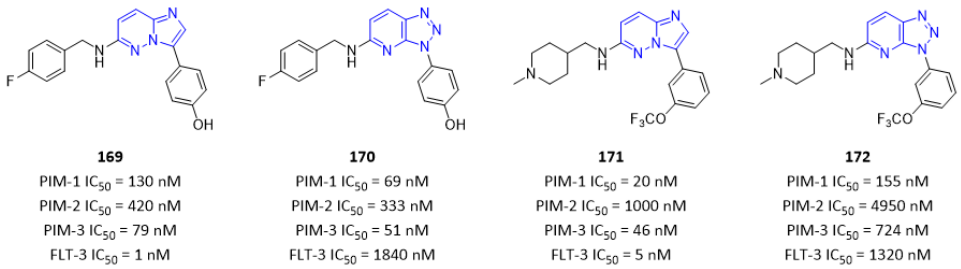

Figure 61. Scaffold hopping resolved selectivity issue.

In order to discover small-molecule inhibitors of TNFalpha, the team examined naphthyridine scaffolds as alternatives to the quinolone core in compound **173**. Compound **174** with a 1,5-naphthyridine core showed comparable potency, while compound **175** with a 1,7-naphthyridine core and compound **176** with a 1,8-naphthyridine core lost potency a lot. This observation can be explained due to better pi-stacking capability of 1,5-naphthyridine in compound **174** with Tyr135. In addition, in the case of 1,7-naphthyridine in compound **175** and 1,8-naphthyridine in compound **176**, the additional nitrogen atom is placed in a hydrophobic environment leading to a significant desolvation penalty, thereby lowering the potency in the binding assay (**Figure 62**). [14]

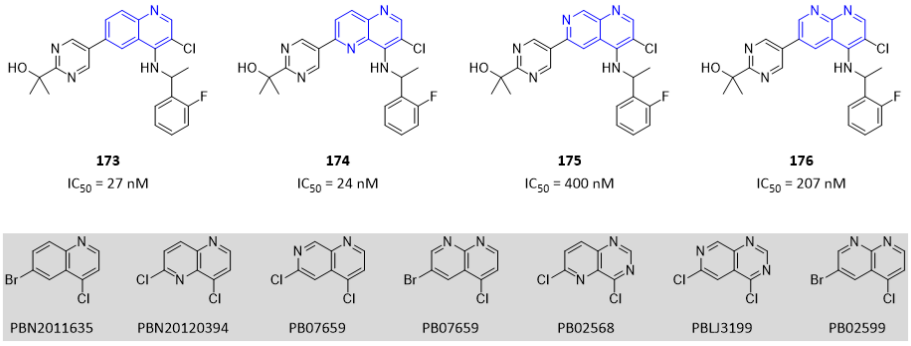

Figure 62. Naphthyridine scaffolds impacted potency in different way.

References

[1] Ye Hu; *et al.* Recent advances in scaffold hopping. *J. Med. Chem.* **2017**, *60*, 1238-1246.
[2] Pan, Z. Y.; *et al.* Discovery of selective irreversible inhibitors for Bruton's tyrosine kinase. *Chem. Med. Chem.* **2007**, *2*, 58-61.
[3] Byrd, J. C.; *et al.* Acalabrutinib (ACP-196) in relapsed chronic lymphocytic leukemia. *N. Engl. J. Med.* **2016**, *374*, 323-332.
[4] Walter, H. S.; *et al.* A phase I clinical trial of the selective BTK inhibitor ONO/GS-4059 in relapsed and refractory mature B-cell malignancies. *Blood* **2016**, *127*, 411-419.
[5] Goel S.; *et al.* Targeting CDK4 and CDK6 in cancer. *Nat. Rev. Cancer* **2022**, *22*, 356-372.
[6] Peter L. Toogood; *et al.* Discovery of a potent and selective inhibitor of cyclin-dependent kinase 4/6. *J. Med. Chem.* **2005**, *48*, 2388-2406.
[7] Richard A. Ward; *et al.* Discovery of a potent and selective oral inhibitor of ERK1/2 (AZD0364) that is efficacious in both monotherapy and combination therapy in models of nonsmall cell lung cancer (NSCLC). *J. Med. Chem.* **2019**, *62*, 11004-11018.
[8] Christel J. Menet; *et al.* Triazolopyridines as selective JAK1 inhibitors: from hit identification to GLPG0634. *J. Med. Chem.* **2014**, *57*, 9323-9342.

[9] Yu Zhang; *et al.* Contributions of intestine and liver to the absorption and disposition of FZJ-003, a selective JAK1 inhibitor with structure modification of filgotinib. *Eur. J. Pharm. Sci.* **2022**, *175*, 106211-106219.
[10] Benjamin J. Eduful; *et al.* Hinge binder scaffold hopping identifies potent calcium/calmodulin-dependent protein kinase 2 (CAMKK2) inhibitor chemotypes. *J. Med. Chem.* **2021**, *64*, 10849-10877.
[11] Nicole Blaquiere; *et al.* Scaffold-hopping approach to discover potent, selective, and efficacious inhibitors of NF-kB inducing kinase. *J. Med. Chem.* **2018**, *61*, 6801-6813.
[12] Yuta Tanaka; *et al.* Discovery of brain-penetrant glucosylceramide synthase inhibitors with a novel pharmacophore. *J. Med. Chem.* **2022**, *65*, 4270-4290.
[13] Gustavo Saluste; *et al.* Fragment-hopping-based discovery of a novel chemical series of proto-oncogene PIM-1 kinase inhibitors. *PLoS One* **2012**, *7*, e45964.
[14] Hai-yun Xiao; *et al.* Biologic-like in vivo efficacy with small molecule inhibitors of TNFa identified using scaffold hopping and structure-based drug design approaches. *J. Med. Chem.* **2020**, *63*, 15050-15071.

Magic Methyl Group in Medicinal Chemistry

The methyl group is one of the most commonly occurring carbon fragments in small-molecule drugs. This simple alkyl fragment appears in more than 60% of the top-selling drugs, highlighting the importance of the simple methyl group as a very useful structural modification in the rational design of bioactive compounds and drugs. One reason the methyl group is so popular in drug discovery is the magic methyl effect: a rare but welcome phenomenon where installation of a methyl group can increase potency, improve selectivity, increase solubility, increase permeability, decrease metabolism or address toxicity issues. [1-2] In **Figure 63**, several drug molecules and clinical candidate molecules which contain methyl group are listed. For each case, methyl group(s) were incorporated into molecules with different purposes which will be introduced below. [3-10]

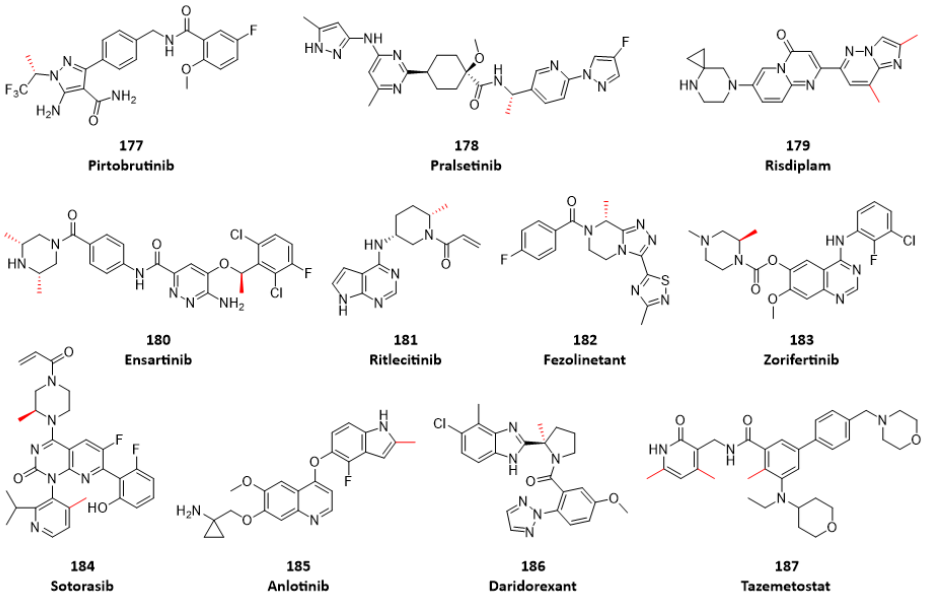

Figure 63. Representative drug and clinical candidate molecules containing methyl group

Compound **188** was identified as a potent and selective JAK3 covalent inhibitor. However, it suffers

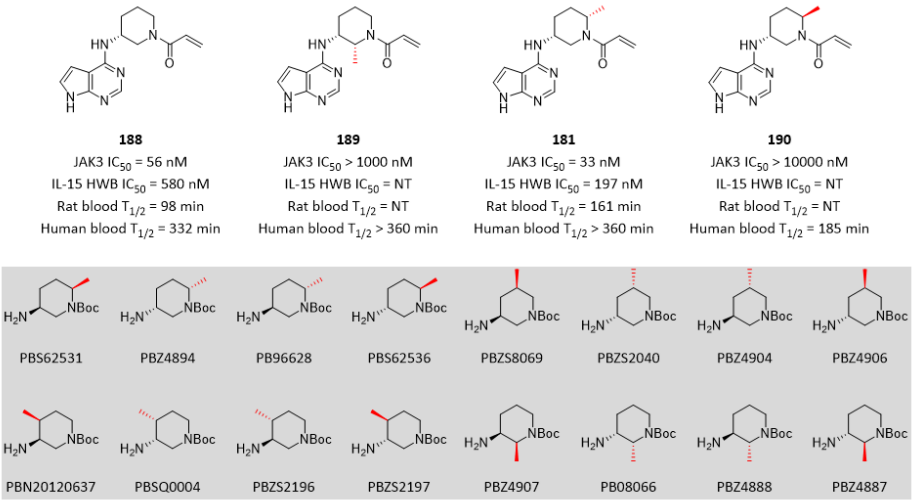

Figure 64. Methyl groups on piperidine ring modulated whole blood stability.

from moderate to poor PK in rat despite very reasonable oxidative stability as judged by liver microsomes. It was speculated that glutathione-S-transferase (GST) mediated glutathione (GSH)

addition to the acrylamide is accounted for this discrepancy. Stability of compound **188** in rat blood is only 98 min, which explained the observed poor PK profile in rat. In order to decrease GSH addition, the team attempted to inhibit chemical reactivity by adding substituents to the acrylamide, as steric hinder around the electrophile should reduce the ability of GST to catalyze GSH addition. As depicted in **Figure 64**, methyl groups were introduced on piperidine ring adjacent to acrylamide in compound **189**, **181** and **190**. Compound **189** lost potency completely due to a potential steric clash between the methyl group with protein side chain residue Leu956 in the ATP pocket. The hypothesis was realized in compound **181** which displayed comparable enzymatic potency and 3-fold higher HWB potency which was consistent with higher stability in HWB assay. It was interesting to found that chirality of the methyl group impacted potency significantly, as seen in compound **190** where the methyl group had an opposite chirality, resulting in potency loss completely. [9-10]

In the course of discovery of a potent, oral and CNS-penetrant EGFR inhibitor, compound **191** was identified as a promising lead with high potency, idea efflux ratio and excellent BBB-penetration. Metabolite identification of compound **191** suggested that the piperazine oxidation was the main metabolic pathway. With this in mind, the team incorporated methyl groups into molecules to block metabolic sites on piperazine ring in compound **192**, **193**, **194** and **195**. Potency of compound **192** and **193** was decreased by 3-4 fold, and PK profile was worse than compound **191**. Although efflux ratio of compound **192** and **193** was decreased, plasma-to-brain ratio was not affected. Both compound **194** and **195** kept comparable potency, while compound **194** had improved both blood exposure and brain exposure comparing to compound **191** and **195** (**Figure 65**). [6] The promising data package of compound **194** (**AZD3759**, **Zorifertinib**) which has excellent central nervous system penetration, strongly supported its selection as a clinical candidate for development for the treatment of brain metastases. Methyl piperazine building blocks (**Figure 66**) played crucial roles in quick access of designed molecules and systematic SAR and SPR studies.

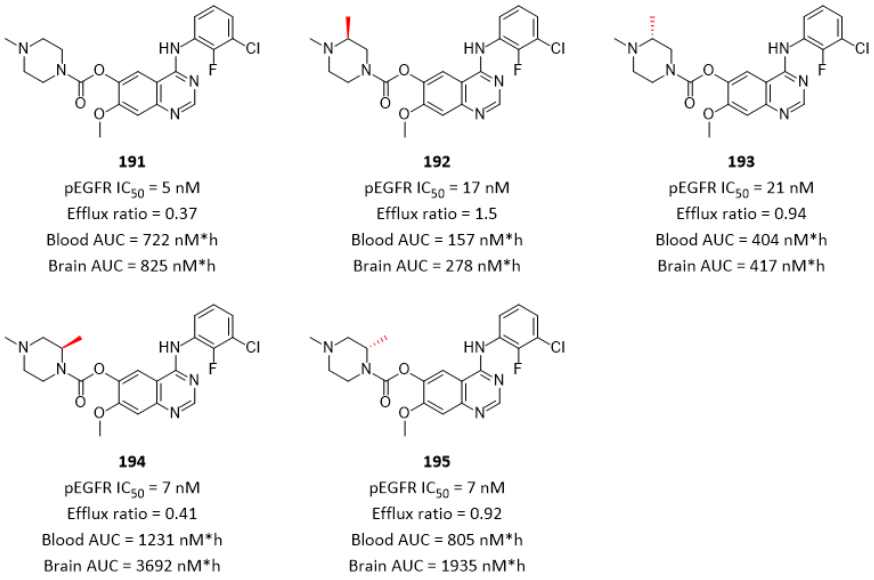

Figure 65. Methyl groups on piperazine modulated potency and PK profile of EGFR inhibitor.

As shown in **Figure 63**, there was also a chiral methyl group on piperazine ring in compound **184** (**AMG510**, **Sotorasib**). In the course of discovery of **Sotorasib**, compound **196** was identified as one of promising hit compounds with high potency. However, PK profile was poor (data not shown). Employing similar strategy in the discovery of compound **194** (**AZD3759**, **Zorifertinib**) described above, a chiral methyl group was incorporated on piperazine ring in compound **197** which had increased cellular potency by 3-fold while oral bioavailability was improved (F = 12%). Comparing

compound **198** and **199**, the same trend was observed with cellular potency and oral bioavailability both increased, especially oral bioavailability, in compound **199** bearing a chiral methyl group on piperazine ring (**Figure 66**). [8]

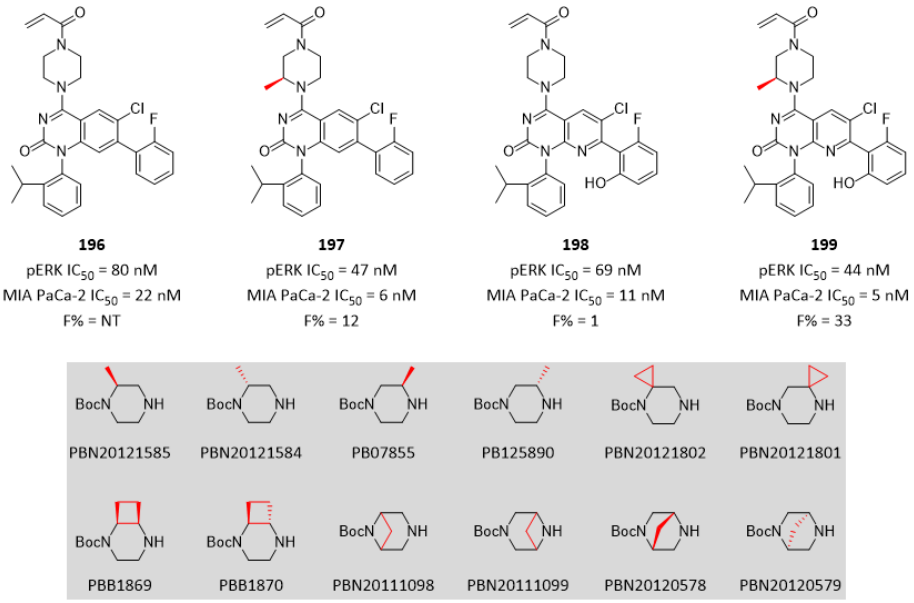

Figure 66. Methyl groups on piperazine ring modulated potency and PK profile of KARS G12C inhibitors.

In the course of discovery of a potent and reversible dual orexin receptor antagonist, compound 200 was identified as a promising lead. As shown in **Figure 66**, both trans-methyl groups in compound **201** and **202** increased potency significantly by 96-fold for OX1R, 145-fold for OX2R and

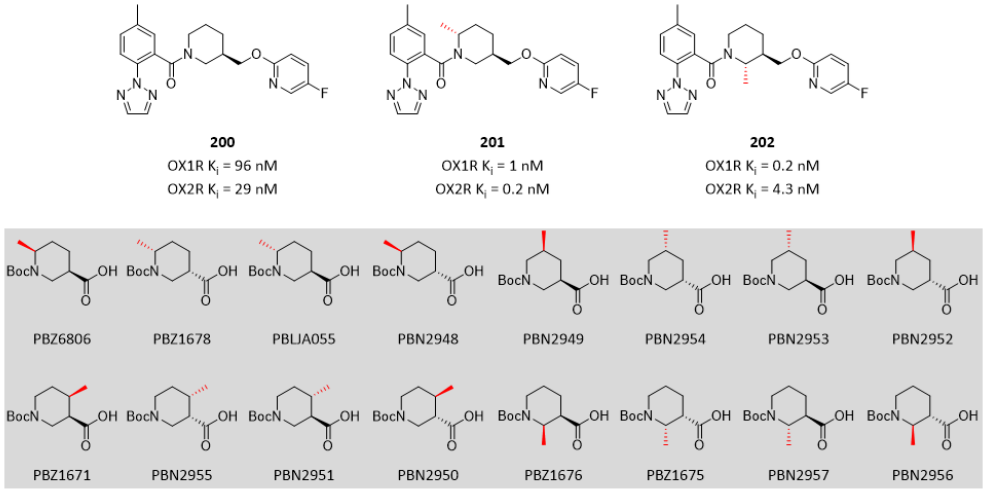

Figure 67. Methyl groups on piperidine ring increased potency.

by 505-fold for OX1R, 6-fold for OX2R respectively. This observation is consistent with structural hypothesis that alpha-methylation favors the trans-diaxially substituted piperidine with axial orientation for the 3-CH_2OAr group (**Figure 67**). [11]

Metabolic studies confirmed that the pyrrolidine moiety in compound **203** was exceptionally metabolically active. Therefore, the initial structural modification was to introduce substituents onto the pyrrolidine to directly block its metabolism. Considering the profile that small substituents on pyrrolidine were preferred for potency against PI3Kdelta along with the availability of starting material, a small (S)-methyl group was introduced onto the pyrrolidine ring in compound **204**.

Compound **204** gave improved clearance compared to compound **203**, which demonstrated the rationality of modification strategy. Moreover, the results of this comparison are reminiscent of the methyl effect in the molecular modification strategy, also known as the magic methyl effect, where the addition of a methyl group in place of hydrogen leads to a dramatic improvement in metabolic stability due to an additional labile group for CYP oxidation (**Figure 68**). [12]

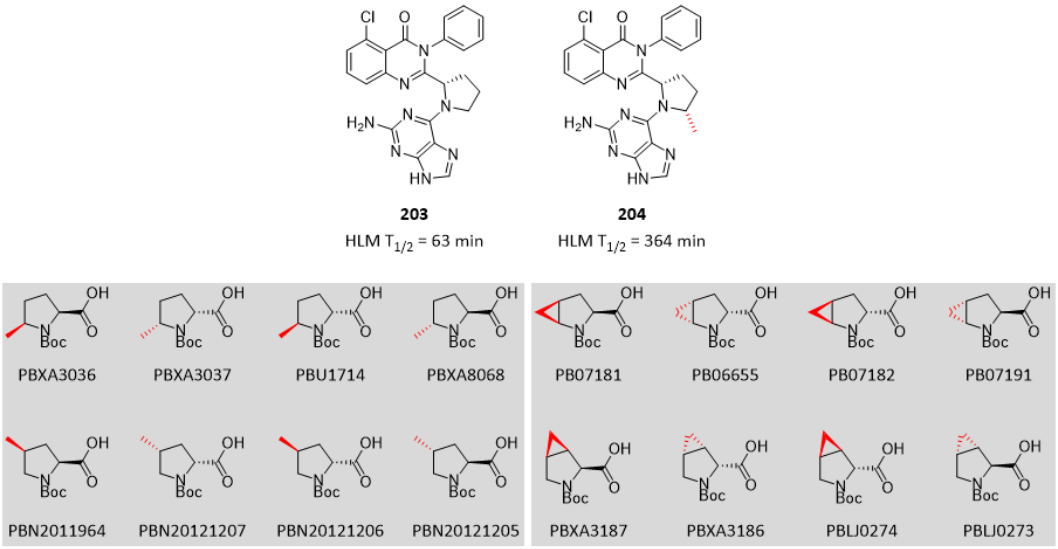

Figure 68. A methyl group increased metabolic stability significantly.

Modifying the initial lead compound **205** to compound **207** resulted in 0.6 log improvement in bioactivity due to the (R)-Me substitution on piperazine ring. Moreover, a stereochemical SAR on piperazine ring methyl substitution was evident with the order of antagonist bioactivity as follows: (R)-Me (compound **207**) > des-Me (compound **205**) > (S)-Me (compound **206**), with compound **207** 10-fold more potent than compound **206** (**Figure 69**). [4-5]

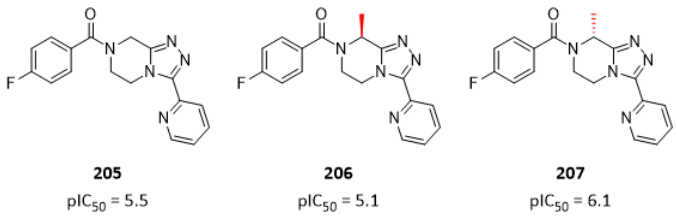

Figure 69. Methyl groups with opposite chirality impacted potency in different way.

In the course of discovery of DNA-PK inhibitors, compound **208** was identified as a promise lead. Ortho- methyl group was added into compound **209** and compound **210**, which confirmed a significant boost in potency for compound **210**, but not compound **209**. Comparing compound **211** and compound **212**, the same trend was observed. The ortho- methyl group on the aniline group gave at least 10-fold increase in biochemical potency while maintaining LogD, thus could be described as “magic methyl”. This striking increase in potency suggests that, in addition to making an effective lipophilic interaction in the hydrophobic pocket consisting of Tyr3791, Leu3806 and Ile3940, the methyl group may also confer a beneficial conformational effect, by favoring a bioactive conformation where there is a twist between the aromatic amine and the purinone core (**Figure 70**). [13]

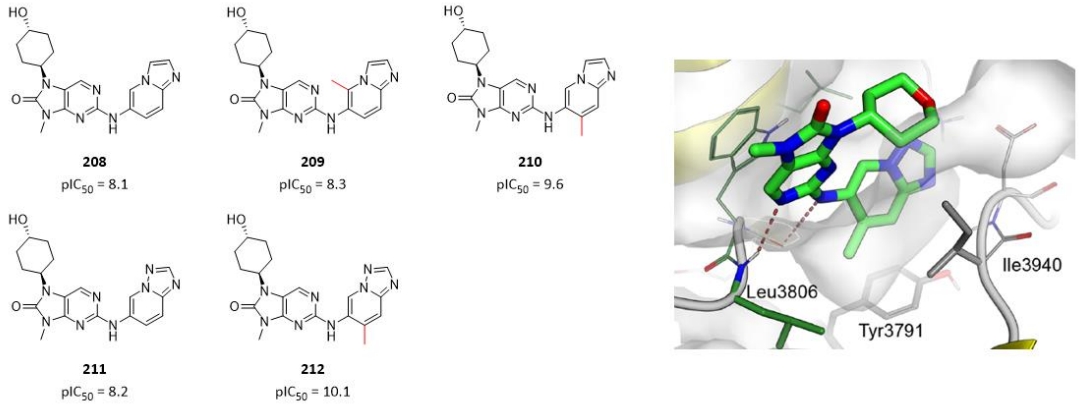

Figure 70. Methyl groups on aniline increased potency by at least 10-fold. (PDB code: 6T3C)

In the course of discovery of **Tazemetostat**, "magic methyl" effect was observed as shown in **Figure 71**. Comparing compound **213** and compound **214**, lacking a methyl group for compound **213**, the activity is significantly decreased by 190-fold. The "magic methyl" effect was magnified in comparison of compound **215** and compound **216**, with a significant 1400-fold difference observed. The steric-directing effect of the methyl group is not limited to the amide moiety, but also has a profound effect on the adjacent aniline substituent. This optimized substitution pattern led to a significant potency breakthrough allowing the team to drive potency to the threshold of single-digit nanomolar levels for the first time (**Figure 71**). Further optimization of compound 216 led to discovery of **Tazemetostat** which was approved as a first EZH2 inhibitor. [7]

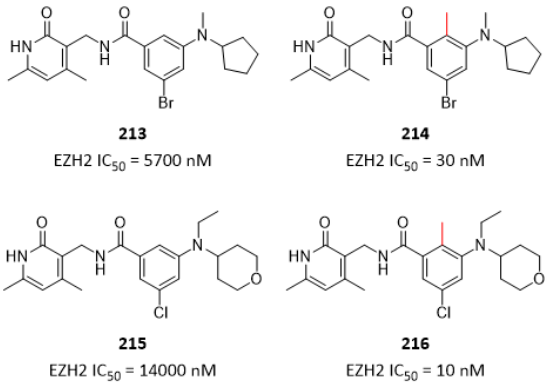

Figure 71. Methyl groups on phenyl ring increased potency significantly.

It is extremely supportive if medicinal chemists have convenient access of diverse building blocks containing methyl groups which could potentially exert "magic methyl" effect to impact positively activity, selectivity or properties of molecules (**Figure 72**). As mentioned in section "**Dihedral Angle in Medicinal Chemistry**", modulating dihedral angle through steric hinder between methyl group and adjacent moieties can influence a lot of properties of molecules.

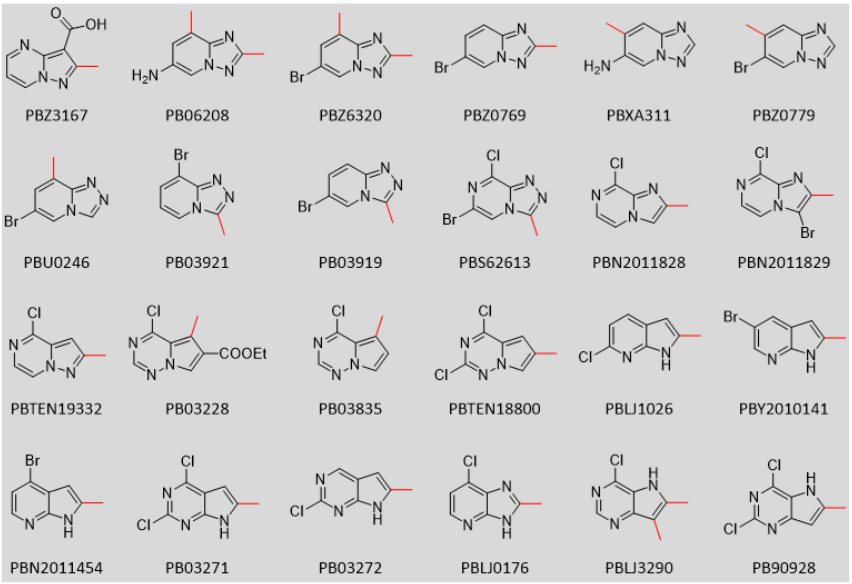

Figure 72. Scaffold building blocks containing a methyl group with potential "magic methyl" effect

With lead compound **217** in hand, the team turned their attention to modification of the benzylic linker, based on hypothesis that the incorporation of an appropriate substituent on the alpha-position of the benzylic amine liker could constrain the linker to adopt the bioactive conformation and, therefore reduce the entropic cost of ligand binding. Moreover, methyl substitution could also block the metabolism at the alpha-position of then benzylic group. Based on modeling, the methyl-substituted linker with (S) stereochemistry is more conformationally constrained, and the bioactive conformation is still near an energy minimum. This extra constraint on the linker conformation would be expected to modestly improve the potency. By contrast, the (R) enantiomer is expected to be substantially less potent, because it has an energy minimum that does not resemble the bioactive conformation observed in the crystal structure. For the (R) enantiomer to adopt the bioactive conformation, there would be a steric clash between the methyl group and the carbonyl oxygen of the quinolinone. As X-ray structure of analogue suggests that the protein can only accommodate a small group in the vicinity of the benzylic group linker, the team selected and investigated small methyl group in compound **218** and compound **219**. As depicted in **Figure 73**, the (S)-methyl group in compound **219** was favored, whereas the (R)-methyl group in compound **218** lost most of its activity. Compound 219 also demonstrated excellent metabolic stability in human microsome and improved solubility. Taken together, the data showed that an (S)-methyl-substituted benzylic linker in compound **219** was the optimal choice, not only providing very potent inhibitory activity against the R132H and R132C mutants but also conferring excellent metabolic stability and enhanced solubility (**Figure 73**). [14] In this context, amine building blocks containing chiral methyl groups at alpha-position of benzylic linker played critical roles in quick synthesis of designed molecules.

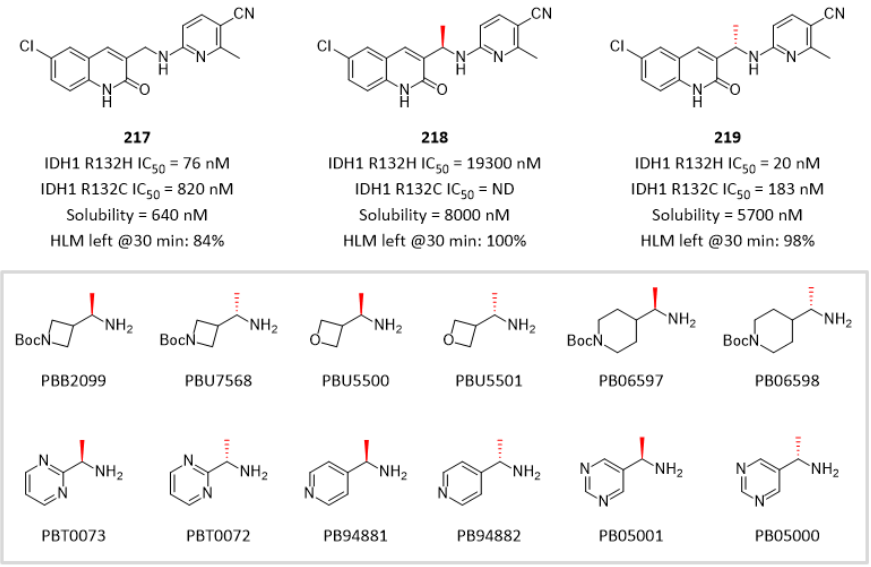

Figure 73. Methyl group at alpha-benzylic position impacted activity and properties.

References

[1] Eliezer J. Barreiro; *et al.* The methylation effect in medicinal chemistry. *Chem. Rev.* **2011**, *111*, 5215-5246.

[2] Heike Schonherr; *et al.* Profound methyl effects in drug discovery and a call for new C-H methylation reactions. *Angew. Chem. Int. Ed.* **2013**, *52*, 2-14.

[3] Hasane Ratni; *et al.* Discovery of Risdiplam, a selective survival of motor neuron-2 (SMN2) gene splicing modifier for the treatment of spinal muscular atrophy (SMA). *J. Med. Chem.* **2018**, *61*, 6501-6517.

[4] Hamid R. Hoveyda; *et al.* Optimization of novel antagonists to the Neurokinin-3 receptor for the treatment of sex-hormone disorders (part II). *ACS Med. Chem. Lett.* **2015**, *6*, 736-740.

[5] Hamid R. Hoveyda; *et al.* Discovery and optimization of novel antagonists to the human Neurokinin-3 receptor for the treatment of sex-hormone disorders (part I). *J. Med. Chem.* **2015**, *58*, 3060-3082.

[6] Qingbei Zeng; *et al.* Discovery and evaluation of clinical candidate AZD3759, a potent, oral active, central nervous system-penetrant, epidermal growth factor receptor tyrosine kinase inhibitor. *J. Med. Chem.* **2015**, *58*, 8200-8215.

[7] Kevin W. Kuntz; *et al.* The importance of being Me: magic methyls, methyltransferase inhibitors, and the discovery of Tazemetostat. *J. Med. Chem.* **2016**, *59*, 1556-1564.

[8] Brian A. Lanman; *et al.* Discovery of a covalent inhibitor of $KRAS^{G12C}$ (AMG 510) for the treatment of solid tumors. *J. Med. Chem.* **2020**, *63*, 52-65.

[9] Atli Thorarensen; *et al.* Design of a Janus kinase 3 (JAK3) specific inhibitor 1-((2S,5R)-5-((7H-pyrrolo[2,3-d]pyrimidin-4-yl)amino)-2-methylpiperidin-1-yl)prop-2-en-1-one (PF-06651600) allowing for the interrogation of JAK3 signaling in humans. *J. Med. Chem.* **2017**, *60*, 1971-1993.

[10] Jean-Baptiste Telliez; *et al.* Discovery of a JAK3-selective inhibitor: functional differentiation of JAK3-selective inhibition over pan-JAK or JAK1-selective inhibition. *ACS Chem. Biol.* **2016**, *11*, 3442-3451.

[11] Paul J. Coleman; *et al.* Discovery of [(2R,5R)-5-{[(5-fluoropyridin-2-yl)oxy]methyl}-2-methylpiperidin-1-yl][5-metyl-2-(pyrimidin-2-yl)phenyl]methanone (MK-6096): a dual orexin receptor antagonist with potent sleep-promoting properties. *ChemMedChem* **2012**, *7*, 415-424.

[12] Kongjun Liu; *et al.* Discovery, optimization, and evaluation of quinazolinone derivatives with novel linkers as orally efficacious phosphoinositide-3-kinase delta inhibitors of treatment of inflammatory diseases. *J. Med. Chem.* **2021**, *64*, 8951-8970.
[13] Frederick W. Goldberg; *et al.* The discovery of 7-methyl-2-[(7-methyl[1,2,4]triazolo[1,5-a]pyridine-6-yl)amino]-9-(tetrahydro-2H-pyran-4-yl)-7,9-dihydro-8H-purin-8-one (AZD7648), a potent and selective DNA-dependent protein kinase (DNA-PK) inhibitor. *J. Med. Chem.* **2020**, *63*, 3461-3471.
[14] Jian Lin; *et al.* Discovery and optimization of quinolinone derivatives as potent, selective, and orally bioavailable mutant isocitrate dehydrogenase 1 (mIDH1) inhibitors. *J. Med. Chem.* **2019**, *62*, 6575-6596.

Acetylene Group in Medicinal Chemistry

The acetylene group has been broadly exploited in drug discovery and development. It has become recognized as a privileged structural feature for targeting a wide range of therapeutic targets. Furthermore, a terminal alkyne is frequently introduced in chemical biology probes as a click handle to identify molecular targets and to assess target engagement. The continued widespread popularity of acetylene group in medicinal chemistry is also apparent from the number of examples of approved drugs and those in clinical evaluations that containing a terminal or internal acetylene group (**Figure 74**). There are lots of roles that acetylene group can play in drug discovery, including potency enhancement by a complementary fit into a protein binding pocket, reactive warhead for irreversible inhibition of a target protein, nonpolar linear rigid spacer which can direct pharmacophore appendages in a favorable geometry, bioisostere of a wide range of functional groups such as cyano, chloro, iodo, carboxamide, phenyl, and modulation of drug metabolism pharmacokinetic (DMPK) profile. [1]

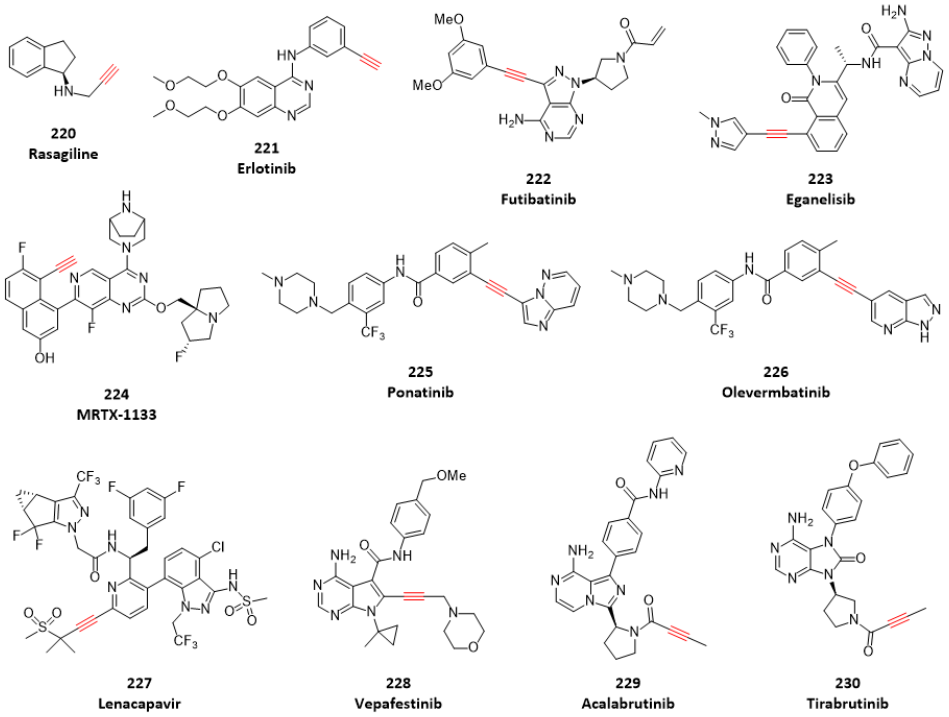

Figure 74. Drug and clinical candidate molecules containing terminal or internal alkyne.

In the medicinal campaign of discovery KRAS G12D inhibitor MRTX-1133, it was recognized that a conserved water molecule makes hydrogen bond interactions with both Gly10 and Thr58, and the team envisioned that a hydrogen bond donor from the 8-position of the naphthyl group in compound **231** might further stabilize this hydrogen bond network (**Figure 75**). The initial attempt with the introduction of a canonical hydroxyl group was unsuccessful. A careful examination suggested that an 8-ethynyl substitution would not only fill the hydrophobic space well, but also engage the conserved water molecule via a non-classical hydrogen bond. Indeed, comparing compound **231** and compound **232**, the 8-ethynyl group in the latter increased potency by 120-fold than the former. The same trend was also observed in paired compound **233** and compound **234** with the latter at 13-fold more potent than the former due to 8-ethynyl group. The X-ray structure of compound **234** in KRAS G12D revealed that the 8-ethynyl group is nicely positioned in a

hydrophobic pocket formed with Val9, Thr58, Phe78, Met72, Tyr96 and Ile100. The conserved water molecule is hydrogen-bonded to two hydrogen bond acceptors, the hydroxyl from Thr58 and the carbonyl oxygen from Gly10, and two hydrogen bond donors, the alkynyl proton of the ligand and NH of Gly10, forming a well-organized hydrogen bond network. [2]

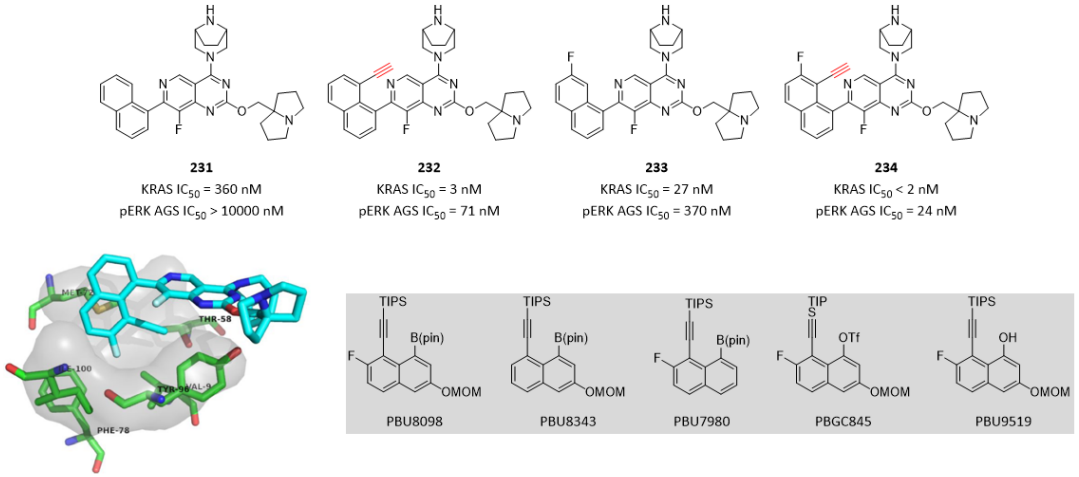

Figure 75. Alkynyl group increased potency and occupied a hydrophobic pocket. (PDB code: 7RT5)

In the course of discovery of clinical candidate **Eganelisib** (**223**) as a selective PI3Kgamma inhibitor, the team evaluated C8-substitution on compound **235** to access a nonconserved region within PI3K

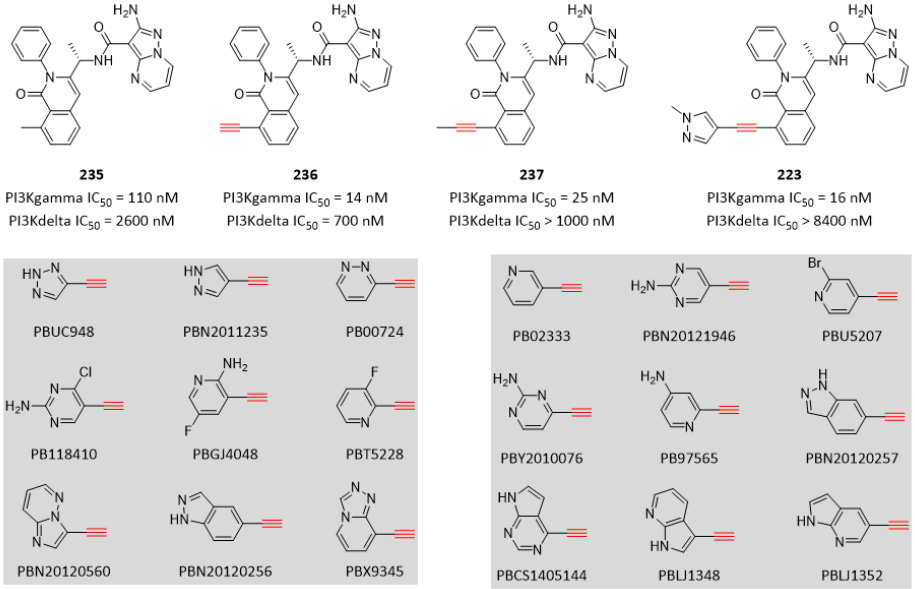

Figure 76. Alkyne group improved potency and selectivity.

Family with the aim of improving the PI3Kgamma potency and selectivity. It was found that small C8 substitution such as methyl in compound **235** did not have a profound impact on PI3Kgamma potency or selectivity. Interestingly, 8-alkyne substitutions in compound **236** and compound **237** unexpectedly provided modest improvements in potency for PI3Kgamma over compound **235**. Importantly, methyl alkyne analogue **237** also demonstrated weaker activity against PI3Kdelta compared to compound **236**, and thus compound **237** had at least 40-fold selectivity for PI3Kgamma over PI3Kdelta, suggesting that the alkyne substitution makes significant nonfavorable interactions with PI3Kdelta at the nonconserved residues adjacent to the specificity pocket (Lys802 for PI3Kgamma *vs* Thr750 for PI3Kdelta) as does the aminopyrazolopyrimidine at the hinge binding

region (**Figure 76**). Further optimization based on compound **237** successfully led to clinical candidate **Eganelisib** (**223**). [3]

In the course of discovery of **Futibatinib** (**222**) as the first covalent FGFR kinase inhibitor, the team found that alkyne compound **222**, which has an extended straight molecule, showed an approximately 200-fold increase in FGFR2 kinase inhibitory activity over compound **238** and flexible compound **239**. As an initial SAR study, only alkyne compound **222** achieved a single-digit nanomolar inhibitory activity on FGFR2. These data suggest that the straight-chain alkyne could correctly place the 3,5-dimethoxybenzene ring in the well-known unique hydrophobic pocket of FGFR (**Figure 77**). [4-5]

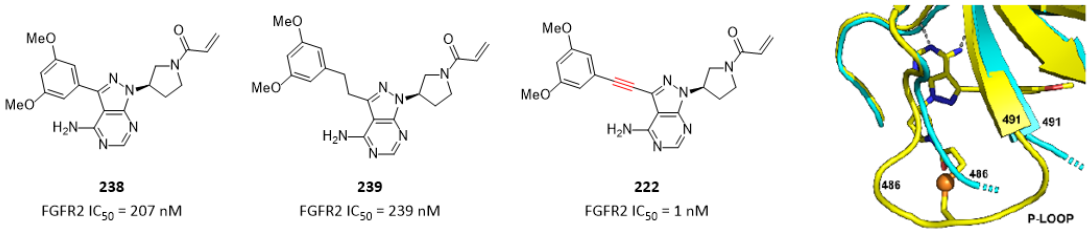

Figure 77. Alkyne group oriented 3,5-dimethoxybenzene to a hydrophobic pocket. (PDB code: 6MZQ)

The X-ray crystal structure of TACE inhibitor **240** bound to the active site of TACE indicated the binding of the phenyl-phenyl system in a shallow hydrophobic S1 pocket surrounded by residues Val314 and Leu350. Although compound **240** showed potent inhibition of TACE, it exhibited poor activity in the presence of human whole blood. Therefore, the team optimized this lead further with the assumption that internal aryl ring can be replaced with an isosteric acetylene while still projecting the terminal aryl ring in a similar orientation as observed in biaryl series. These efforts culminated in the discovery of compound **241** with comparable TACE inhibitory activity and improved activity in a human whole blood assay (**Figure 78**). [6-7]

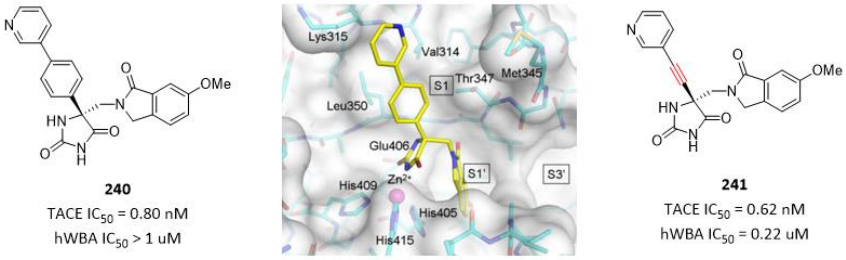

Figure 78. Alkyne group as bioisostere of phenyl ring improved hWBA. (PDB code: 3LEA)

Addition of a propargyl substituent onto the piperazine ring in compound **242** led to the discovery of compound **243** with at least 20-fold increased potency (**Figure 79**). [8] Installation of an acetylene group at the C5-position of 2-cyanopyrrolidine moiety in compound **244** to obtain compound **245** with a considerable improvement in DDP-4 selectivity over DPP-8 and DPP-9 (**Figure 79**). [9] Building blocks containing terminal or internal acetylene groups play critical roles in quick exploration of SAR and SPR.

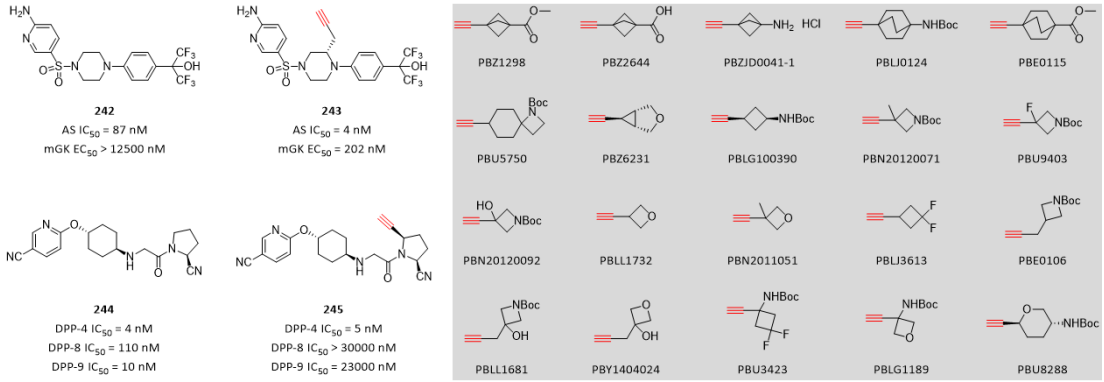

Figure 78. Two case stories where acetylene group increased potency.

References

[1] Tanaji T. Talele; Acetylene group, friend or foe in medicinal chemistry. *J. Med. Chem.* **2020**, *63*, 5625-5663.
[2] Xiaolun Wang; *et al.* Identification of MRTX1133, a noncovalent, potent, and selective KRAS G12D inhibitor. *J. Med. Chem.* **2022**, *65*, 3123-3133.
[3] Catherine A. Evans; *et al.* Discovery of a selective phosphoinositide-3-kinase (PI3K)-gamma inhibitor (IPI-549) as an immuno-oncology clinical candidate. *ACS Med. Chem. Lett.* **2016**, *7*, 862-867.
[4] Satoru Ito; *et al.* Discovery of Futibatinib: the first covalent FGFR kinase inhibitor in clinical use. *ACS Med. Chem. Lett.* **2023**, *14*, 396-404.
[5] Maria Kalyukina; *et al.* TAS-120 cancer target binding; defining reactivity and revealing the first FGFR1 irreversible structure. *ChemMedChem* **2019**, *14*, 494-500.
[6] Wensheng Yu; *et al.* Biaryl substituted hydantoin compounds as TACE inhibitors. *Bioorg. Med. Chem. Lett.* **2010**, *20*, 5286-5289.
[7] Vinay M. Girijavallabhan; *et al.* Novel TNF-alpha converting enzyme (TACE) inhibitors as potential treatment for inflammatory diseases. *Bioorg. Med. Chem. Lett.* **2010**, *20*, 7283-7287.
[8] St. Jean; *et al.* Small molecule disruptors of the glucokinase-glucokinase regulatory protein interaction: 2. Leveraging structure-based drug design to identify analogues with improved pharmacokinetic profiles. *J. Med. Chem.* **2014**, *57*, 325-338.
[9] Madar D. J.; *et al.* Discovery of 2-[4-{{2-(2S,5R)-2-cyano-5-ethynyl-1-pyrrolidinyl}-2-oxoethyl}amino]-4-methyl-1-piperidinyl]-4-pyridinecarboxylic acid (ABT-279): a very potent, selective, effective, and well-tolerated inhibitor of dipeptidyl peptidase-IV, useful for the treatment of diabetes. *J. Med. Chem.* **2006**, *49*, 6416-6420.

Spirocyclic Rings in Medicinal Chemistry

Spirocyclic scaffolds are the focus of modern drug discovery, as can be observed by the number of publications and contributions to a variety of approved drugs and clinical candidates (**Figure 79**). Studies that endorse the use of scaffolds with high Fsp^3 further enhance the interest in novel and established spirocycles. The increase in rigidity resulting from spirocyclization can influence important factors, such as potency and selectivity. Furthermore, significant improvements in physicochemical properties, such as logD, lipophilicity and solubility, as well as ADMET properties, are achievable, ultimately leading to improved pharmacokinetic profiles. However, their full potential has not yet been exploited. Methodologies for the systematic exploration of the spirocyclic chemical space are still in their infancy. Taken together, spirocycle is a powerful tool for medicinal chemists with further potential to advance in the near future. As expected, it is often associated with increased synthetic effort, resulting from an increased number of synthetic steps and stereocenters or unusual reaction procedures. Recent advances in the development of synthetic methods and efficient supplies of diverse **spirocyclic building blocks** have allowed the introduction and increase in spirocycles in medicinal chemistry in the past decade. [1-5]

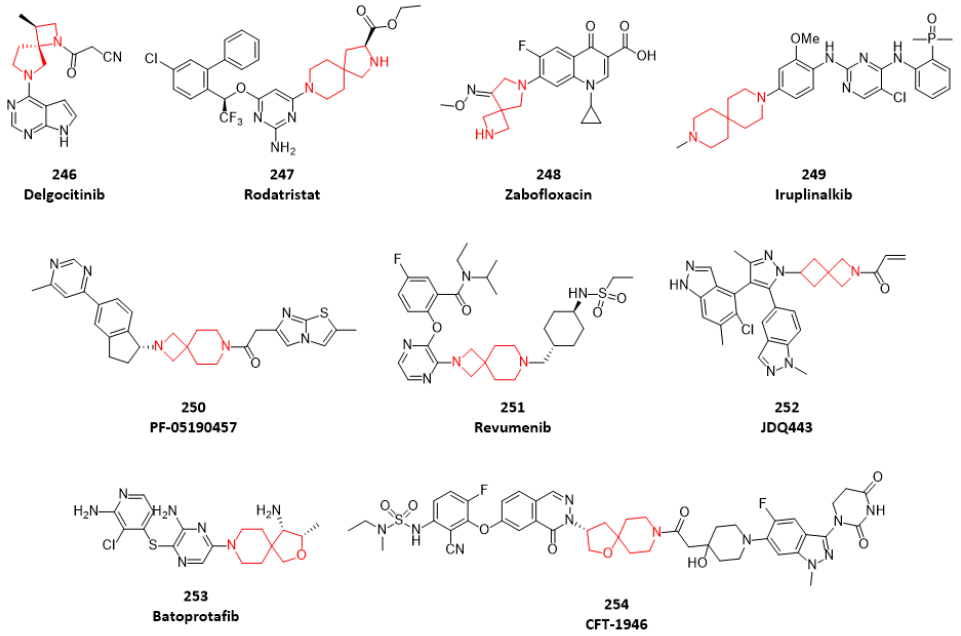

Figure 79. Spirocycles contribute to a variety of approved drugs and clinical candidates.

In order to develop a new series of JAK inhibitors, the team replaced piperidine in approved drug **Tofacitinib** (**255**) with a variety of spirocyclic diamine rings as depicted in **Figure 80**. Replacing pyrrolidine ring in the spirocycle of compound **256** with azetidine ring in the spirocycle of compound **257** increased both cellular potency and metabolic stability in both human and monkey microsomes. Adding a methyl group on azetidine ring in the spirocycle of compound **258** further increased JAK3 inhibition by 4-5 fold compared to compound **257**. It was explained that the methyl group occupied the lipophilic pocket neighborhood the JAK3 hinge region. However, cellular potency was not increased proportionally, and metabolic stability was decreased. Adding two fluorine atoms on azetidine ring in the spirocycle of compound **259** kept comparable potency, but metabolic stability was decreased slightly. Replacing piperidine rings in the spirocycle of compound **259** and **258** with pyrrolidine rings generated compound **260** and **246** (**Delgocitinib**) respectively.

Compound **246** (**Delgocitinib**) has both excellent potency and metabolic stabilities, and was moved into clinical trials. [6]

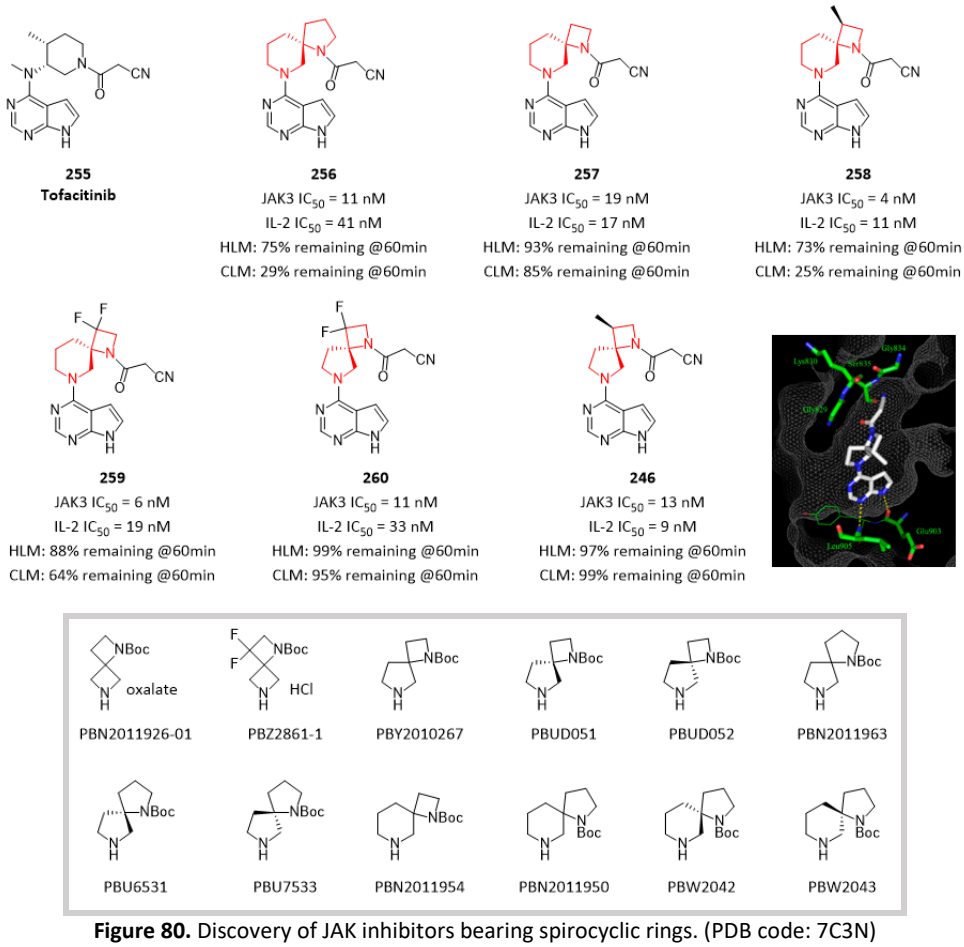

Figure 80. Discovery of JAK inhibitors bearing spirocyclic rings. (PDB code: 7C3N)

In the course of discovery of a novel covalent KRAS G12C inhibitor **JDQ443**, compound **261** was identified as one promising hit compound. Initial SAR exploration aimed to balance specific reactivity toward KRAS G12C versus intrinsic chemical cysteine reactivity. Several drugs containing an acrylamide electrophile have been approved by FDA and demonstrate favorable safety profiles. However, excessively reactive electrophiles increase the risk of nonspecific covalent protein adduct formation and the potential for immune-mediated adverse reactions. Intrinsic chemical reactivity was determined by assessing the disappearance of the compound in the presence of 5 mM reduced GSH, representing a concentration close to intracellular conditions. Compound **261** exhibited modest inhibition of ERK phosphorylation with IC_{50} = 500 nM, but suffered low stability in GSH addition assay with $T_{1/2}$ = 20 min. In compound **262**, replacement of the eletron-withdrawing fluorine atom with a methyl group decreased inhibition of ERK phosphorylation, but stability in GSH addition assay was increased remarkably with $T_{1/2}$ = 107 min. To further optimize the linker geometry and, most importantly, to reduce the intrinsic chemical reactivity of the acrylamide, the team evaluated aliphatic linkers as phenyl replacement. A spiro-azetidine moiety, as in compound **263**, turned out to be the best suitable linker identified. For compound **263**, intrinsic chemical reactivity was significantly lowered with $T_{1/2}$ = 241 min, while reasonable inhibition of ERK phosphorylation was maintained with IC_{50} = 3900 nM. Therefore, the spirocyclic moiety was kept constant in subsequent SAR studies. Further exploration based on compound **263** led to identification of clinical candidate **JDQ443** (**Figure 81**). [7]

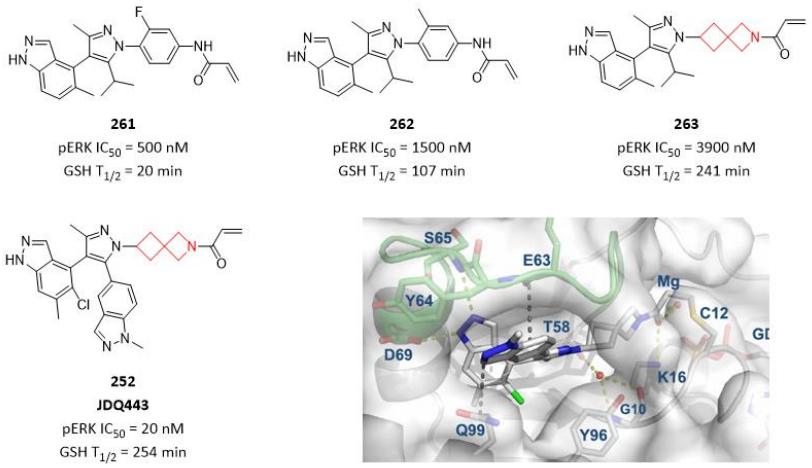

Figure 81. Spriocyclic rings were used in discovery of JDQ443. (PDB code: 7R0M)

In the course of discovery of LSD1 inhibitors, the team examined the impact of linker between the two amines on the activity and ADME properties. A variety of spirocyclic rings were surveyed as linkers in compound **265** (4,6-spiro) and compound **266** (4,4-spiro). Compared to compound **264** (piperidine), two types of spirocyclic rings in compound **265** (4,6-spiro) and compound **266** (4,4-spiro) both increased microsome stabilities in various species, while keeping comparable potency (**Figure 82**). [8]

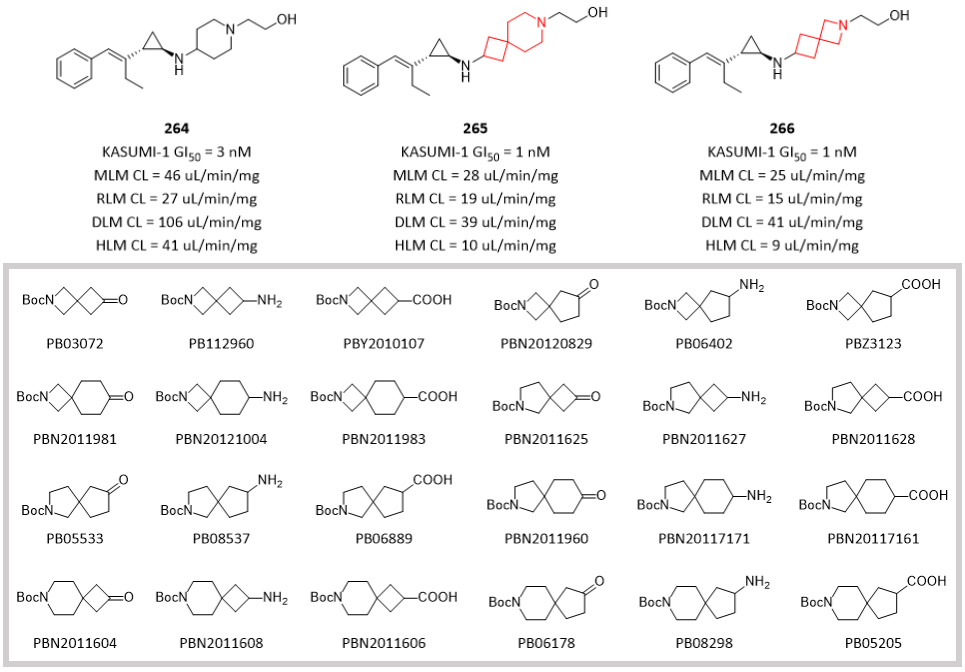

Figure 82. Spriocyclic rings increased microsome stabilities in various species.

Drug repurposing is an economical and effective approach to discover new drugs. Starting from a HTS of an epigenetic inhibitor library, clinical candidate **Quisinostat** (**267**) was revealed as a potent antimalarial agent. However, the extensive inhibitory activity of **Quisinostat** on HDACs results in serious safety issues, which limits its further development as an antimalarial drug. Hence, **Quisinostat** (**267**) was treated as the lead compound for medicinal chemistry investigation to find new chemical entities with good antimalarial efficacy and adequate safety. A conformational restriction and homologues strategy was adopted by replacing the 4-aminomethylpiperidine moiety with a 2,6-diazaspiro[3.4]octane moiety to give compound **268**. As expected, the antimalarial

activity of compound **268** was preserved, and a cell viability assay confirmed that the cytotoxicity of compound **268** indeed decreased considerably with 159-fold and 336-fold safety index (SI) compared with that of **Quisinostat** (**267**). Further optimization by introducing a cyano group on indole ring generated compound **269** with higher antimalarial activity and higher safety index (SI) (**Figure 83**). [9]

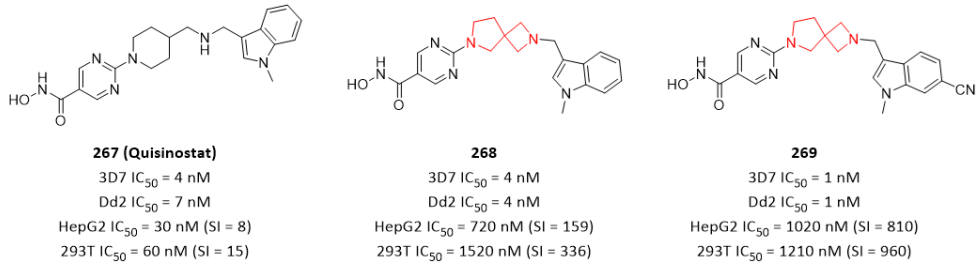

Figure 83. Spirocyclic ring increased safety index.

In order to reduce DNA damage and cytotoxicity of **Olaparib** (**270**), the team examined the pharmacological consequences of replacing the piperazine core in **Olaparib** (**270**) with a variety of diazaspiro systems, in hopes of developing a noncytotoxicity congener of the FDA-approved drug. This work afforded best-in-class compound **271** with a 4,4-spirocyclic ring, an **Olaparib** congener with nanomolar PARP-1 affinity and poor DNA damaging properties, which can be explored as a potential therapeutic for inflammation or neurodegeneration applications where cytotoxicity is not desired. Compound **271** inhibits PARP activity in a manner similar to **Olaparib**. However, compared to the FDA approved drug, higher concentration level of compound **271** was required to completely block PAR synthesis. Compound **271** was unable to induce DNA damage at concentrations as high as 10 uM. These data provide strong evidence that compound **271** showed high PARP-1 affinity and good catalytic inhibitory properties without DNA damaging properties. Compound **272** with a 6,6-spirocyclic ring also reduced DNA damaging and cytotoxicity, but PARP-1 affinity was also decreased by 7-fold compared with **Olaparib** (**270**) (**Figure 84**). [10]

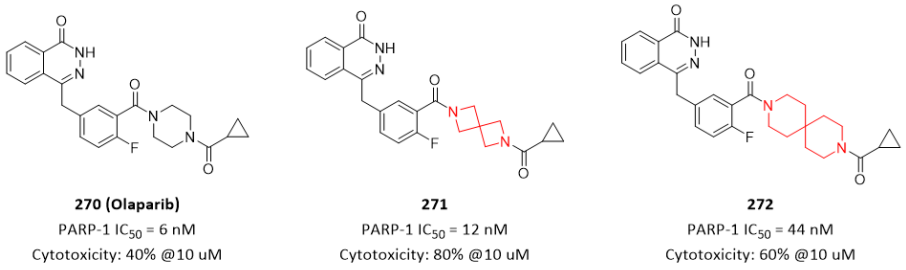

Figure 84. Spirocyclic rings reduced DNA damage and cytotoxicity of Olaparib.

In order to discover highly selective dopamine D3 receptor (D3R) antagonists, the team examined a series of diazaspiro alkane cores as depicted in compound **274**-**279**. Compound **273** was a potent D3R antagonist, but selectivity against D2R was modest with SI = 40. Replacing piperazine in compound **273** with various spirocyclic rings in compound **274**-**279** impacted potency and selectivity in a remarkable way. Among of them, 5,5-spirocyclic ring in compound **276**, 6,5-spirocyclic ring in compound **278**, and 6,6-spirocyclic ring in compound **279** kept comparable potency while increasing selectivity significantly. Especially, compound **279** exhibited a high potency with D3R Ki = 12 nM and a high selectivity against D2R with SI = 905 (**Figure 85**). [11]

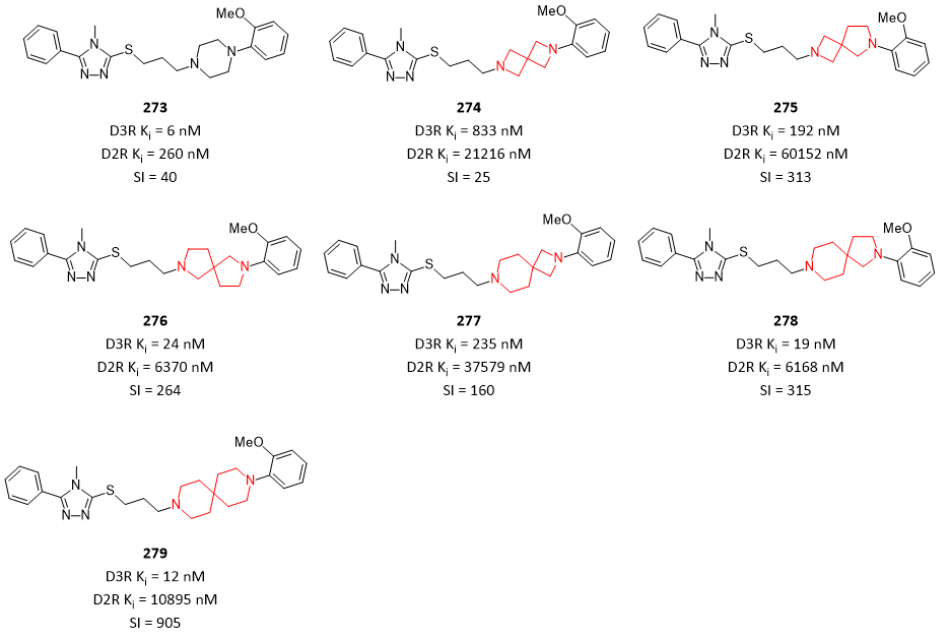

Figure 85. Spirocyclic rings impacted potency and selectivity remarkably.

Two 6,5-spirocyclic rings in compound **281** and **282** respectively, were used as replacements of piperazine ring in compound **280**. Both of them resulted in improvement in the LSD1 inhibitory activity compared with compound **280**. However, compound **281** demonstrated 62% hERG inhibition at 10 uM. It was extremely interesting that compound **282** where nitrogen atom was in a different place had little hERG inhibition with only 10% inhibition at 10 uM (**Figure 86**). [12]

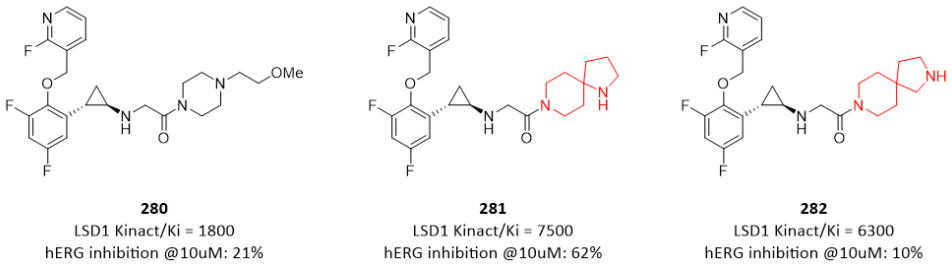

Figure 86. Spirocyclic rings increased potency and decreased hERG inhibition.

As described in above case stories, there is a great variant for diazaspirocylic rings with different ring size, or different orientation resulted from different place of nitrogen atoms. So a diverse library of diazaspirocyclic building blocks is of great value for medicinal chemists to quickly evaluate SAR or SPR in their medicinal programs (**Figure 86**).

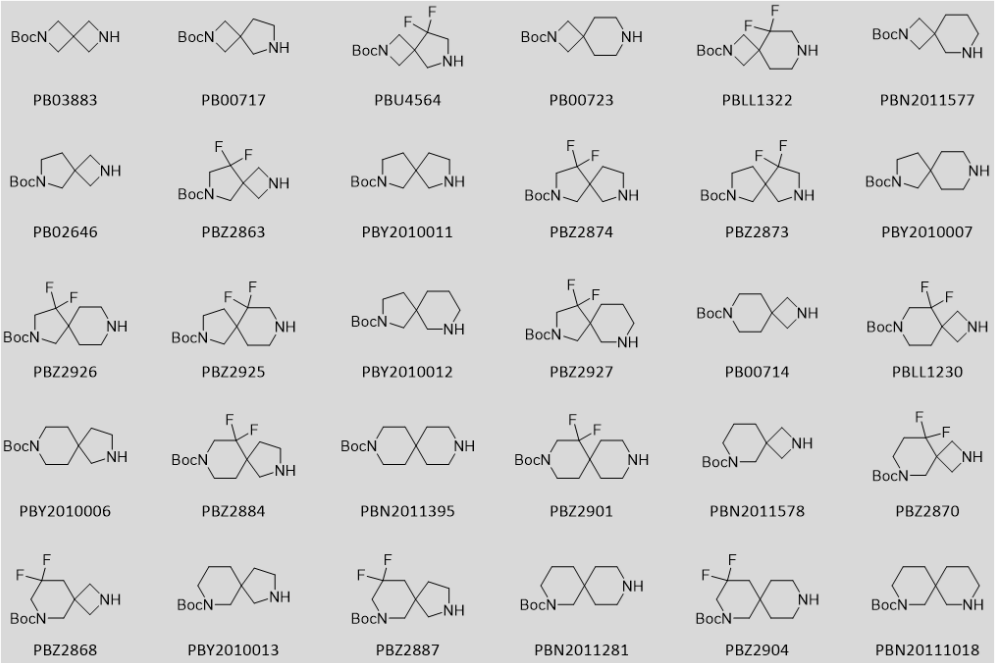

Figure 86. A diverse library of diazaspirocyclic building blocks

Rigidization of the primary amine by a spriocycle has been performed by researcher at Novartis during optimization of SHP2 inhibitors for cancer treatment. Two teams reported on two lead series **283** and **285** respectively, making use of the same spirocyclic rigidization. Both lead series started with compounds bearing a 4-methylpiperidin-4-ylmethanamine moiety, which exhibited very good in vitro potency. However, cellular potency and antiproliferative effects were significantly diminished. X-ray structure analysis revealed that the primary amine group is engaged in three directed hydrogen bond interactions. Rigidization of the aminomethyl moiety could be achieved by introduction of spirocyclic systems carrying the exocyclic amine. All spirocyclic variants, especially compound **284** and compound **286**, exhibited comparable in vitro potency. However, the cellular efficacy was improved by increased lipophilicity (**Figure 87**). [13-14]

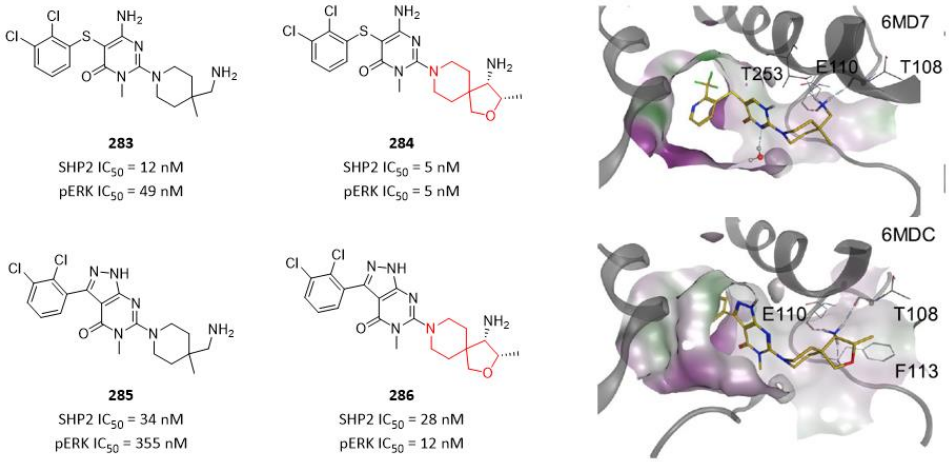

Figure 87. Spirocyclic rings increased potency. (PDB code: 6MD7, 6MDC)

Like diazaspirocyclic rings, oxa-azaspirocyclic rings also have a great variety defined by different ring size, or different orientation resulted from different place of nitrogen and oxygen atoms. So a diverse library of oxa-azaspirocyclic building blocks is of great value for medicinal chemists to

quickly evaluate SAR or SPR in their medicinal programs (**Figure 88**). More interesting case stories where oxa-azaspirocyclic rings have remarkable impacts were discussed below.

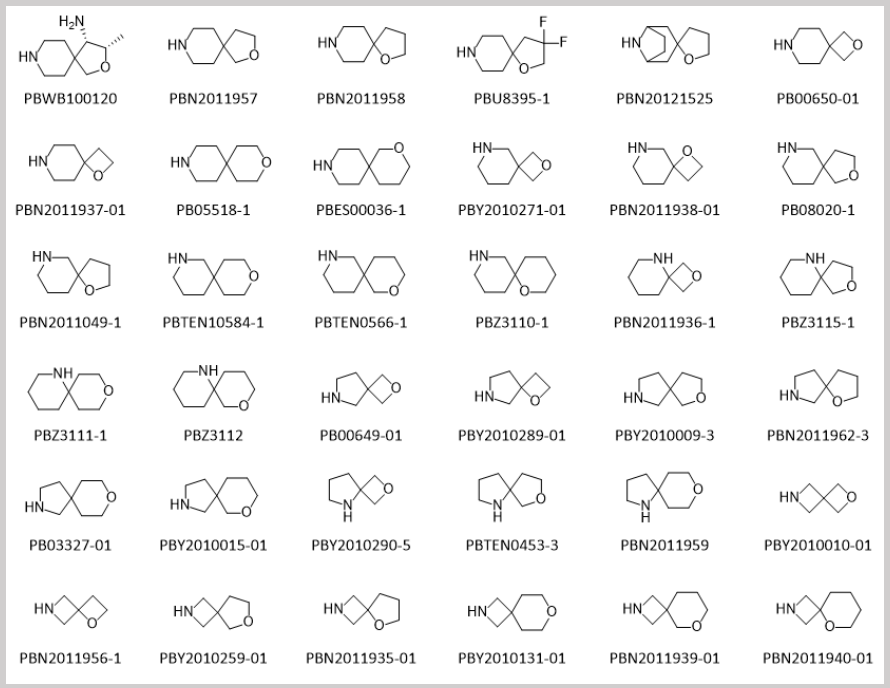

Figure 88. A diverse library of oxa-azaspirocyclic building blocks

In the course of discovery of MCHr1 antagonist **AZD1979** (**290**), the homomorpholine derivative **287** was identified which offered an improvement in properties over morpholines, but metabolic turnover rate was still too high with a high clearance in human microsome. The team's attention was turned to replace homomorpholine ring in compound **281** with some oxa-azaspirocyclic rings in compound **288**, compound **289** and **AZD1979** (**290**). It was interesting to find that compound **288** and compound **290** have decreased clearance in human microsome, while keeping comparable potency (**Figure 89**). [15]

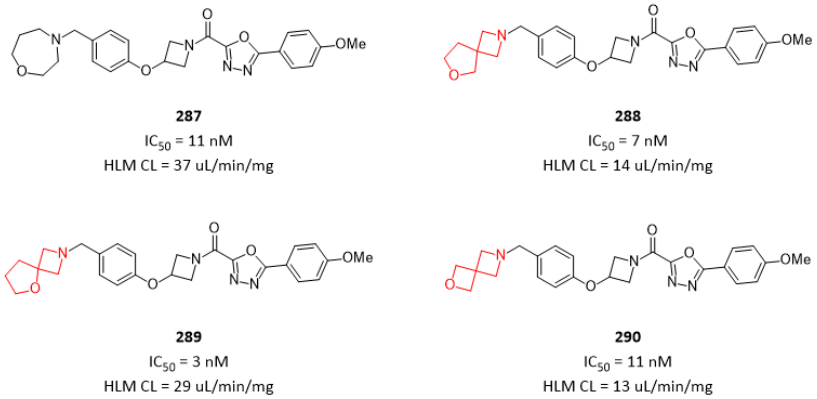

Figure 89. Spirocyclic rings decreased clearance in human microsome.

As the early lead compound, **291** looked very promising. However, particular attention was paid to hERG inhibition which was determined to be 7 uM. The basic lipophilic amine was the most likely contributor to the hERG inhibition. Therefore, strategy focused on reducing basicity of piperidine to decrease hERG inhibition while retaining excellent potency. In compound **292**, a common strategy to introduce fluorine atoms was employed. Indeed, as expected hERG inhibition was decreased remarkably. However, the potency was decreased by 4-fold. In compound **293**, pyrrolidine ring was

used instead of piperidine ring which decreased hERG inhibition while keeping potency. Installation of a sprio-oxetane ring on pyrrolidine in compound **294** decreased hERG inhibition while keeping comparable potency (**Figure 90**). [16]

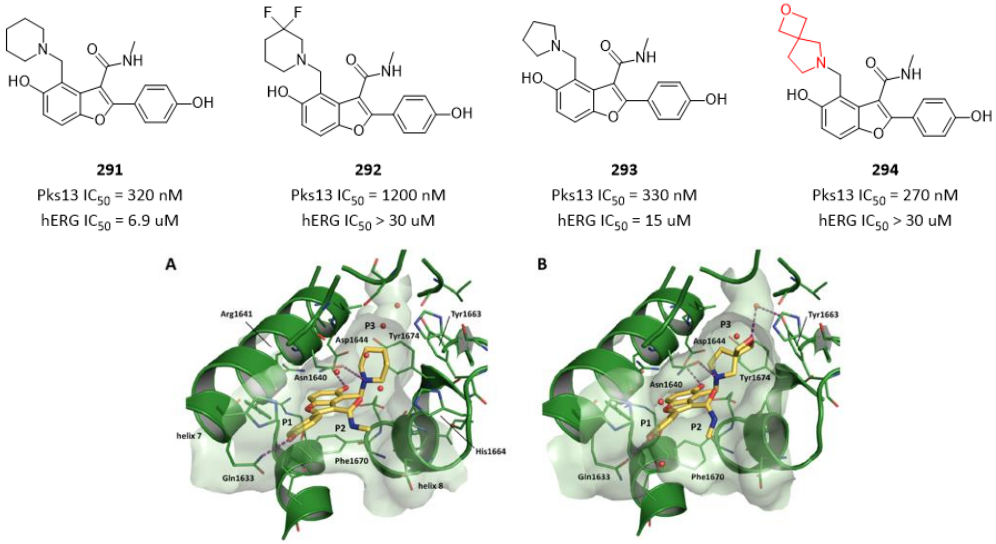

Figure 90. Spirocyclic rings decreased hERG inhibition. (PDB code: 5V3Y and 7M7V)

Compound **295** was identified as a highly potent hDGAT1 inhibitor, but suffered off-target CYP3A4 inhibition with IC_{50} = 6 uM, CYP2C9 inhibition with IC_{50} = 10 uM, and hERG inhibition with IC_{50} = 5 uM. Besides, there was a low solubility issue (< 4 uM) at pH=2 for compound **295**. In order to solve

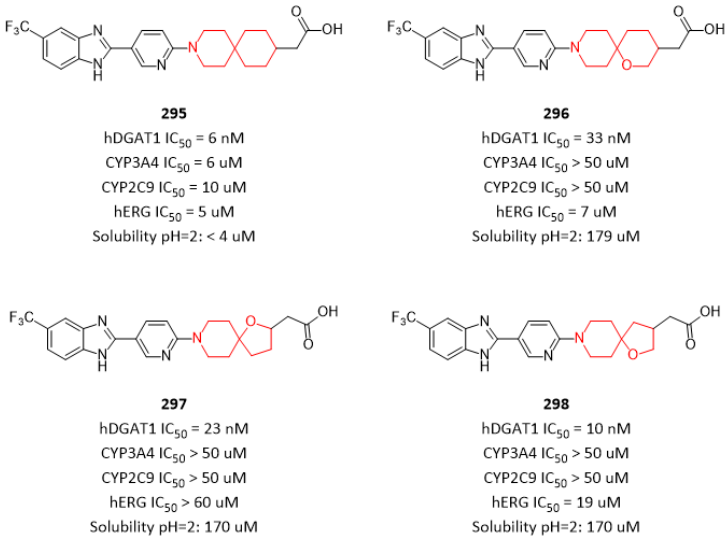

Figure 91. Oxa-spirocyclic rings solved CYP inhibition, hERG inhibition and solubility issues.

these problems, additional oxygen atom was introduced into the spirocyclic ring in compound **296**. Although potency was decreased by 5-fold, compound **296** decreased both CYP3A4 and CYP2C9 inhibition, and increased solubility dramatically. However, hERG inhibition issue was not solved for compound **296**. It was interesting that when ring size was reduced to five-membered tetrahydrofuran in compound **297**, both CYP inhibition and hERG inhibition were not detected, while solubility was increased significantly. Compound **298** also contained a tetrahydrofuran ring, like compound **297**, which decreased both CYP inhibition and hERG inhibition and increased solubility while keeping comparable potency (**Figure 91**). [17]

In many cases, spirocyclic rings brought several issues, such as solubility and metabolic stability, caused by increased number of carbon atoms which made molecule more lipophilic. So, a general strategy is to replace on carbon atom with a polar oxygen atom to balance properties of the whole molecule (**Figure 92**).

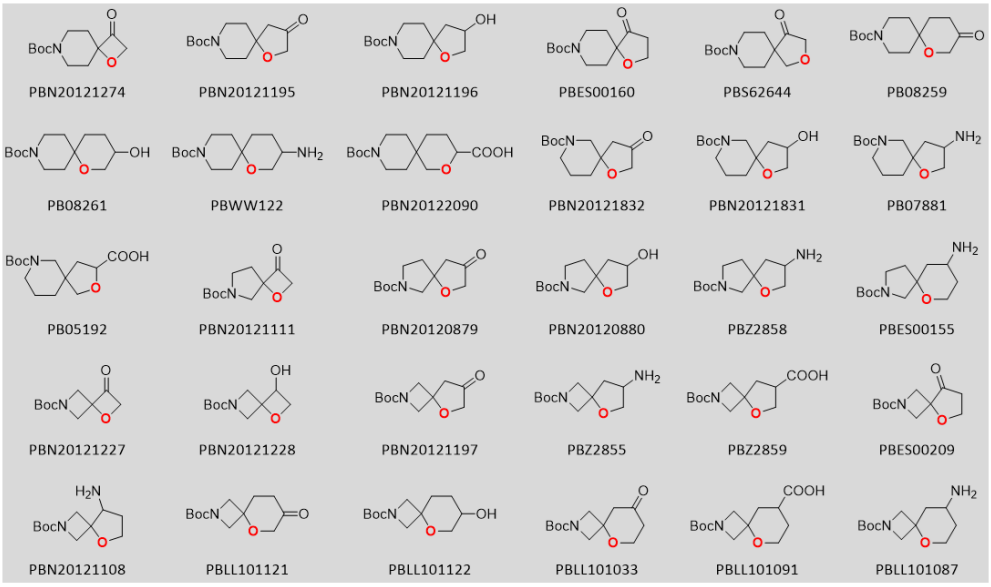

Figure 92. Spirocyclic rings containing a polar oxygen atom in the ring

In order to discover a potent, orally bioavailable small-molecule inhibitor of WNT signaling, the team identified a promising lead compound **299**. With compound **299** in hand, the team decided to further explore the piperidine carboxamide in order to understand the optimal geometry. Although a germinal methyl group in compound **300** decreased potency slightly by 2-fold, it suggested that spirocyclic carboxamides might be tolerated. With this in mind, the spirocyclic ring in compound **301** kept potency, while additional carbonyl in compound **302** resulted in a very potent inhibitor caused by improved hydrogen bond donor ability (**Figure 93**). [18]

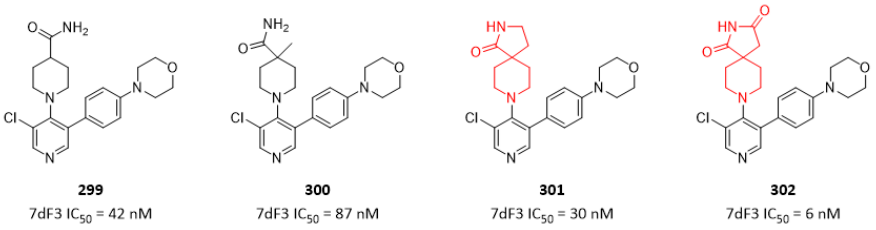

Figure 93. Spirocyclic amide increased potency

Spriocyclic amides were used in discovery of selective dual TYK2/JAK1 inhibitor **303**, where NH of lactam formed a key hydrogen bond with protein. In compound **304**, a selective CYP11B2 inhibitor, oxygen of carbonyl of lactam formed a key hydrogen bond with protein (**Figure 94**). [19-20]

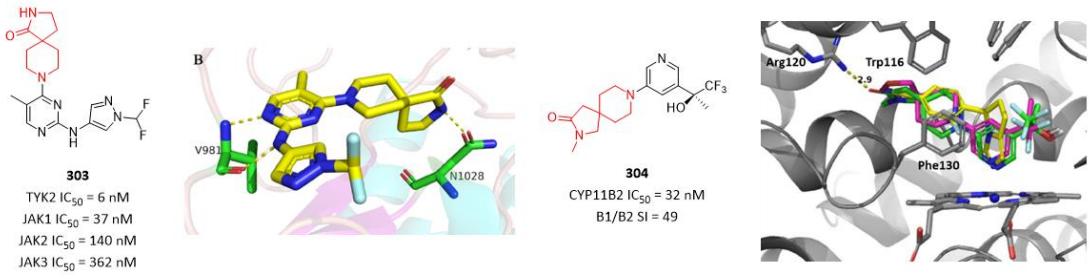

Figure 94. Spirocyclic amides used in discovery of selective inhibitors

In above case stories, spirocyclic amide building blocks played critical roles in quick access of designed molecules and SAR/SPR data (**Figure 95**). Oxygen of carbonyl of lactam can be a strong hydrogen bond acceptor, while NH of lactam can be a strong hydrogen bond donor.

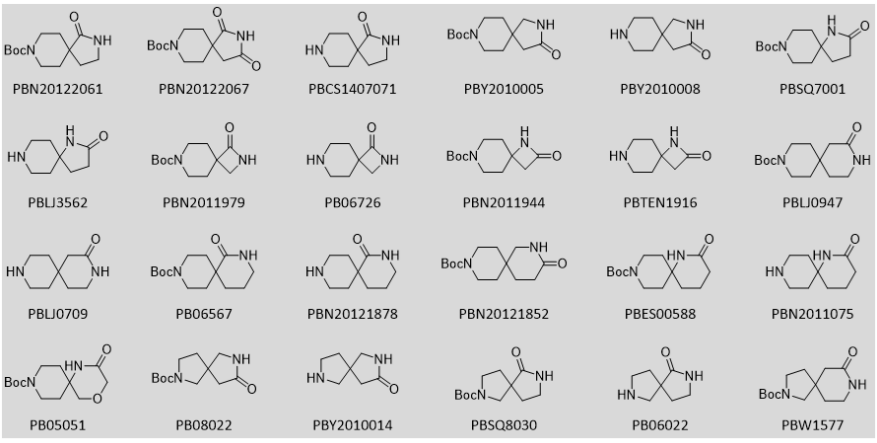

Figure 95. Spirocyclic amide building blocks

In **Figure 96**, a variety of spirocyclic rings were explored in discovery of JAK1 selective inhibitors, and resulted in identification of clinical candidate **306** based on **Filgotinib** (**305**) approved as a JAK1

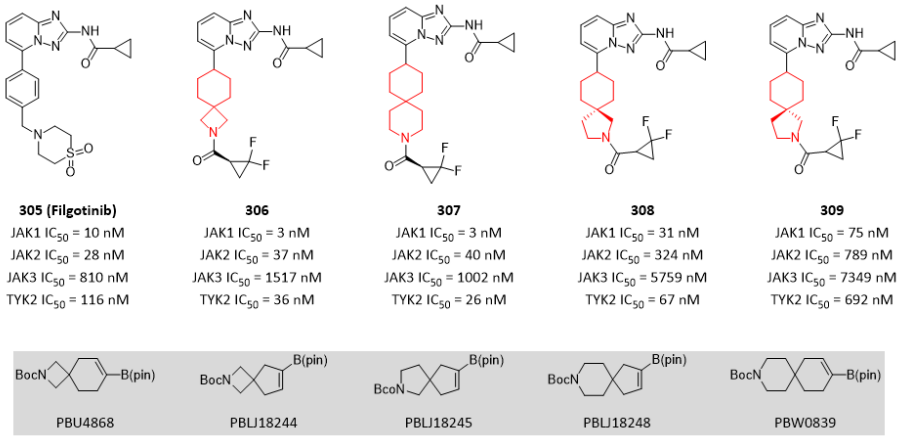

Figure 96. Spirocyclic rings used in discovery of selective JAK1 inhibitors

inhibitor for treatment of autoimmune and inflammatory diseases. Both compound **306** and compound **307** showed excellent JAK1 inhibition and selectivity against other JAK family members. In compound **308** and compound **309**, JAK1 inhibition was decreased by > 10-fold, most likely due to unfavored geometry of the molecule for JAK binding (**Figure 96**). [21]

References

[1] Kerstin Hiesinger; *et al.* Spirocyclic scaffolds in medicinal chemistry. *J. Med. Chem.* **2021**, *64*, 150-183.

[2] Oleksandr O. Grygorenko; *et al.* Bicyclic conformationally restricted diamines. *Chem. Rev.* **2011**, *111*, 5506-5568.

[3] Nicholas A. Meanwell; *et al.* Applications of isosteres of piperazine in the design of biologically active compounds: part 1. *J. Agric. Food Chem.* **2022**, *70*, 10942-10971.

[4] Sebastien L. Degorce; *et al.* Lowering lipophilicity by adding carbon: azaspiroheptanes, a logD lowering twist. *ACS Med. Chem. Lett.* **2019**, *10*, 1198-1204.

[5] Ilaria Proietti Silvestri; *et al.* The growing importance of chirality in 3D chemical space exploration and modern drug discovery approaches for hit-ID. *ACS Med. Chem. Lett.* **2021**, *12*, 1220-1229.
[6] Satoru Noji; *et al.* Discovery of a Janus kinase inhibitor bearing a highly three-dimensional spiro scaffold: JTE-052 (Delgocitinib) as a new dermatological agent to treat inflammatory skin disorders. *J. Med. Chem.* **2020**, *63*, 7163-7185.
[7] Edwige Lorthiois; *et al.* JDQ443, a structurally novel, pyrazole-based, covalent inhibitor of KRAS G12C for the treatment of solid tumors. *J. Med. Chem.* **2022**, *65*, 16173-16203.
[8] Victor S. Gehling; *et al.* Design and synthesis of styrenylcyclopropylamine LSD1 inhibitors. *ACS Med. Chem. Lett.* **2020**, *11*, 1213-1220.
[9] Manjiong Wang; *et al.* Drug repurposing of Quisinostat to discover novel Plasmodium falciparum HDAC1 inhibitors with enhanced triple-stage antimalarial activity and improved safety. *J. Med. Chem.* **2022**, *65*, 4156-4181.
[10] Sean W. Reilly; *et al.* Examination of diazaspiro cores as piperazine bioisosteres in the Olaparib framework shows reduced DNA damage and cytotoxicity. *J. Med. Chem.* **2018**, *61*, 5367-5379.
[11] Sean W. Reilly; *et al.* Highly selective dopamine D3 receptor antagonists with arylated diazaspiro alkane cores. *J. Med. Chem.* **2017**, *60*, 9905-9910.
[12] Yasuko Koda; *et al.* Design and synthesis of tranylcypromine-derived LSD1 inhibitors with improved hERG and microsomal stability profiles. *ACS Med. Chem. Lett.* **2022**, *13*, 848-854.
[13] Patrick Sarver; *et al.* 6-Amino-3-methylpyrimidinones as potent, selective, and orally efficacious SHP2 inhibitors. *J. Med. Chem.* **2019**, *62*, 1793-1802.
[14] Bagdanoff J. T.; *et al.* Optimization of fused bicyclic allosteric SHP2 inhibitors. *J. Med. Chem.* **2019**, *62*, 1781-1792.
[15] Anders Johansson; *et al.* Discovery of (3-(4-(2-oxa-6-azaspiro[3.3]heptan-6-ylmethyl)phenoxy) azetidin-1-yl)(5-(4-methoxyphenyl)-1,3,4-oxadiazol-2-yl)methanone (AZD1979), a melanin concentrating hormone receptor 1 (MCHr1) antagonist with favorable physicochemical properties. *J. Med. Chem.* **2016**, *59*, 2497-2511.
[16] Caroline Wilson; *et al.* Optimization of TAM16, a benzofuran that inhibits the thioesterase activity of Pks13; evaluation toward a preclinical candidate for a novel antituberculosis clinical target. *J. Med. Chem.* **2022**, *65*, 409-423.
[17] Tim Cernak; *et al.* Microscale high-throughput experimentation as an enabling technology in drug discovery: application in the discovery of (piperidinyl)pyridinyl-1H-benzimidazole diacylglycerol acyltransferase 1 inhibitors. *J. Med. Chem.* **2017**, *60*, 3594-3605.
[18] Aurelie Mallinger; *at al.* Discovery of potent, orally bioavailable, small-molecule inhibitors of WNT signaling from a cell-based pathway screen. *J. Med. Chem.* **2015**, *58*, 1717-1735.
[19] Tao Yang; *et al.* Identification of a novel 2,8-diazaspiro[4.5]decan-1-one derivative as a potent and selective dual TYK2/JAK1 inhibitor for the treatment of inflammatory bowel disease. *J. Med. Chem.* **2022**, *65*, 3151-3172.
[20] Whitney L. Petrilli; *et al.* Discovery of spirocyclic aldosterone synthase inhibitors as potential treatments for resistant hypertension. *ACS Med. Chem. Lett.* **2017**, *8*, 128-132.
[21] Shuhao Zhou; *et al.* Identification of TUL01101: a novel potent and selective JAK1 inhibitor for the treatment of rheumatoid arthritis. *J. Med. Chem.* **2022**, *65*, 16716-16740.

Fused Cyclic Rings in Medicinal Chemistry

There are three types of bicyclic aliphatic rings: spirocyclic, fused cyclic and bridged cyclic, all of which have been gaining substantial interest in medicinal chemistry. [1-3] Like spirocyclic rings, fused cyclic ring system is also one of the most popular strategies of modern medicinal chemistry, as can be seen by the number of publications and contributions to a variety of approved drugs and clinical candidates (**Figure 97**). The increase in rigidity resulting from fused cyclization can influence important factors, such as potency and selectivity. Furthermore, significant improvements in physicochemical properties, such as logD, lipophilicity and solubility, as well as ADMET properties, are achievable, ultimately leading to improved pharmacokinetic profiles. Recent advances in the development of synthetic methods and efficient supplies of diverse **fused cyclic building blocks** have allowed the introduction and increase in fused cycles in medicinal chemistry in the past decade.

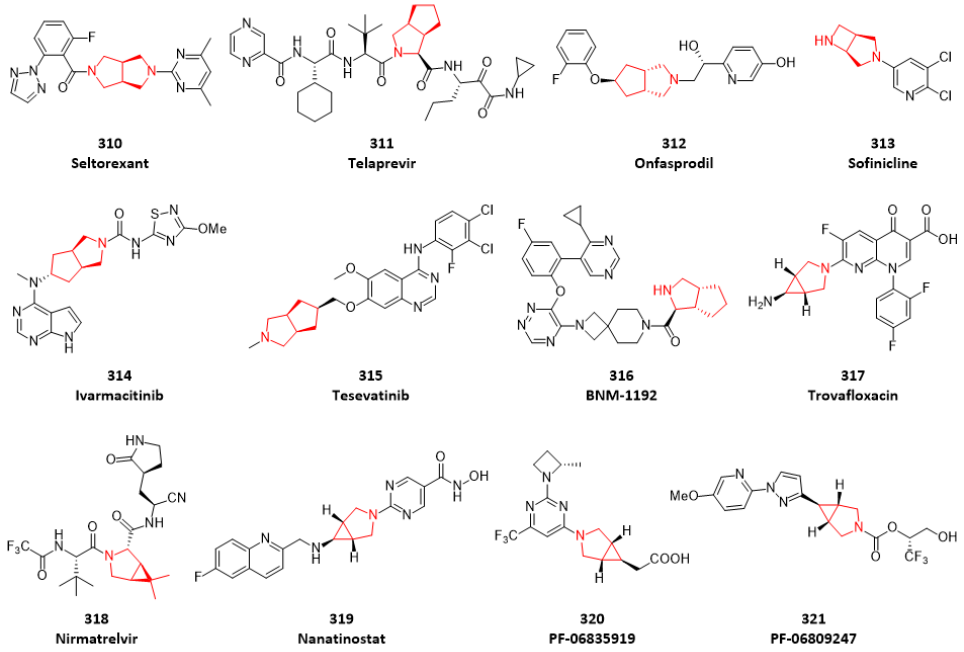

Figure 97. Fused cyclic rings in drug or clinical candidate molecules

In order to discover novel KHK inhibitors, compound **322** was identified as a promising hit. X-ray structure of compound **322** bound to KHK protein revealed that the cis-dihydroxypyrrolidine substituent is in line with the Arg108 residue at the polar back portion of the ATP binding site normally occupied by the triphosphate side chain in KHK. The team sought to exploit this vector in the direction of Arg108 in an effort to improve potency, possibly utilizing a Coulombic interaction. Additionally, a HydroSite calculation predicted a high-energy virtual water molecule in this pocket present within the hydrogen-bonding distance between Arg108, a backbone carbonyl oxygen atom of Thr253, and a backbone NH of Gly257 respectively, suggesting the possibility of making energetically favorable interactions with an appropriately chosen side chain attachment in this regioin. With this in mind, initial exploration of this vector by parallel medicinal chemistry using a diverse array of amines culminated in the identification of compound **323**, possessing a fused cyclic 3-azabicyclo[3.1.0]hexane ring system as one of the most potent neutral azetidine analogues among those tested from parallel medicinal chemistry effort (**Figure 98**). [4] X-ray structure of compound **323** bound in KHK protein showed that the terminal hydroxyl group on the newly

introduced 3-azabicyclo[3.1.0]hexane ring system effectively reached proximally to Arg108. This terminal hydroxyl group indirectly forms a hydrogen bond with Arg108 through a bound water, while within the hydrogen bond distance with the backbone carbonyl oxygen atom of Thr253. With compound **323** in hand, further optimization of the terminal polar groups was targeted as next design strategy to improve potency. Among the polar group known to interact with the arginine residue, the carboxylic acid group was considered as one of the top candidates given its potential to form a strong salt bridge with the guanidinium group of Arg108. This was proved by compound **324**, which demonstrated significantly increased potency by > 20-fold compared to compound **323**. X-ray structure of compound **324** bound to KHK protein displayed that the carboxylic acid group was well positioned to interact with cationic guanidinium group of Arg108. In addition, the backbone NH of Gly255 and Gly257, as well as a bound water nearby, were all within the hydrogen bond distance. Thus, a complex network of polar interactions through the carboxylic acid is likely responsible for the significant potency improvement. Further optimization based on compound **324** led to identification of clinical candidate **PF-06835919** (compound **320**).

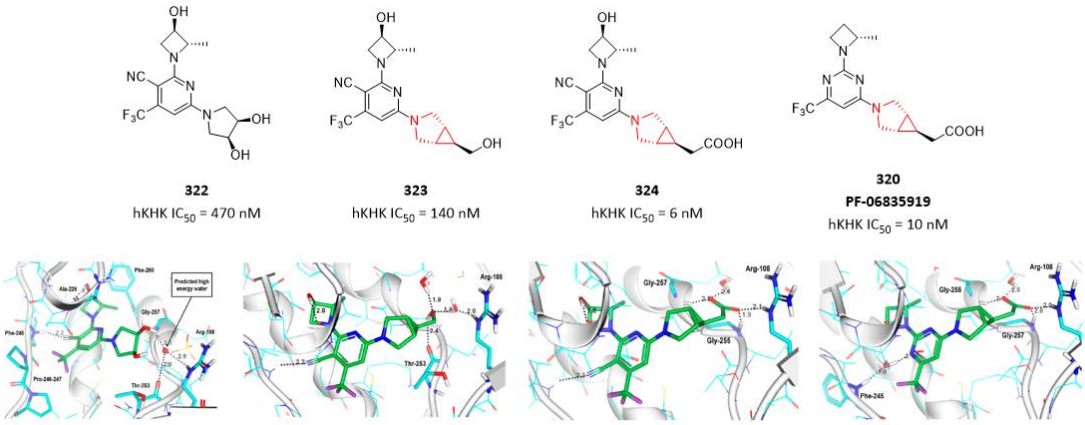

Figure 98. Fused 3-azabicyclo[3.1.0]hexane ring in KHK inhibitors (PDB codes: 6W0W, 6W0X, 6W0Y, 6W0Z)

In the course of discovery of MAGL inhibitor **PF-06795071** (compound **321**), the team previously identified a series of azetidine analogs such as compound **325**, which displayed excellent MAGL potency with IC_{50} = 0.3 nM and a good selectivity profile. However, in vivo PK-PD studies, only a transient elevation in 2-AG was observed. Cellular activity based protein profiling studies confirmed that this class of compounds covalently inhibited MAGL transiently and led the team to speculate that the azetidine adducts formed at the MAGL site were rapidly hydrolyzed from the enzyme. With an observation in mind that analogs containing larger ring cores, such as piperidines, resulted in improved MAGL adduct stability and thus prolonged PD effects, efforts to optimize the core system resulted in the discovery of compounds based on 3-azabicyclo[3.1.0]hexane ring system, such as compound **326**. Compound **326** retained MAGL potency with IC_{50} = 1.4 nM and had excellent selectivity. Despite a promising pharmacology profile, compound **326** had poor solubility (< 1 uM). To address this issue, the team systematically explored leaving group with the goal of improving drug-like properties, which led to discovery of clinical candidate **PF-06809247** (compound **321**) with significantly increased solubility. X-ray structure of compound **326** bound to MAGL protein revealed that 3-azabicyclo[3.1.0]hexane core with aryl pyrazole tail complements the shape of the lipophilic MAGL acyl chain binding pocket (**Figure 99**). [5]

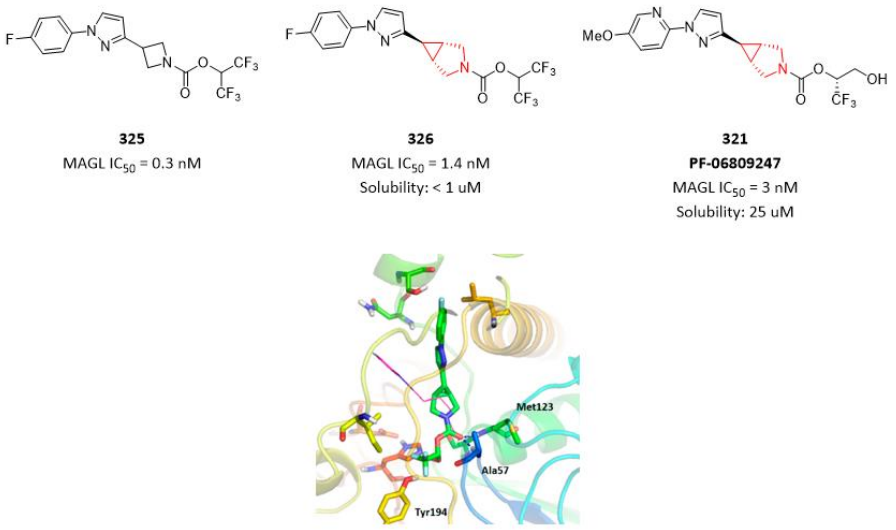

Figure 99. Fused 3-azabicyclo[3.1.0]hexane ring in MAGL inhibitors (PDB codes: 6BQ0)

PBTZ169 (compound **327**) is a promising compound which possesses extraordinary while-cell activity with a minimum inhibitory concentration (MIC) of 1 nM. While impressive, **PBTZ169** has liabilities emanating from its extremely poor solubility (< 0.01 ug/mL) that portend poor penetration. This may affect oral bioavailability (F) and volume of distribution (V_d), neither of which have been reported. To address this issue, disruption of molecular symmetry and planarity was used to improve aqueous solubility by replacing piperazine moiety with a wide variety of bioisosteric spirocyclic, fused cyclic and bridged cyclic diamines. This effort led to identification of compound **328** and compound **329** which possess a bridged cyclic ring and a fused cyclic ring respectively. Both compounds had high potency with MIC_{90} = 32 nM, although 15-fold less potent than **PBTZ169**. Fused 3-azabicyclo[3.1.0]hexane ring in compound **329** significantly increased aqueous solubility by at least 480-fold, while metabolic stability in both human and mouse liver microsome were both improved. However, compound **328** failed to improve solubility, and had a similar metabolic stability profile with **PBTZ169** (**Figure 100**). [6]

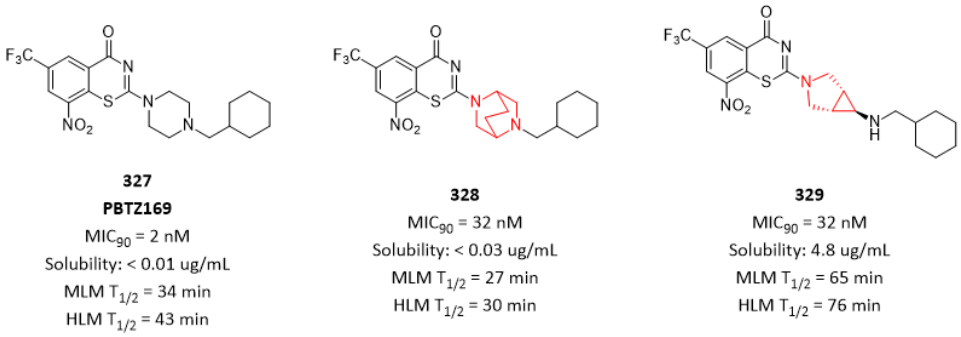

Figure 100. Fused 3-azabicyclo[3.1.0]hexane ring improved both solubility and metabolic stability.

To identify new potent and selective allosteric SHP2 inhibitors, the team led to discovery of a promising hit compound **330**, which exhibited modest SHP2 inhibition with IC_{50} = 225 nM. An attempt to optimize the novel amino moiety was undertaken with objectives: (a) maximize SHP2 inhibition; (b) remove secondary amine groups which are potentially detrimental to cell penetration; (c) make molecule constrained to likely control metabolic stability. With these goals in mind, a variety of fused cyclic diamines were examined and these efforts led to identification of compound **331** which possesses a bicyclo[3.1.0]hexane ring. Compound **331** had an excellent SHP2

inhibition with IC_{50} = 9 nM, and a modest pERK inhibition with IC_{50} = 210 nM. In order to further increase potency, a bicyclic pyrazopyrazole scaffold in compound **332** was employed with pERK inhibition increased by up to 10-fold. Despite promising in vitro potency, compound **332** inhibited hERG with IC_{50} = 58 nM. In order to address this critical issue, dichlorophenyl group was replaced by various bicyclic heterocycles. Among of them, indazole in compound **333** was found to decrease hERG inhibition while keeping excellent in vitro potency. Surprisingly, the corresponding 3-azabicyclo[3.1.0]hexane ring in compound **334** showed excellent in vitro potency and significantly lower hERG inhibition (**Figure 101**). [7]

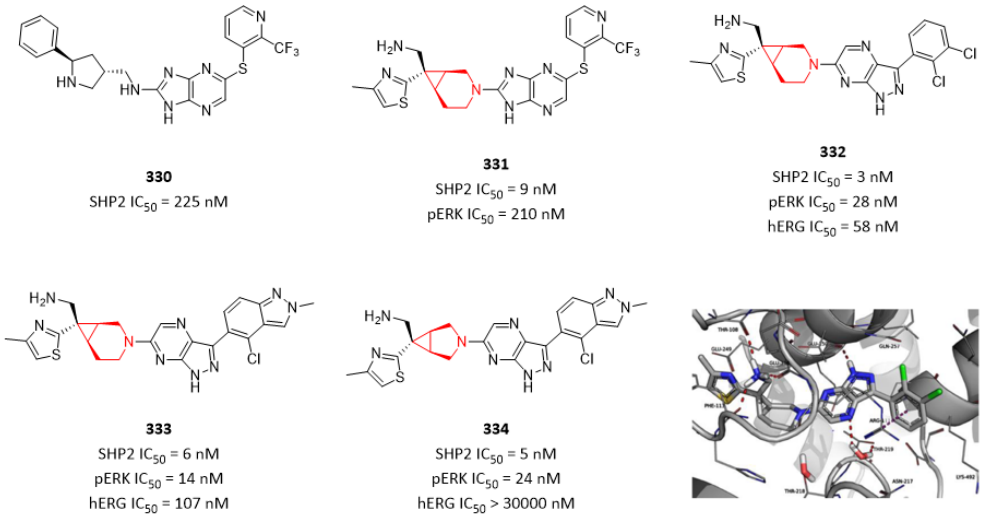

Figure 101. Fused 3-azabicyclo[3.1.0]hexane ring decreased hERG inhibition. (PDB code: 8CBH)

As can be seen in above case stories, a quick access of a diverse collection of fused cyclic building blocks is of great value for medicinal chemists to get SAR or SPR results in their program as soon as possible (**Figure 102**).

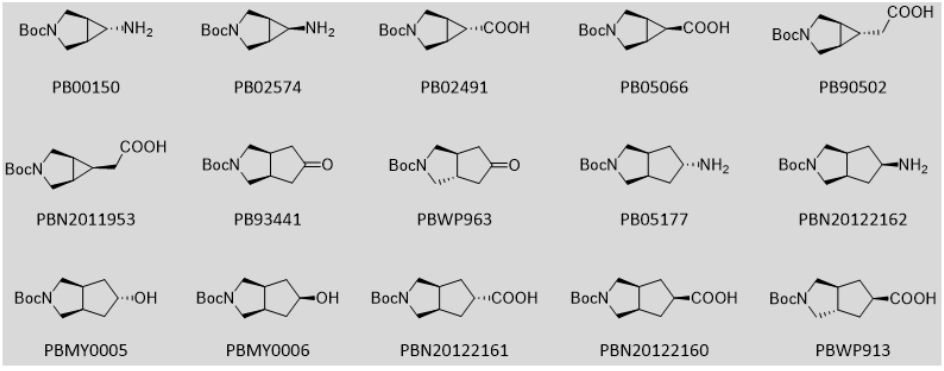

Figure 102. Fused cyclic building blocks with different functional groups

Discovery of compound **339** (**SAR707**) was started from reported compound **335**. Replacement of piperazine moiety with fused hexahydro-pyrrolo-pyrrole ring in compound **336** increased potency by 5-fold. SAR study around the left chain identified compound **337** as the most potent compound, which possesses a cyclopropane. Replacing pyridine with pyridazine in compound **338** didn't change potency. Surprisingly, in compound **339** (**SAR707**), phenyl ring increased SCD1 potency significantly by 25-fold (**Figure 103**). [8]

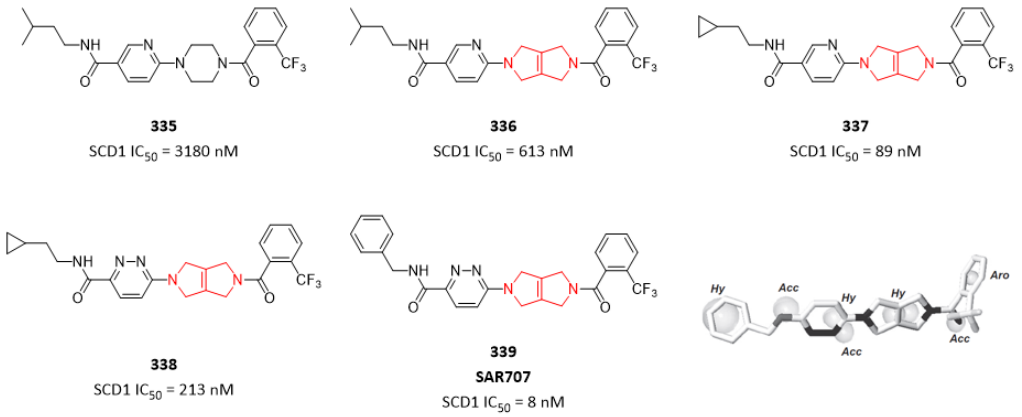

Figure 103. Fused hexahydro-pyrrolo-pyrrole ring in discovery of **SAR707**.

Compound **341** was discovered through an optimization program based on hit compound **340**, and potency was increased by 7-fold. However, compound **341** had CYP inhibition with IC_{50} = 7 uM for CYP3A4 and IC_{50} = 12 uM for CYP2D6 respectively. In order to address this critical issue, replacing piperazine with bioisosteres was employed. One piperazine isostere of interest was the fused octahydropyrrolo[3,4-c]pyrrole ring. As showed in compound **342**, fused octahydropyrrolo[3,4-c]pyrrole also increased potency by 7-fold, but still had CYP inhibition with IC_{50} = 6 uM for CYP3A4 and IC_{50} = 24 uM for CYP2D6 respectively. Further optimization led to compound **343** where adamantly group was replaced with a spirocyclic ring, which demonstrated no CYP3A4 and CYP2D6 inhibition (**Figure 104**). [9]

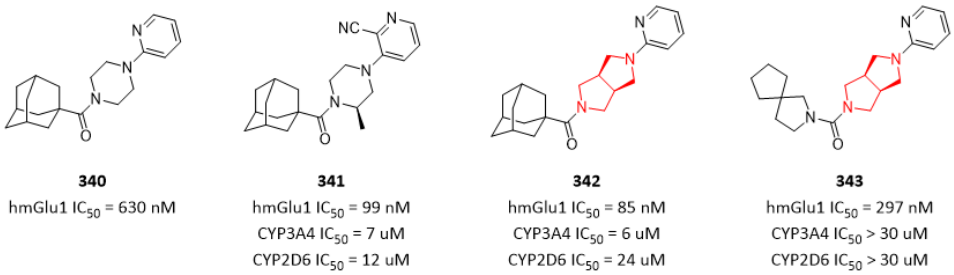

Figure 104. Fused octahydropyrrolo[3,4-c]pyrrole ring increased potency.

In order to discover novel, selective OX2R antagonists that were orally bioavailable and safe with an optimal pharmacokinetic profile for the treatment of primary insomnia, a high-throughput screening campaign was conducted identified a promising hit compound **344**. To further optimize compound **344**, the team decided to investigate SAR and selectivity of compounds with novel core structures. These efforts generated compound **345** possessing a fused octahydropyrrolo[3,4-c]pyrrole ring, which decreased potency significantly by 88-fold. Despite low potency, iterative SAR led to great improvements in both OX2R affinity and selectivity against OX1R, and culminated in discovery of clinical candidate **Seltorexant** (compound **310**) (**Figure 105**). [10]

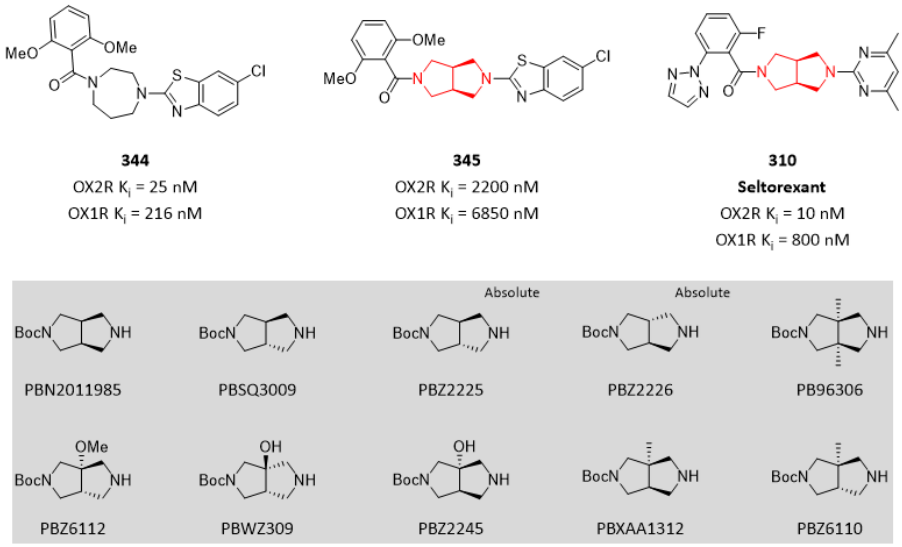

Figure 105. Fused octahydropyrrolo[3,4-c]pyrrole ring in selective OX2R antagonists

To optimize compound **346**, a series of potent neuronal nAChR ligands based on fused 3,8-diazabicylco[4.2.0]octane ring have been synthesized and evaluated for affinity and agonist efficacy at human high affinity nicotine recognition site and in a rat model of persistent nociceptive pain. Among of them, compound **347** and compound **348** exhibited equivalent or greater affinity relative to epibatidine, and demonstrated robust analgesic efficacy in the rat formalin model of persistent pain (**Figure 106**). [11] Fused 3,8-diazabicylco[4.2.0]octane ring was also used in discovery of novel dual orexin receptor antagonists via scaffold hopping approach based on compound **349** (**Suvorexant**). Compound **350** displayed comparable potency to compound **349** (**Suvorexant**). [12]

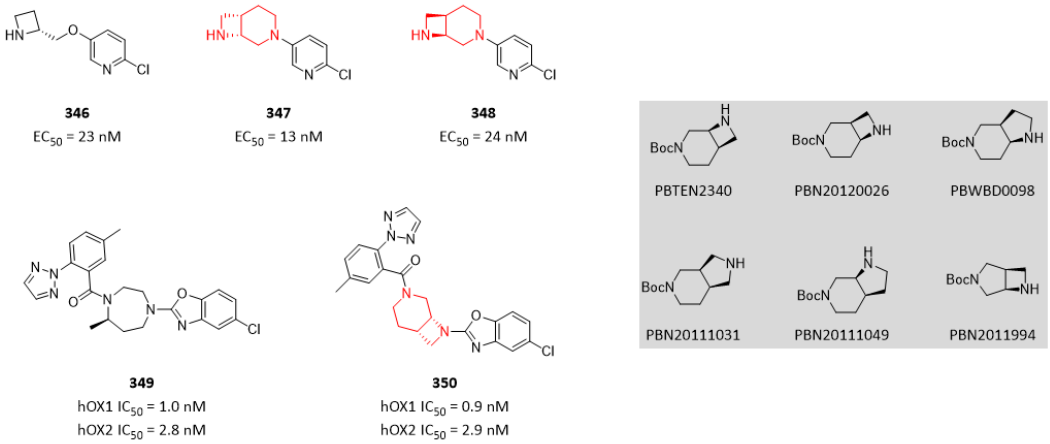

Figure 106. Fused 3,8-diazabicylco[4.2.0]octane ring used in drug discovery

Fused cyclic diamines have been widely used in discovery of novel antibacterial drugs. Based on compound **351**, an additional ring was formed to generate compound **352** which increased potency by 7-fold. However, compound **352** inhibited hERG with 36% inhibition at 100 uM. To address this critical issue, a polar oxygen atom was inserted in compound **353**, and interestingly hERG inhibition was not observed (**Figure 107**). [13] In another work, compound **354** was identified as a highly potent antibacterial inhibitor. Further optimization by introduction of a fused cyclic ring and two fluorine atoms, led to discovery of compound **355** which significantly increased antibacterial potency by 33-

fold. Furthermore, compound **355** also decreased *in vivo* clearance and increased *in vivo* exposure and oral bioavailability. [14]

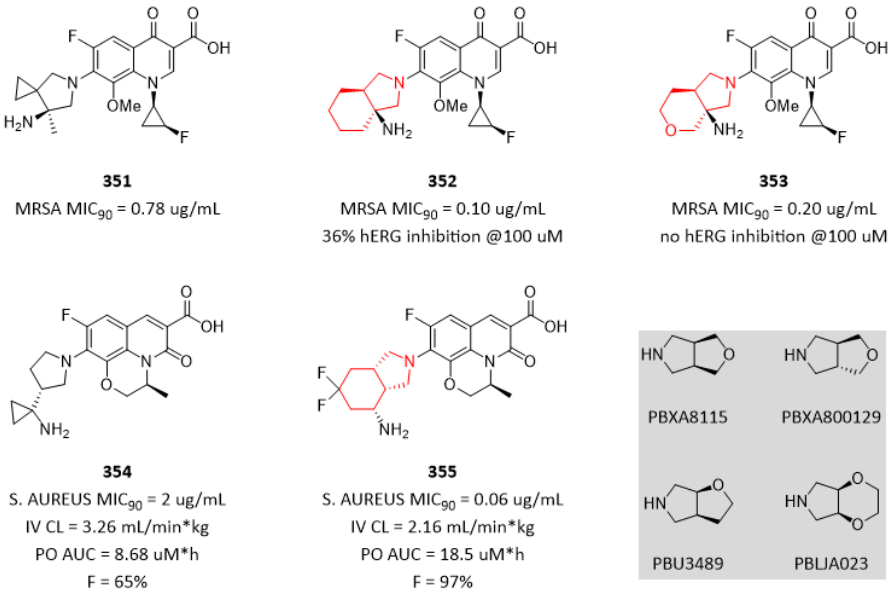

Figure 107. Fused cyclic rings used in discovery of novel antibacterial drugs

The fusion of a cyclopropane ring with two of the carbon of piperazine reduces the basicity of the nitrogen atom. This is attributed to a combination of the known effect of the cyclopropane ring on amine basicity which typically reduces pKa values by 1.15 units, coupled with an effect resulting from the two nitrogen atoms being slightly closer in proximity, disposing at a distance of 2.77 A compared to 2.86 A in the piperazine. The ring fusion also confers an element of conformational constraint. In an effort to assess the potential fused 2,5-diazabicyclo[4.1.0]heptane ring to substitute for the C-7 piperazine ring of compound **356**, analogue **357** was synthesized and evaluated for its in vitro antibacterial properties. The antibacterial potency of compound **357** was comparable to that of compound **356**. In the single crystal X-ray structure of compound **357**, the fused 2,5-diazabicyclo[4.1.0]heptane ring exists in a twist boat-like conformation that results in some distortion of cyclopropane ring (**Figure 108**). [15]

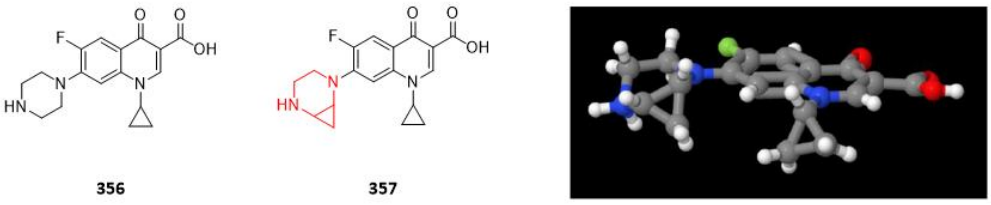

Figure 108. Conformation of fused 2,5-diazabicyclo[4.1.0]heptane ring

It would be greatly interesting to investigate conformation and impact on biological activity of other fused piperazine rings. An efficient access of this kind of building blocks can provide us more insights in potential applications in drug discovery (**Figure 109**).

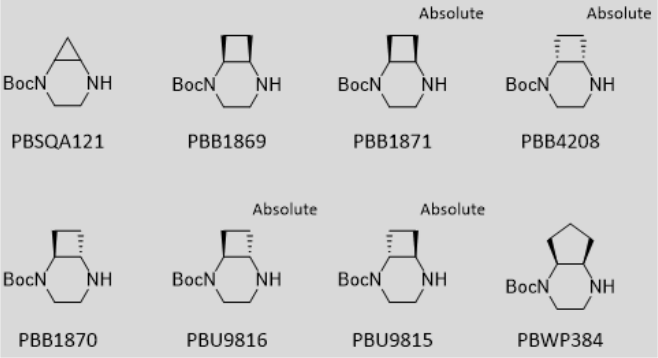

Figure 109. Fused piperazine building blocks

In the course of discovery of clinical candidate **NTQ1062** (compound **359**) as an AKT inhibitor, it was surprisingly to found that the inhibitory of fused piperazine compound **359** was improved by 4-fold compared with compound **358**, and more importantly the exposure was increased by 9-fold. The predicted binding model of compound **359** revealed that the distance between the sulfur in the amino acid residue of Met281 and the cyclopropyl was 3.6 A. The cyclopropyl ring has properties similar to those of carbon-carbon double bond of alkene. Therefore, it was speculated that additional sulfur-pi interaction might contribute to the increase in the potency of compound **359** (**Figure 110**). [16]

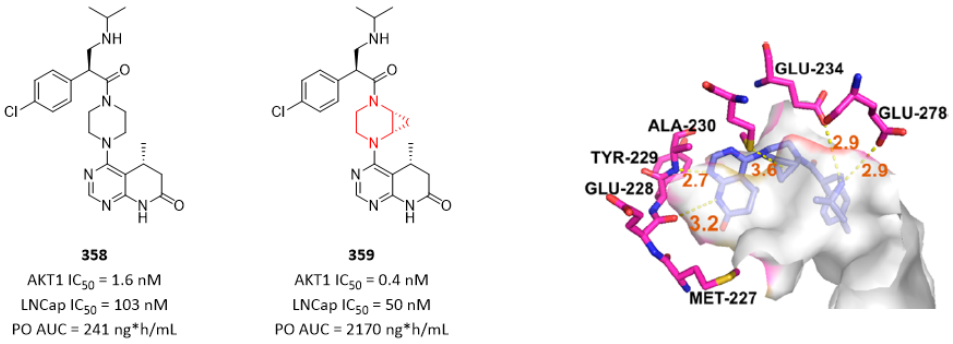

Figure 110. Fused piperazine increased both potency and exposure.

References

[1] Oleksandr O. Grygorenko; *et al.* Bicyclic conformationally restricted diamines. *Chem. Rev.* **2011**, *111*, 5506-5568.
[2] Nicholas A. Meanwell; *et al.* Applications of isosteres of piperazine in the design of biologically active compounds: part 1. *J. Agric. Food Chem.* **2022**, *70*, 10942-10971.
[3] Nicholas A. Meanwell; *et al.* Applications of isosteres of piperazine in the design of biologically active compounds: part 1. *J. Agric. Food Chem.* **2022**, *70*, 10972-11004.
[4] Kentaro Futatsugi; *et al.* Discovery of PF-06835919: a potent inhibitor of ketohexokinase (KHK) for the treatment of metabolic disorders driven by the overconsumption of fructose. *J. Med. Chem.* **2020**, *63*, 13546-13560.
[5] Laura A. McAllister; *et al.* Discovery of trifluoromethyl glycol carbamates as potent and selective covalent monoacylglycerol lipase (MAGL) inhibitors for treatment of neuroinflammation. *J. Med. Chem.* **2018**, *61*, 3008-3026.
[6] Gang Zhang; *et al.* Spirocyclic and bicyclic 8-nitrobenzothiazinones for tuberculosis with improved physicochemical and pharmacokinetic properties. *J. Med. Chem.* **2019**, *10*, 348-351.

[7] Alessia Petrocchi; *et al.* Discovery of a novel series of potent SHP2 allosteric inhibitors. *ACS Med. Chem. Lett.* **2023**, *14*, 645-651.
[8] Marc D. Voss; *et al.* Discovery and pharmacological characterization of SAR707 as novel and selective small molecule inhibitor of stearoyl-CoA desaturase (SCD1). *Eur. J. Pharmacol.* **2013**, *707*, 140-146.
[9] Jason T. Manka; *et al.* Octahydropyrrolo[3,4-c]pyrrole negative allosteric modulators of mGlu1. *Bioorg. Med. Chem. Lett.* **2013**, *18*, 5091-5096.
[10] Michael A. Letavic; *et al.* Novel octahydropyrrolo[3,4-c]pyrroles are selective orexin-2 antagonists: SAR leading to a clinical candidate. *J. Med. Chem.* **2015**, *58*, 5620-5636.
[11] Jennifer M. Frost; *et al.* Synthesis and structure-activity relationships of 3,8-diazabicyclo[4.2.0]octane ligands, potent nicotinic acetylcholine receptor agonists. *J. Med. Chem.* **2006**, *49*, 7843-7853.
[12] Bibia Heidmann; *et al.* Discovery of highly potent dual orexin receptor antagonists via a scaffold-hopping approach. *ChemMedChem* **2016**, *11*, 1-16.
[13] Takashi Odagiri; *et al.* Design, synthesis, and biological evaluation of novel 7-[(3aS,7aS)-3a-aminohexahydropyrano[3,4-c]pyrrol-2(3H)-yl]-8-methoxyquinolines with potent antibacterial activity against respiratory pathogens. *J. Med. Chem.* **2018**, *61*, 7234-7244.
[14] Guillaume Lapointe; *et al.* Discovery and optimization of DNA gyrase and topoisomerase IV inhibitors with potent activity against fluoroquinolone-resistant gram-positive bacteria. *J. Med. Chem.* **2021**, *64*, 6329-6357.
[15] Taylor R. R. R.; *et al.* Substituted 2,5-diazabicyclo[4.1.0]heptanes and their application as general piperazine surrogates: synthesis and biological activity of a ciprofloxacin analogue. *Tetrahedron* **2010**, *66*, 3370-3377.
[16] Changyou Ma; *et al.* Discovery of clinical candidate NTQ1062 as a potent and bioavailable Akt inhibitor for the treatment of human tumors. *J. Med. Chem.* **2022**, *65*, 8144-8168.

Bridged Cyclic Rings in Medicinal Chemistry

Like spirocyclic rings and fused cyclic rings, bridged cyclic ring system is also one of the most popular focus of modern medicinal chemistry, as can be seen by a wide range of applications of bridged cyclic rings in approved drug and clinical candidate molecules (**Figure 111**).

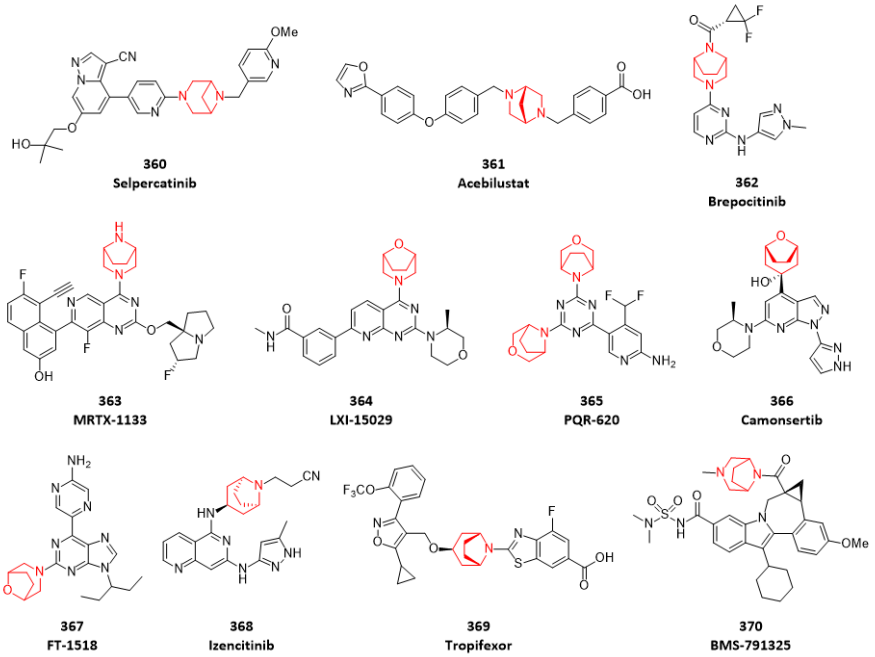

Figure 111. Approved drug and clinical candidate molecules containing bridged cyclic rings

Bridging piperazines, piperidines, morpholines and other mono-rings with one, two or even more carbon atoms can confer them with unexpected observations due to conformational restrictions (**Figure 112**). For instance, it was recommended that medicinal chemists consider the use of one-carbon bridges as a potential strategy to modulate the physicochemical properties of morpholines and piperazines, especially in cases where issues are observed with metabolism, hERG inhibition, or other detrimental properties correlated with lipophilicity. In addition, specific benefits, particularly where the conformational restrictions can potentially be used to improve selectivity or increase potency via subtly changing the shape of the moiety. [1]

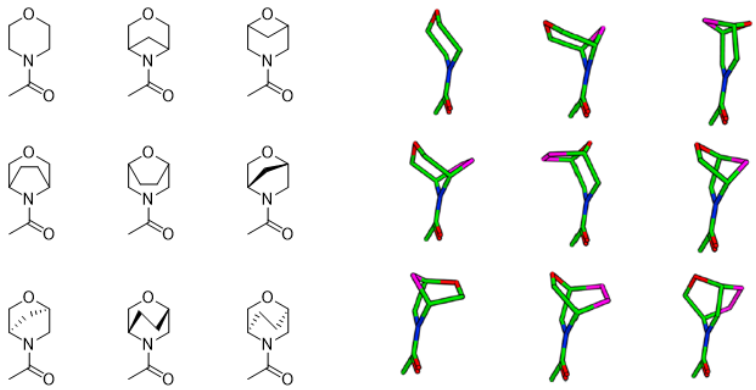

Figure 112. 3-D models of various bridged N-acetylmorpholines (bridged carbons are shown in purple)

In the course of discovery of clinical candidate **Brepocitinib** (compound **362**), a variety of bridged rings were examined in compound **371**, **372**, **373**, **374**, **375**, **376** and **362**. A clear stereochemical

preference is evident from the biochemical activity of compound **371** and compound **372**. Potency against TYK2 improved for compound **374**, compound **375** and compound **376** compared to compound **373**, presumably due to improved hydrophobic interactions of bridged carbon atoms with the residues at the bottom of the binding site. Among of these compounds, compound **376** containing 3,8-diazabicyclo[3.2.1]octane ring demonstrated the highest potency. Further optimization led to discovery of clinical candidate **Brepocitinib** (compound **362**). To better understand the TYK2 potency, a crystal structure of compound **362** bound to TYK2 was obtained. The ethylene bridge of the [3.2.1]-diazabicycle projects into the lower hydrophobic portion of the binding site (**Figure 113**). [2]

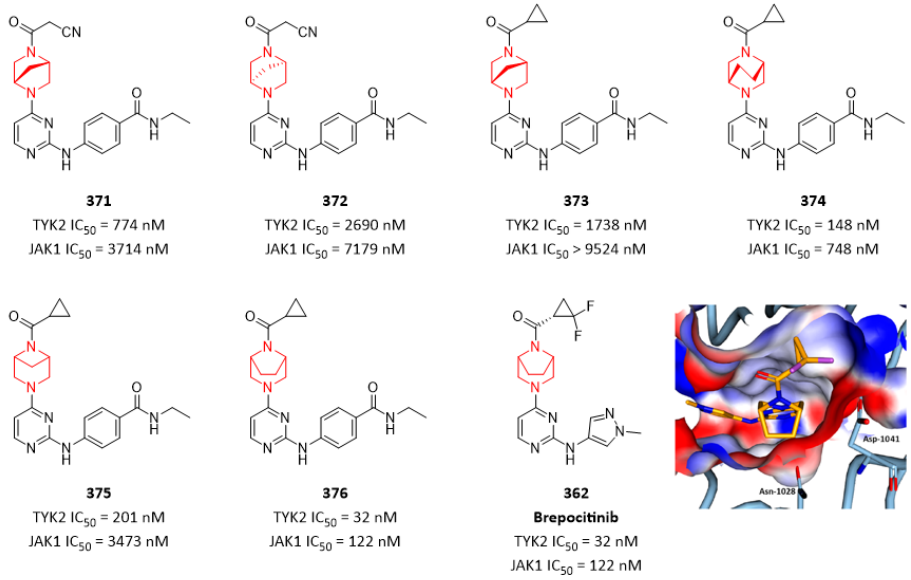

Figure 113. Bridged cyclic rings used in discovery of **Brepocitinib** (PDB code: 6DBM)

As described in above case story, an efficient access of diverse **bridged piperazine building blocks** is of great value for quick exploration of SAR and SPR (**Figure 114**).

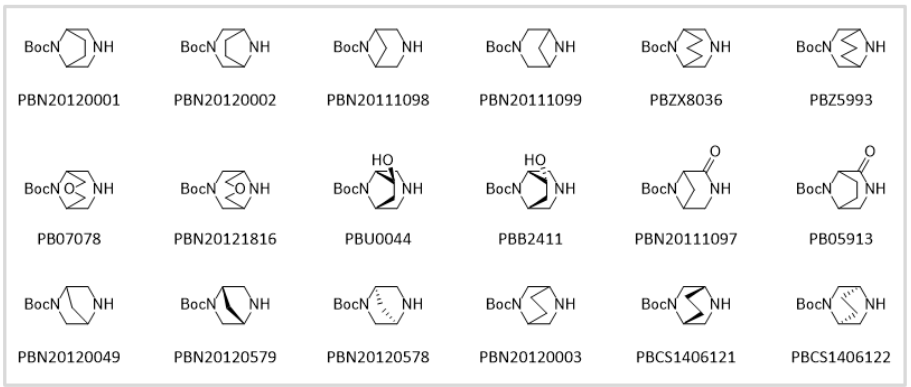

Figure 114. Bridged piperazine building blocks

In order to discover novel KRAS G12D inhibitor, like discovery of **Brepocitinib** (compound **362**) in above, a variety of bridged rings were examined in compound **378**, **379**, **380**, **381**, and **363**. Comparing with compound **377**, all rigidification of bioactive conformation with bridged piperazine increased affinity. Among of them, compound **381** containing a [3.2.1]bicyclic diamino substituent had a 200-fold greater affinity than compound **377**. The X-ray structure of compound **381** bound to KRAS G12D revealed that two-carbon bridge of the bicyclic group occupies a small pocket, while

one of the endo C-Hs forms a non-classical hydrogen bond with the Gly10 carbonyl oxygen (**Figure115**). [3]

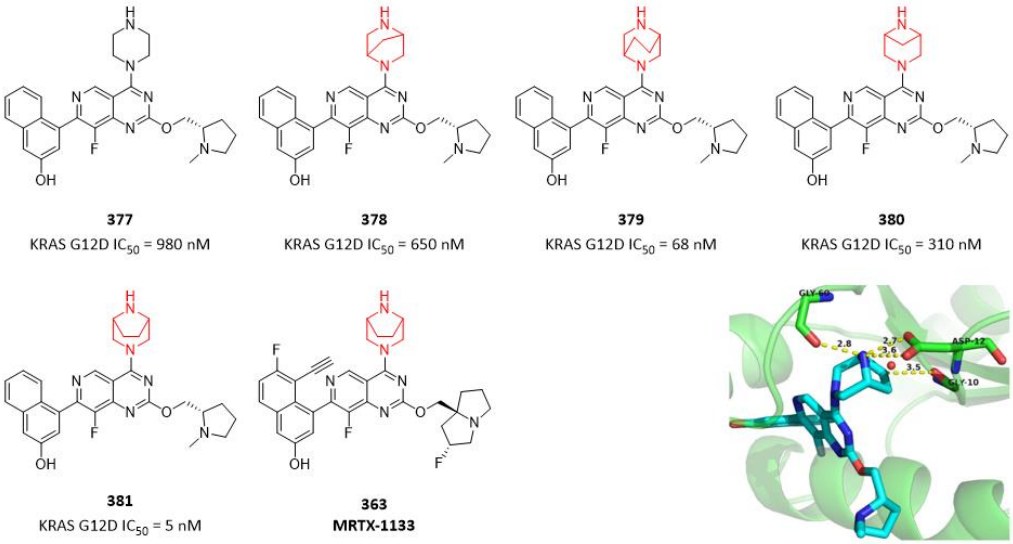

Figure 115. Bridged cyclic rings used in discovery of **MRTX-1133** (PDB code: 7RT1)

In the last section "**Fused Cyclic Rings in Medicinal Chemistry**", we described further optimization of compound **358** which suffered poor oral exposure. Besides fused cyclic rings, the team also investigated bridged cyclic piperazines for improving oral exposure. As shown in compound **382** and compound **383**, 3,8-diazabicyclo[3.2.1]octane ring increased oral exposure by 4-fold and 6-fold respectively (**Figure 116**). However, compound **383** decreased cellular potency by 4-fold. [4]

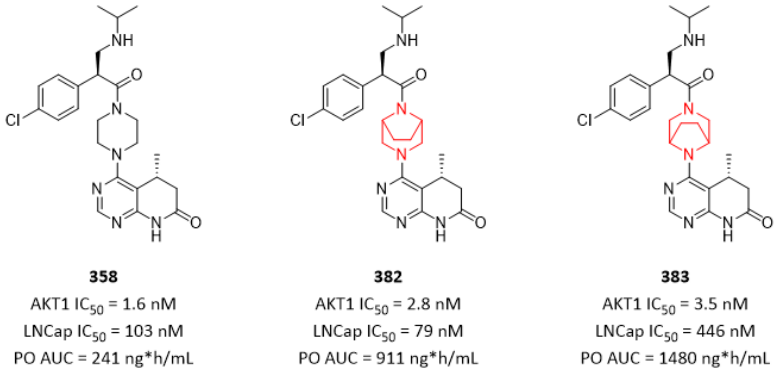

Figure 116. Bridged rings increased oral exposure.

In the course of discovery of clinical candidate **BMS-791325** (compound **370**) as a potent allosteric inhibitor of the hepatitis C virus NS5B polymerase, a variety of bridged cyclic rings were examined to address off-target activities, most notably hPXR transactivation which led to identification of compound **384**. Compound **384**, containing a 3,6-diazabicyclo[3.1.1]heptane ring, had a highly potency and no hPXR issue, but inhibited CYP3A4 with IC_{50} = 14 uM. It was interesting that in compound **370** (**BMS-791325**), containing a 3,8-diazabicyclo[3.2.1]octane ring, demonstrated no CYP3A4 inhibition (**Figure 117**). [5] X-ray structure of compound **370** bound in NS5B revealed that additional contacts between two-carbon bridge of the bicyclic group and proximal protein residues L492, T399 and A400 were observed.

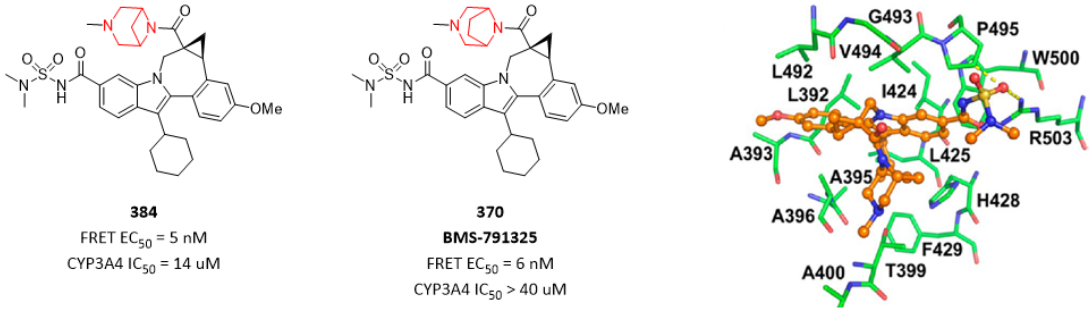

384
FRET EC_{50} = 5 nM
CYP3A4 IC_{50} = 14 uM

370
BMS-791325
FRET EC_{50} = 6 nM
CYP3A4 IC_{50} > 40 uM

Figure 117. 3,8-Diazabicyclo[3.2.1]octane ring address CYP3A4 inhibition.

Compound **385** was identified as a potent, brain-penetrant and selective M1R antagonist, but showed low metabolic stability and inhibition against hERG. To address these issues, many bridged cyclic rings in compound **386** (**PIPE-359**), compound **387** and compound **388** were examined. A 3,8-diazabicyclo[3.2.1]octane ring in compound **386** (**PIPE-359**) not only increased activity, but also improved metabolic stability and hERG inhibition. However, in compound **387** and compound **388**, two bridged cyclic rings displayed inferior activity (**Figure 118**). [6]

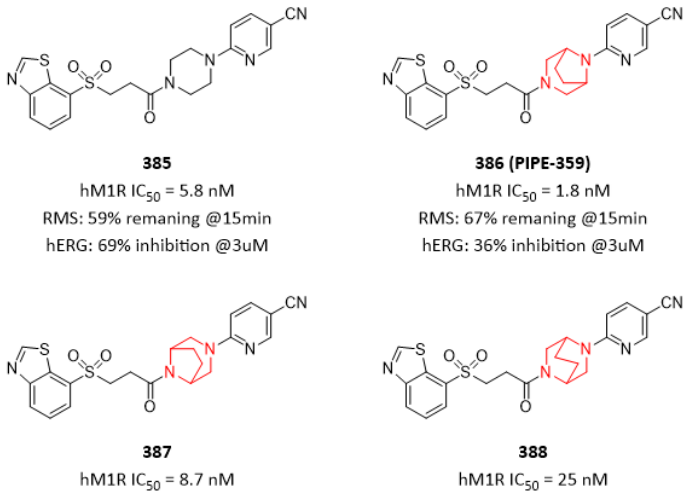

385
hM1R IC_{50} = 5.8 nM
RMS: 59% remaning @15min
hERG: 69% inhibition @3uM

386 (PIPE-359)
hM1R IC_{50} = 1.8 nM
RMS: 67% remaning @15min
hERG: 36% inhibition @3uM

387
hM1R IC_{50} = 8.7 nM

388
hM1R IC_{50} = 25 nM

Figure 118. 3,8-Diazabicyclo[3.2.1]octane ring address metabolic stability and hERG inhibition issues.

In order to discover FGFR2 and FGFR3 dual inhibitors with high selectivity against FGFR1 and FGFR4, compound **389** was selected as starting point. Encouraged by previous work, piperazine bearing 2,6-dimethyl group displayed improved FGFR3 potency in comparison to unsubstituted piperazine, suggesting an opportunity to enhance potency and selectivity by introduction of carbon bridge on piperazinone ring. Pleasingly, compound **390**, featuring an ethylene bridge between C-2 and C-6 of the piperazinone, displayed single-digit-nanomolar potency against FGFR3 while maintaining good selectivity against FGFR1 (16-fold). Further optimization led to identification of more promising compound **391**. Docking of compound **391** in binding site revealed that the bridged piperazinone occupies the pocket under the P loop, wherein the ethylene bridge is oriented toward a hydrophobic groove formed by Leu624 and Ala634, placing the amide carbonyl group in the proper position to form a strong hydrogen bond with the catalytic Lys508 (**Figure 119**). [7]

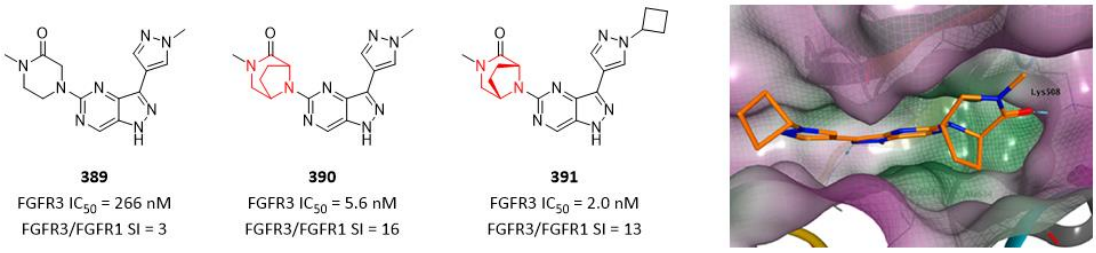

Figure 119. Bridged piperazinone increased both potency and selectivity.

In the course of discovery of clinical candidate **PQR-620** (compound **365**) as a highly potent and selective mTORC1/2 inhibitor, a variety of bridged cyclic rings were investigated to improved selectivity against PI3K. Compound **392**, featuring two morpholines, displayed a high potency, but suffured a low selectivity against PI3K. 8-Oxa-3-azabicyclo[3.2.1]octane ring in compound **393** increased selectivity significantly while keeping a comparable potency. 2-Oxa-5-azabicyclo[2.2.1]heptane ring in compound **394** also increased selectivity significantly while keeping a comparable potency. However, in compound **395** 2-oxa-5-azabicyclo[2.2.1]heptane ring decreased potency dramatically, indicating a preference of chiral conformation. 3-Oxa-6-azabicyclo[3.1.1]heptane ring in compound **396** decreased potency dramatically, although selectivity index was increased to 49 (**Figure 120**). [8]

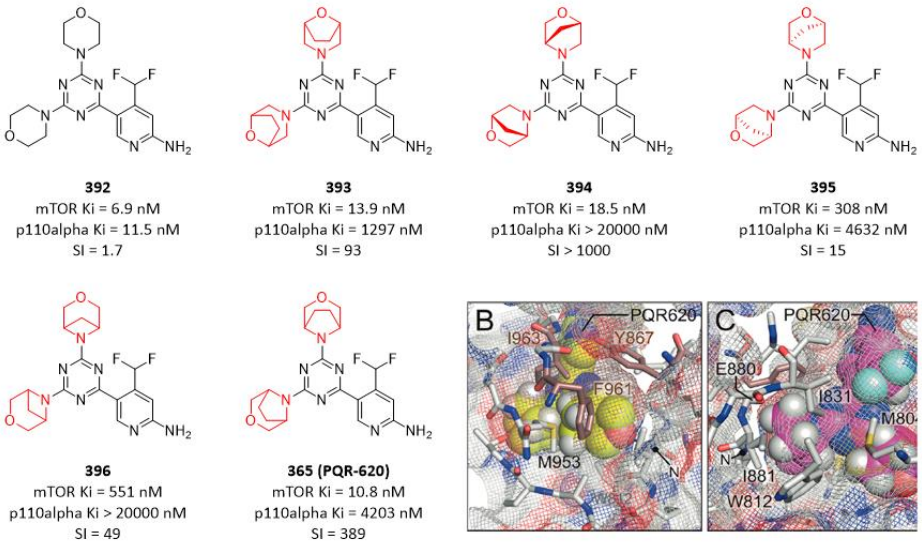

Figure 120. Bridged cyclic rings increased selectivity due to steric clash with protein.

3-Oxa-8-azabicyclo[3.2.1]octane ring in compound **365** (**PQR-620**) increased selectivity significantly with SI = 389, while keeping a comparable potency. Computational modeling studies were used to elucidate the binding mode of compound **365** and ultimately provided structural features defining the compound's high selectivity toward mTOR versus PI3K. The ethylene bridge of the morpholine pointing toward Val882 can take two main conformations, with the bridge oriented toward Met953 defined as bridge-up, or toward Ile881 defined as bridge-down. The bridge-up conformation induces steric clashes within a region of the ATP-binding pocket that has previously been identified as very rigid in PI3K and is defined by residues Tyr867, Phe961 and Ile963. The bridge-down conformation generates steric clash within the backbone of Ile881 and Glu880 and side chains of Ile831 and Ile881. Steric clashes, and as a consequence the weakening of the essential hydrogen bond to the PI3K hinge region explain the reduced affinity of compound **365** for PI3K (**Figure 120**). [8]

As described in above case story, an efficient access of diverse **bridged morpholine building blocks** is of great value for quick exploration of SAR and SPR (**Figure 121**).

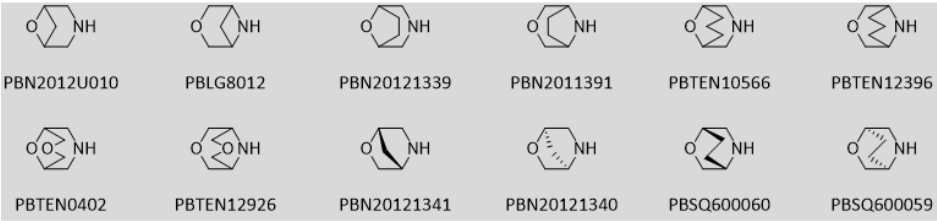

Figure 121. Bridged morpholine building blocks

The trend of selectivity against PI3K in above case story (**Figure 120**) was also observed in another series of mTOR inhibitors. Compared to compound **397** with morpholine ring unsubstituted, 8-oxa-

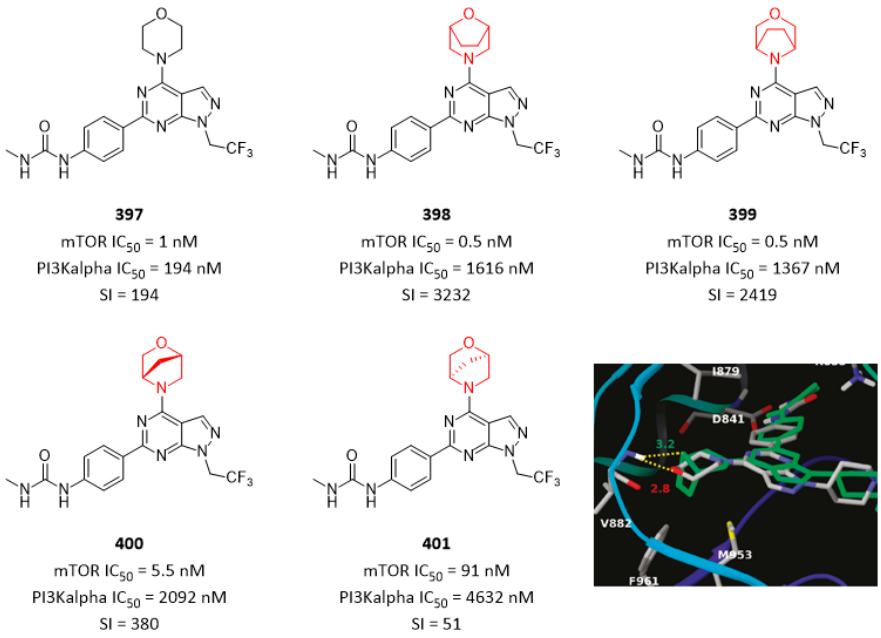

Figure 122. Bridged morpholines increased selectivity due to steric clash.

3-azabicyclo[3.2.1]octane ring in compound **398** and 3-oxa-8-azabicyclo[3.2.1]octane ring in compound **399** both increased selectivity significantly, while keeping comparable potency. However, 2-oxa-5-azabicyclo[2.2.1]heptane rings in compound **400** and compound **401** decreased potency. Docking of the bridged morpholine analogue suggests that a single amino acid difference between mTOR and PI3K causes a difference in the depth of the morpholine binding pockets that is responsible for the increased selectivity observed. Modeling indicates that Phe961 of PI3K is too large to comfortably accommodate the ethylene-bridged morpholine, causing displacement of the morpholine oxygen away from its hydrogen bonding partner, the backbone NH of Val882 (**Figure 122**). [9]

In order to obtain an orally available GSM without covalent binding and phototoxicity, compound **402** was identified as a promising starting point, which has moderate potency and very low human plasma-free fraction and low solubility. By exploring replacements for the central ring with various bridged, bicyclic or azaspiro-piperidine analogues, it was realized that the best replacement was [3.2.1] bridged piperidine as existed in compound **403**. Compound **403** gave an excellent

improvement in potency along with decreased protein binding with human plasma free fraction increased to 40% compared to compound **402**. The potency improvement can be caused by a most favorable conformational change due to the repulsion between the bridge and the lone electron pair from the piperidine nitrogen that enforces an almost linear orientation of the two exit vectors from the piperidine, enabling an optimal binding to gamma-secretase (**Figure 123**). [10]

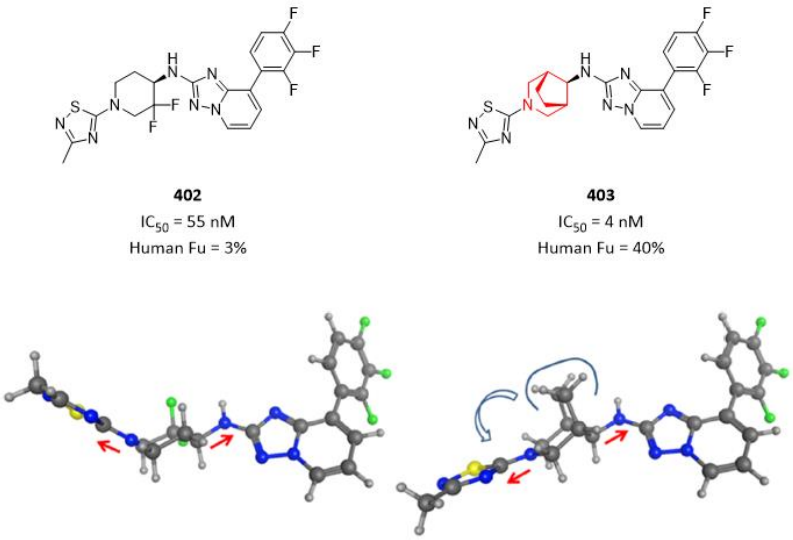

Figure 123. Bridged piperidine increased potency by conformational modulation.

In the course of discovery **EPZ030456** (compound **406**) as the first orally bioavailable small-molecule SMYD3 inhibitor, compound **404** was identified as a promising starting point. Further restriction of conformational freedom with the bridged piperidine core, compound **405**, gave a 17-fold potency improvement over compound **404**. Further optimization led to identification of **EPZ030456** (compound **406**) which displayed stronger potency in cellular assay and demonstrated superior PK profile. To better understand binding model, X-ray crystal structure of compound **406** bound to **SMYD3** was obtained (**Figure 124**). [11]

As described in above two case stories where various bridged piperidine were used to solve critical issues in medicinal chemistry, it is obvious that an efficient access of diverse bridged piperidine building blocks is of great value for medicinal chemists (**Figure 124**).

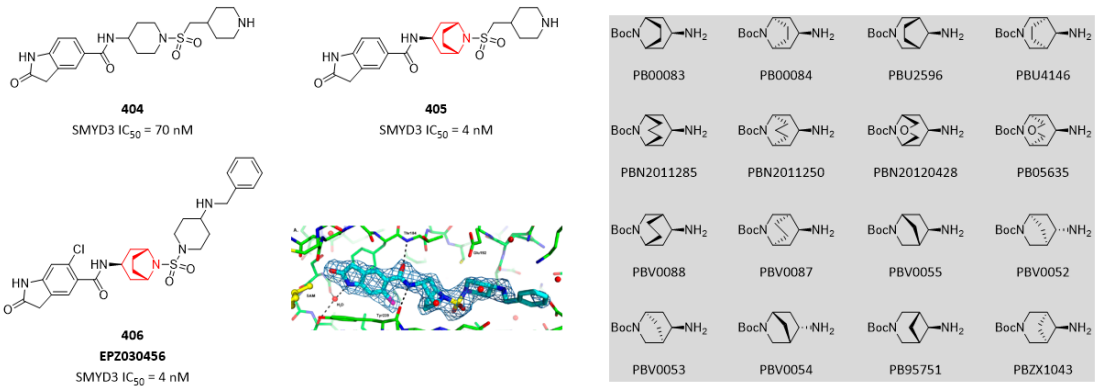

Figure 124. Bridged piperidine increased potency and related building blocks

It was found that compound **408** can fully antagonize an agonist response, while compound **407** can antagonize to approximately 20% of maximum. Taken together with the pharmacology results, the

conformational analysis of compound **407**, compound **408** and compound **409** led the team to propose the agonist conformation hypothesis shown in **Figure 125**. Compound **407** can explore the agonist and antagonist forms from the accessible axial and equatorial conformations and shows partial agonist activity. Compound **408** is constrained to the antagonist conformation and is an antagonist. The agonist conformation is energetically preferred by compound **409**, and this accounts for the greater functional response observed. Complete switching in the functional profile can be attributed to conformational differences in the ligand. [12]

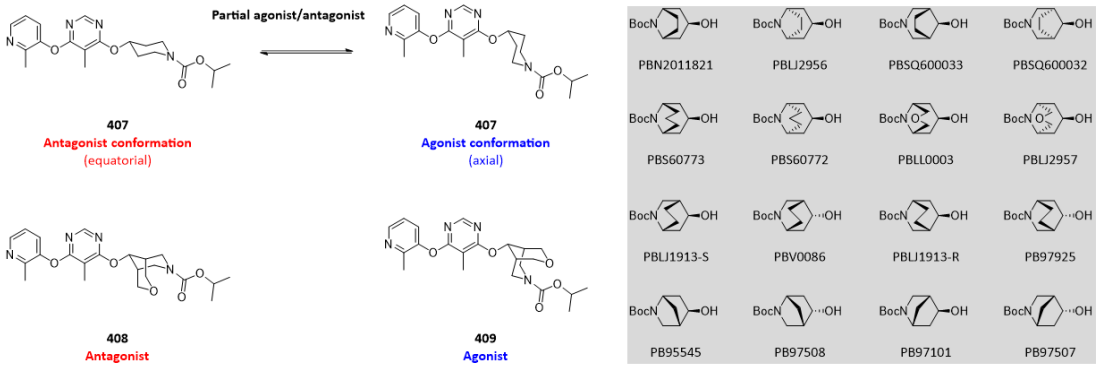

Figure 125. Conformational differences changed mechanism of action.

In order to discover potent, selective, and brain-penetrant LRRK2 inhibitors, the team identified compound **410** as a promising lead compound with high potency. However, this compound suffered very low solubility (< 2 uM), which hinder further development. To address this critical issue, the team focused on disrupting planarity through the introduction of additional complex Fsp^3-riched fragment in the solvent front. With respect to design, the team sought to incorporate fused and/or bridged bicyclic ring systems that, in addition to improving solubility, could also decrease oxidative metabolism of the pyrrolidine and potentially reduce P-gp efflux by further masking the tertiary alcohol polarity. This design logic resulted in the synthesis of azabicyclo[2.1.1]hexane compound **411**, which demonstrated a significantly increased solubility while keeping a comparable potency (**Figure 126**). [13] This kind of caged pyrrolidine building blocks are of great value for exploring SAR and SPR.

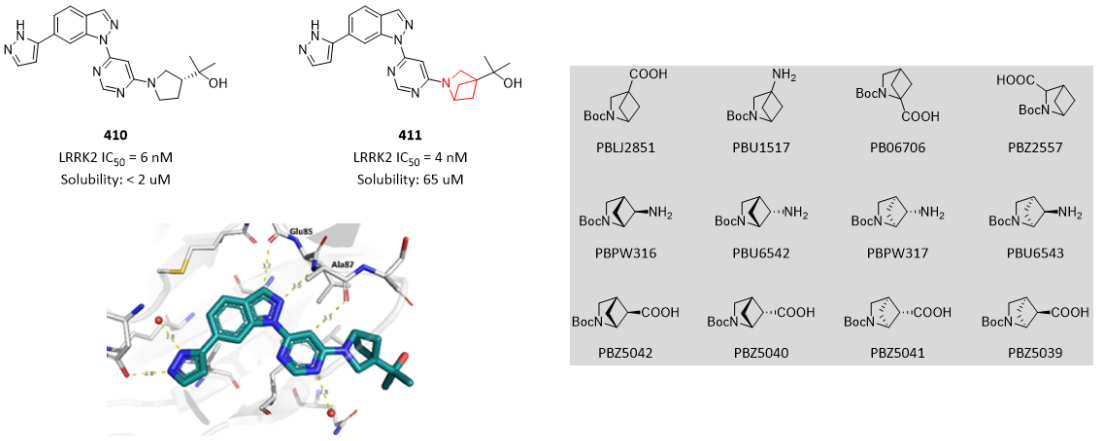

Figure 126. Caged pyrrolidine increased aqueous solubility. (PDB code: 8E80)

Initial evaluation of the SAR from the HTS screen suggested that the diazepane ring found in compound **412** was essential for GCSi activity. Substituted with ethyl group in compound **413**

caused > 10-fold lower potency. However, cyclizing the ethyl group into a 1,4-diazabicyclo[3.2.2]nonane in compound **414** improved the potency > 1000-fold (**Figure 127**). [14]

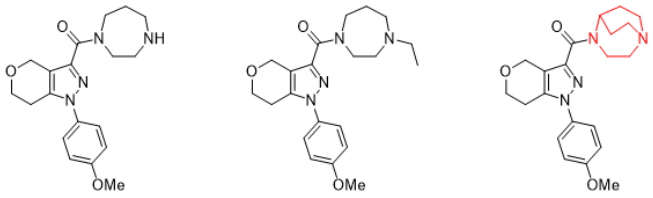

Figure 127. 1,4-Diazabicyclo[3.2.2]nonane increased potency significantly.

References

[1] Sebastien L. Degorce; *et al.* Lowering lipophilicity by adding carbon: one-carbon bridges of morpholines and piperazines. *J. Med. Chem.* **2018**, *61*, 8934-8943.
[2] Andrew Fensome; *et al.* Dual inhibition of TYK2 and JAK1 for the treatment of autoimmune diseases: discovery of ((S)-2,2-difluorocyclopropyl)((1R,5S)-3-(2-((1-methyl-1H-pyrazol-4-yl)amino)pyrimidin-4-yl)-3,8-diazabicyclo[3.2.1]octan-8-yl)methanone (PF-06700841). *J. Med. Chem.* **2018**, *61*, 8597-8612.
[3] Xiaolun Wang; *et al.* Identification of MRTX1133, a noncovalent, potent, and selective KRAS G12D inhibitor. *J. Med. Chem.* **2022**, *65*, 3123-3133.
[4] Changyou Ma; *et al.* Discovery of clinical candidate NTQ1062 as a potent and bioavailable Akt inhibitor for the treatment of human tumors. *J. Med. Chem.* **2022**, *65*, 8144-8168.
[5] Robert G. Gentles; *et al.* Discovery and preclinical characterization of the cyclopropylindolobenzazepine BMS-791325, a potent allosteric inhibitor of the hepatitis C virus NS5B polymerase. *J. Med. Chem.* **2014**, *57*, 1855-1879.
[6] Thomas O. Schrader; *et al.* Discovery of PIPE-359, a brain-penetrant, selective M1 receptor antagonist with robust efficacy in murine MOG-EAE. *ACS Med. Chem. Lett.* **2021**, *12*, 155-161.
[7] Minh H. Nguyen; *et al.* Discovery of orally bioavailable FGFR2/FGFR3 dual inhibitors via structure-guided scaffold repurposing approach. *ACS Med. Chem. Lett.* **2023**, *14*, 312-318.
[8] Denise Rageot; *et al.* Discovery and preclinical characterization of 5-[4,6-bis({3-oxa-8-azabicyclo[3.2.1]octan-8-yl})-1,3,5-triazin-2-yl]-4-(difluoromethyl)pyridine-2-amine (PQR620), a highly potent and selective mTORC1/2 inhibitor for cancer and neurological disorders. *J. Med. Chem.* **2018**, *61*, 10084-10105.
[9] Arie Zask; *et al.* Morpholine derivatives greatly enhance the selectivity of mammalian target of rapamycin (mTOR) inhibitors. *J. Med. Chem.* **2009**, *52*, 7942-7945.
[10] Rosa Maria Rodriguez Sarmiento; *et al.* Stepwise design of r-secretase modulators with an advanced profile by judicious coordinated structural replacements and an unconventional phenyl ring bioisostere. *J. Med. Chem.* **2020**, *63*, 8534-8553.
[11] Lorna H. Mitchell; *et al.* Novel oxindole sulfonamides and sulfamides: EPZ031686, the first orally bioavailable small molecule SMYD3 inhibitor. *ACS Med. Chem. Lett.* **2016**, *7*, 134-138.
[12] Kim F. McClure; *et al.* Activation of the G-protein-coupled receptor 119: a conformation-based hypothesis understanding agonist response. *J. Med. Chem.* **2011**, *54*, 1948-1952.
[13] David A. Candito; *et al.* Discovery and optimization of potent, selective, and brain-penetrant 1-heteroaryl-1H-indazole LRRK2 kinase inhibitors for the treatment of Parkinson's disease. *J. Med. Chem.* **2022**, *65*, 16801-16817.

[14] Anthony J. Roecker; *et al.* Pyrazole ureas as low dose, CNS penetrant glucosylceramide synthase inhibitors for the treatment of Parkinson's disease. *ACS Med. Chem. Lett.* **2023**, *14*, 146-155.

Cyclopropane in Medicinal Chemistry

Cyclopropyl ring has been playing versatile roles in drug discovery, as can be seen from approved drug and clinical candidate molecules (**Figure 128**). Important features of the cyclopropyl ring are: 1) coplanarity of the three carbon atoms, 2) relatively shorter C-C bonds, 3) enhanced pi-character of C-C bonds, and 4) C-H bonds are shorter and stronger than those in alkanes. These distinct features confer cyclopropyl ring with great value in molecule design and ability to address multiple critical issues that can occur during drug discovery such as: a) enhancing potency, b) increasing selectivity, c) increasing metabolic stability, d) increasing permeability and BBB-penetration, e) increasing solubility, f) contributing to an entropically more favorable binding to target and g) improve PK profile. Cyclopropyl ring can be exploited either as a substituent, as a chiral bridge, and as a spiro or fused ring (discussed in previous sections) in solving multiple challenges that occurs during the course of drug discovery program. [1]

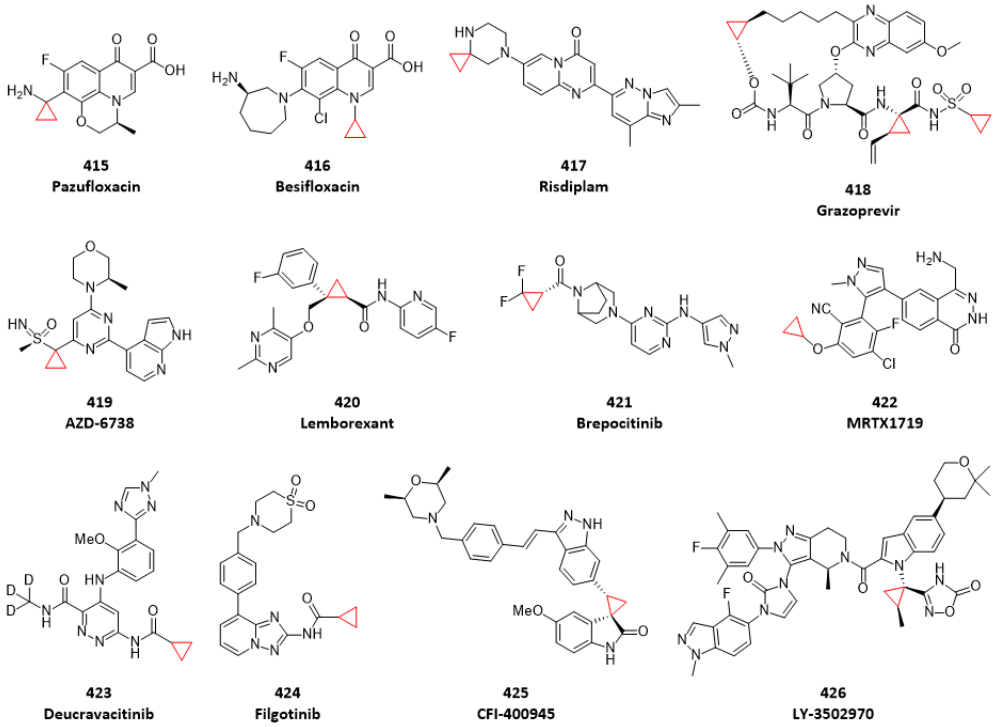

Figure 128. Approved drug and clinical candidate molecules containing cyclopropyl rings

Cyclopropanes and other hydrocarbons containing three-membered rings have a certain sp2 character and gain substantial H-bond acidity which can serve as a hydrogen bond donor. In the course of discovery of **Filgotinib** (compound **424**) as a selective JAK1 inhibitor, compound **429** was identified as a primary hit with modest JAK1 inhibition. Replacement of the cyclopropyl amide moiety showed the importance of this position on the activity. Surprisingly, close amide analogues, such as isopropylamide **428** or acetamide **427** displayed much reduced potency against JAK1. Addition of a methyl group on cyclopropane in compound **429** was also detrimental to JAK1 inhibition. Only the crystal structure of **Filgotinib** (compound **424**) obtained later gave a possible explanation for this SAR observations. It was hypothesized that the superior ability of the cyclopropane ring to donate an H-bond could explain the SAR observations. The crystal structure demonstrates a putative hydrogen bond between the C-H of the cyclopropylamide and the carbonyl

oxygen of Leu932 and of Pro933 (**Figure 129**). This type of interaction has been previously described in the literature. [2-3]

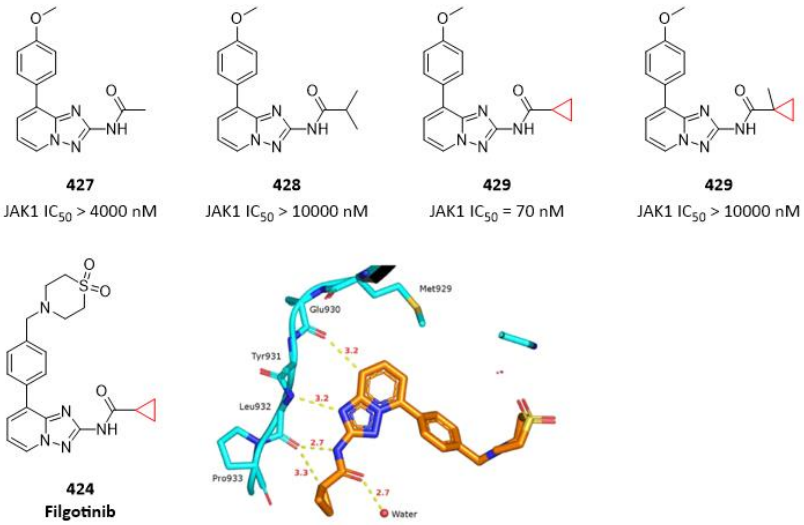

Figure 129. C-H of cyclopropylamide serves as a hydrogen bond donor. (PDB code: 4P7E)

The special ability to serve as a hydrogen bond donor makes cyclopropane-1-carboxylic acid building blocks of great value for molecule design (**Figure 130**).

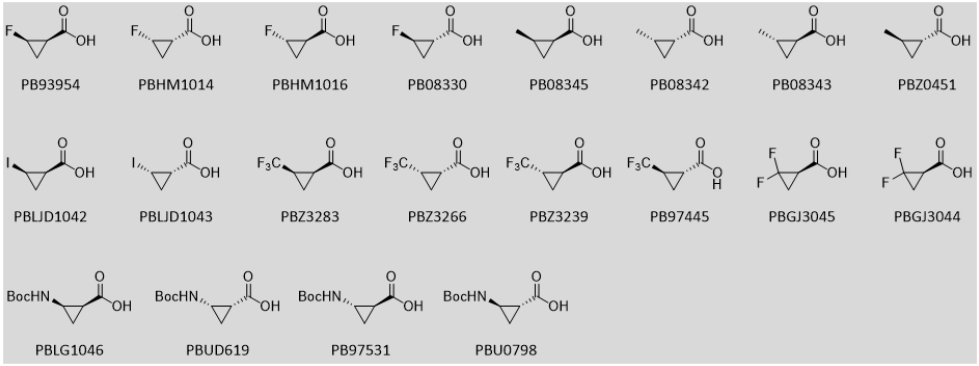

Figure 130. Cyclopropane-1-carboxylic acid building blocks

In the course of discovery of **MRTX1719** (compound **422**) as a synthetic lethal inhibitor of the PRMT5 MTA complex for the treatment of MTAP-deleted cancers, compound **430** was identified from a fragment-based campaign which displayed a modest cellular potency. In order to further increase cellular potency, X-ray crystal structure indicated that there was a small lipophilic pocket sandwiched between Phe300 and Tyr304 around methoxyl group of compound **430**. With this in mind, a variety of small, lipophilic substituents on oxygen were examined. Among of them, cyclopropane ring in compound **431** demonstrated increased cellular potency by 7-fold. Further optimization based on compound **431** aiming to increase cellular potency and improve ADMET profile led to identification of **MRTX1719** (compound **422**). The X-ray crystal structure of **MRTX1719** (compound **422**) bound to PRMT5 MTA demonstrated that cyclopropane ring occupied the small lipophilic pocket sandwiched between Phe300 and Tyr304 (**Figure 131**). [4]

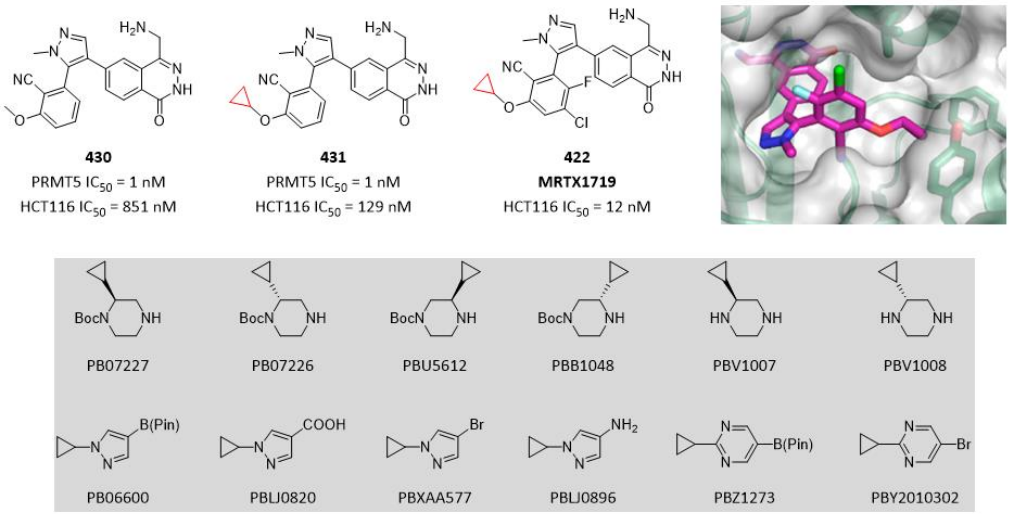

Figure 131. Cyclopropane ring increased potency by occupying a small lipophilic pocket. (PDB code: 7S1S)

Compound **432** was discovery by a fragment-based drug discovery (FBDD) campaign, which was a potent PDE10 inhibitor. The team sought to functionalize selected positions in the aliphatic chain with the goal of blocking possible sites of metabolism. It was soon realized that significant improvements by incorporation of cyclopropane constraint in compound **433** and compound **434**. While the potency of *cis*-cyclopropane linker in compound **433** was compromised relative to compounds with more flexible linkers, the corresponding *trans*-cyclopropane linker in compound **434** provided a dramatic improvement in potency (> 10-fold). Further optimization of compound **434** led to discovery of compound **435** with more promising ADMET and PK profiles which was advanced to *in vivo* study (**Figure 132**). [5]

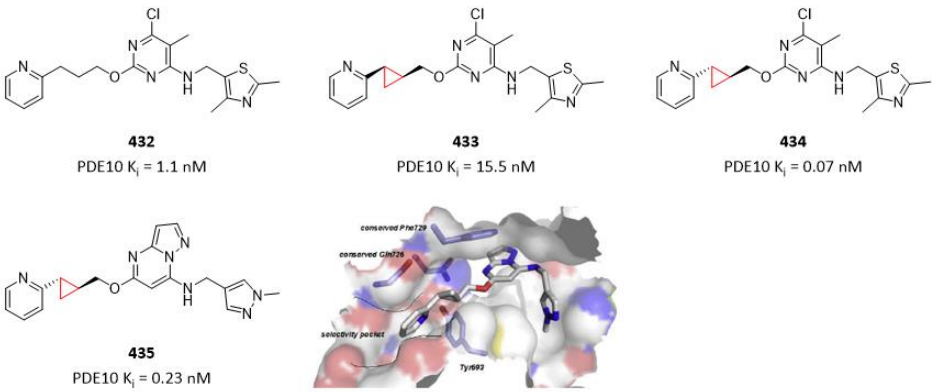

Figure 132. Cyclopropane linker increased potency by locking conformation. (PDE code: 5DH5)

In the course of discovery of clinical candidate **CFI-400945** (compound **425**) as a PLK4 selective inhibitor, compound **436** was identified as a promising hit. In order to lock the molecule into a stable configuration, it was computationally to predict whether compound activity would be retained upon replacing the *E*-alkene in compound **436** with the *trans*-cyclopropane in compound **437**. PLK4 docking predicted retention of activity for this bioisostere replacement. It can be seen that the *E*-form of compound **436** and *1R,2S* stereoisomer **437** have nearly identical topology and similar binding poses. It was equally pleasing to see that compound **437** was active against PLK4 and performed favorably with respect to compound **436** in terms of selectivity toward FLT3 and KDR. Furthermore, it was found that the cyclopropane modification imparts improved aqueous solubility. This improvement is attributed to the nature of the cyclopropane ring, being orthogonal to the

plane of the indolinone, it serves to counter crystal packing forces. Compound **437** also demonstrated desirable ADMET properties, which included an improved profile for CYP isomers, and better microsome stability. More significantly, compound **437** achieved up to 100-fold higher level of exposure in mouse plasma. Further optimization led to discovery of compound **438** and clinical candidate **CFI-400945** (compound **425**) (**Figure 133**). [6]

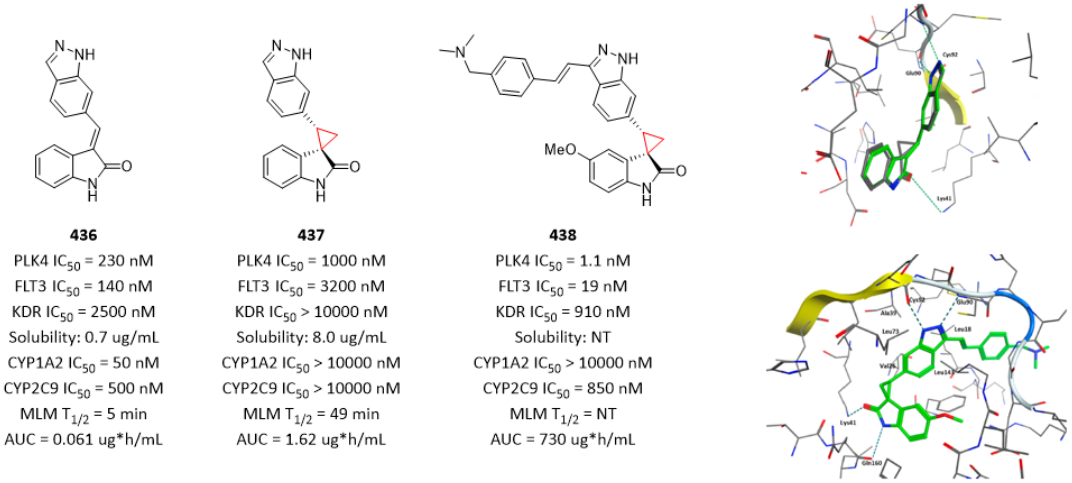

Figure 133. Cyclopropane addressed selectivity and ADMET profile issues. (PDB code: 4JXF)

From above two case stories, 2-phenylcyclopropane building blocks are of great value as bioisosteres of styrene, potentially addressing critical issues associated with styrene (**Figure 134**).

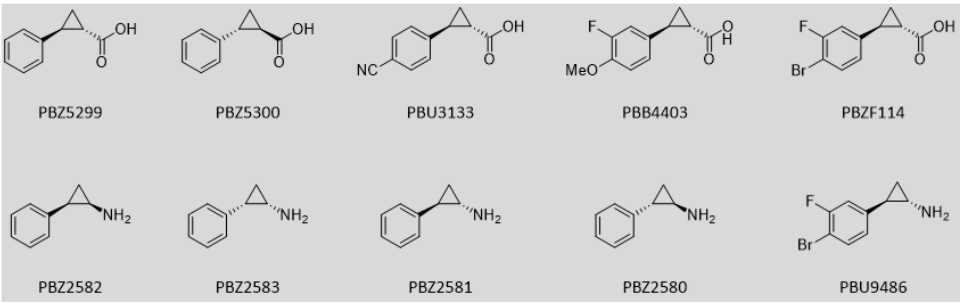

Figure 134. 2-Phenylcyclopropane building blocks as bioisosteres of styrene

Guided by the model, the prime side SAR was further explored by introducing structural features designed to more effectively complement the uniquely defined S1' subsite. Most immediately, the cyclopropylacylsulfonamide compound **441** was evaluated and this compound inhibited HCV NS3/4A activity with IC_{50} of 1 nM, which is 30-fold potent than compound **439**. Close analogues were significantly less active, with ethylacylsulfonamide compound **440** showing 6-fold reduced activity, isopropylacylsulfonamide compound **442** showing 19-fold reduced activity, and cyclobutylacylsulfonamide compound **443** showing 7-fold reduced activity. It can be concluded that this specific aliphatic binding element was critical to activity while also sensitive to small structural modification. These prime side SAR were rationalized using a plot of the van der Waals surface of the protein which highlights the shallow cavity within the S1' site that is defined by Gln41, Phe43, Val55 and Gly58. An assessment of the optimized geometries of the sulfonamide caps suggested that the cyclopropane exhibited a shape most complementary with the S1' pocket, thus maximizing van der Waals surface contact and explaining the potency of compound **441** (**Figure 135**). [7]

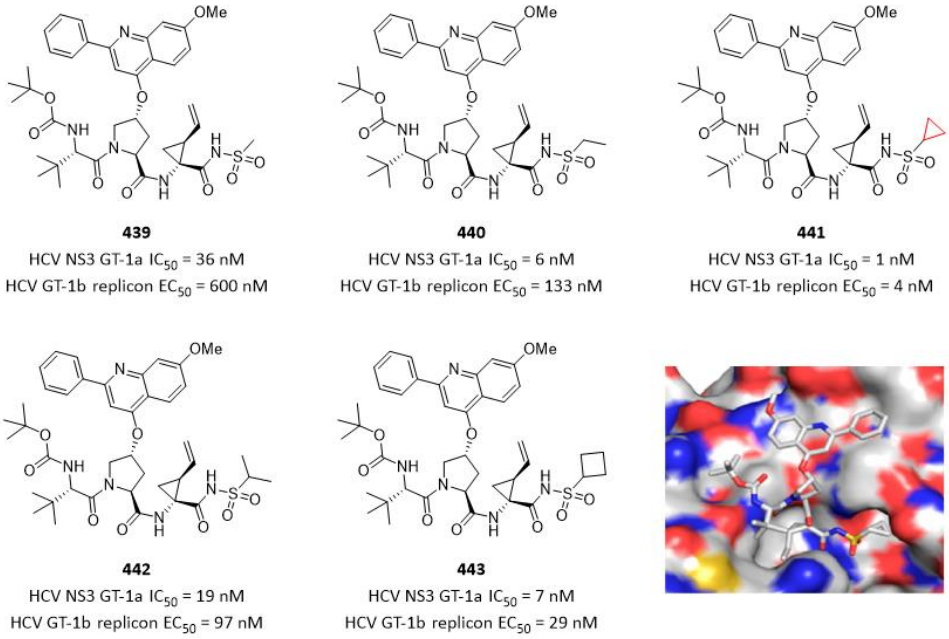

Figure 135. Cyclopropane increased anti-HCV potency by occupying a small hydrophobic pocket.

In the lead optimization course of small-molecule IL-17 inhibitors, although compound **444** gave the best potency, it came with significant metabolic instability in human live microsome. In contrast, biscyclopropylalanine compound **445** was stable in human liver microsome even with the increased lipophilicity. The X-ray crystal structure of compound **445** bound to IL-17 revealed that the biscyclopropyl moiety makes hydrophobic contacts with Tyr85, Leu120, Leu122, and Leu135 of subunit B (**Figure 136**). [8]

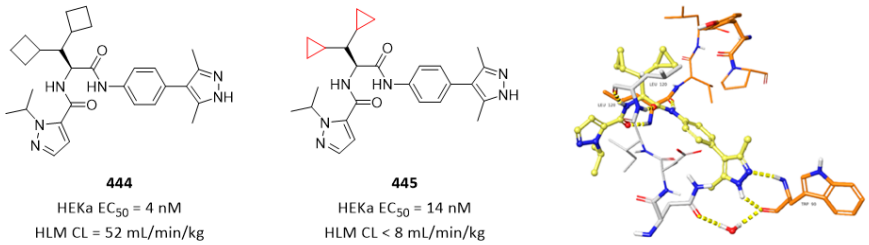

Figure 136. Cyclopropane increased metabolic stability in human liver microsome. (PDB code: 7AMA)

Further development of compound **446** was hampered by realization that this scaffold formed reactive metabolites. To overcome this metabolic liability, the team discovered that the problematic diaminopyridine scaffold could be efficiently replaced with a cyclopropylamino acid moiety. The design concept yielded compound **447** with an improved PK profile (**Figure 137**). [9]

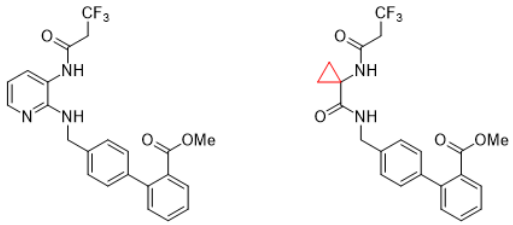

446
hBK1 K_i = 12 nM
$T_{1/2}$ = 0.2 h
CL = 35 mL/min/kg
F: 9%

447
hBK1 K_i = 63 nM
$T_{1/2}$ = 9.5 h
CL = 9.3 mL/min/kg
F: 26%

Figure 137. Cyclopropylamino acid amide as a bioisostere of 2,3-diaminopyridine

References

[1] Tanaji T. Talele. The “cyclopropyl fragment” is a versatile player that frequently appears in preclinical/clinical drug molecules. *J. Med. Chem.* **2016**, *59*, 8712-8756.
[2] Ibon Alkorta; *et al.* Ring strain and hydrogen bond acidity. *J. Org. Chem.* **1998**, *63*, 7759-7763.
[3] Christel J. Menet; *et al.* Triazolopyridines as selective JAK1 inhibitors: from hit identification to GLP0634. *J. Med. Chem.* **2014**, *57*, 9323-9342.
[4] Christopher R. Smith; *et al.* Fragment-based discovery of MRTX1719, a synthetic lethal inhibitor of the PRMT5 MTA complex for the treatment of MTAP-deleted cancers. *J. Med. Chem.* **2022**, *65*, 1749-1766.
[5] Izzat T. Raheem; *et al.* Discovery of pyrazolopyrimidine phosphodiesterase 10A inhibitors for the treatment of schizophrenia. *Bioorg. Med. Chem. Lett.* **2016**, *26*, 126-132.
[6] Peter B. Sampson; *et al.* The discovery of Polo-like kinase 4 inhibitors: design and optimization of spiro[cyclopropane-1,3’[3H]indol]-2’(1’H)-ones as orally bioavailable antitumor agents. *J. Med. Chem.* **2015**, *58*, 130-146.
[7] Paul M. Scola; *et al.* Discovery and early clinical evaluation of BMS-605339, a potent and orally efficacious tripeptidic acylsulfonamide NS3 protease inhibitor for the treatment of hepatitis C virus infection. *J. Med. Chem.* **2014**, *57*, 1708-1729.
[8] Mark D. Andrews; *et al.* Discovery of an oral, rule of 5 compliant, interleukin 17A protein-protein interaction modulator for the potential treatment of psoriasis and other inflammatory diseases. *J. Med. Chem.* **2022**, *65*, 8828-8842.
[9] Michael R. Wood; *et al.* Cyclopropylamino acid amide as a pharmacophoric replacement for 2,3-diaminopyridine. Application to the design of novel bradykinin B1 receptor antagonists. *J. Med. Chem.* **2006**, *49*, 1231-1234.

Nitrile in Medicinal Chemistry

The nitrile group has played an increasingly important role in medicinal chemistry, with more than 60 small-molecule approved drugs and a tremendous number of clinical candidates containing nitrile (**Figure 138**). [1-3] Since 2010, the FDA has approved at least one nitrile-containing drug every year, and reached the maximum number of five drugs in 2020. The marketed drugs with a nitrile moiety target a wide range of clinical disorders, including heart failure, hypertension, chronic myeloid leukemia, breast cancer, virus infection, etc.

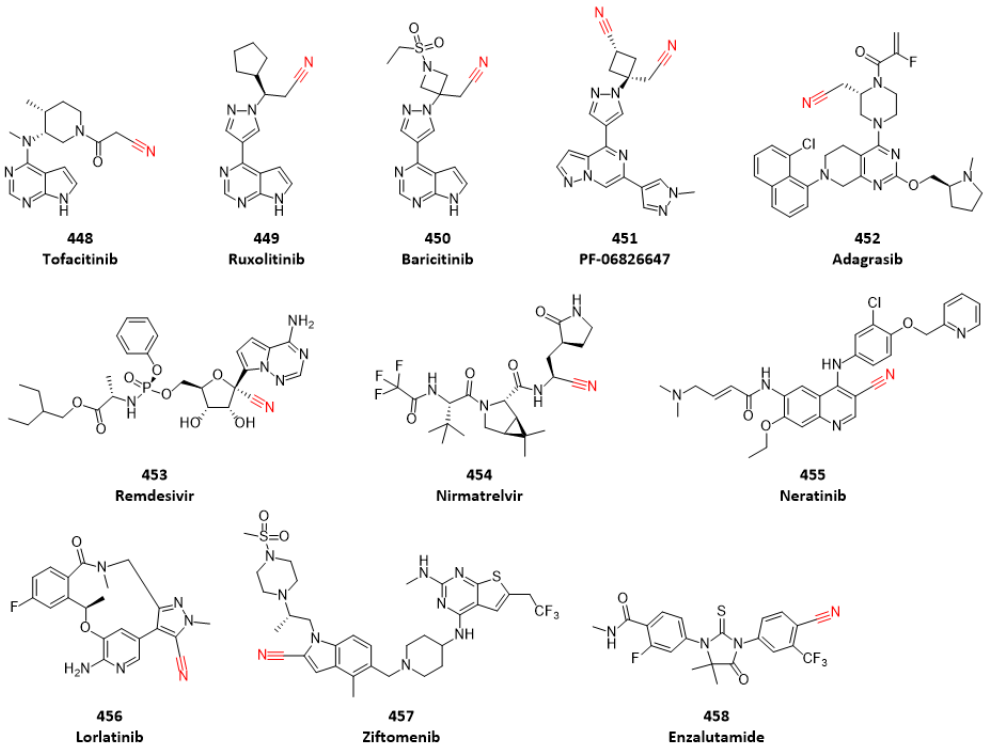

Figure 138. Approved drugs and clinical candidates containing nitrile group

Underpinning a wide range of applications of nitrile group in drug discovery are its unique features, including but not limited to the followings (**Figure 139**): [1-3]

a) Owing to its linear shape and low molecular volume, nitrile group can properly fit in the subsites of proteins and perform lipophilic interactions *via* the triple bond π system. The molecular volume of nitrile group is only one-eighth the size of methyl group, with 1.16 Å length of CN triple bond.

b) The carbon atom can act as an electrophile due to its electron deficiency, promoted by the high electronegativity of the nitrogen atom and high dipole moment in the triple bond; while the nitrogen atom can act as a hydrogen bond acceptor by its lone pair. So a nitrile group can simultaneously form two interactions with protein.

c) In addition to the non-bonded interactions, nitrile is a remarkable group that can for covalent adduct with proteins, mainly linked to a reactive cysteine or serine side chain. The most popular examples are DDP-4 inhibitors (**Vildagliptin** and **Saxagliptin**) and 3CL inhibitors (**Nirmatrelvir**).

d) Compounds containing nitrile group generally have a lower cLogP which indicates enhanced solubility. Compared to alkyne, nitrile decreases cLogP by 0.84 unit.

e) Nitrile group is considerably metabolically stable and non-toxic. It usually remains unchanged when it is eliminated from human body.

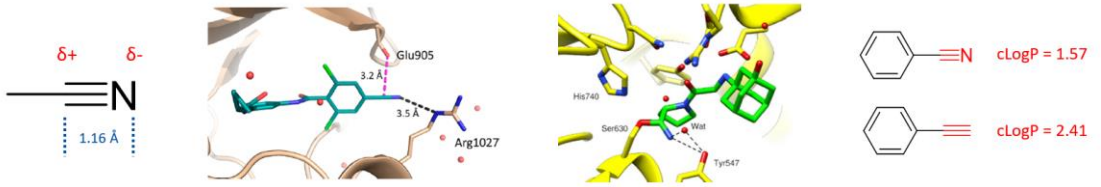

Figure 139. Unique features of nitrile group: an example where nitrile forms two interactions with protein (PDB code: 4GI1); [11] an example where nitrile forms a covalent bond with protein (PDB code: 6B1E); [2] compared to alkyne, nitrile decreases cLogP by 0.84 unit.

In the course of discovery of clinical candidate **Adagrasib** (compound **452**), in order to increase potency of compound **459**, X-ray crystal structure was obtained. Notable in this crystal structure is a bound water molecule complexed to Gly10 and Thr58 which is near the piperazine ring. This water molecule forms hydrogen bonds with the side chain hydroxyl of Thr58 and the carbonyl of Gly10. Analysis of the proximal hydrogen bonding network suggested that displacement of this water could lead to a large potency increase. An appropriately substituted piperazine ring would have the correct trajectory to displace this bound water. With this hypothesis in mind, a series of analogues were designed and synthesized. Among of them, compound **460** with *S*-CH_2CN was determined to be 440-fold more potent than compound **459** and 100-fold more potent than diastereomer **461**. In addition to binding, CH_2CN also impacted chemical reactivity of acrylamide. For example, compound **459** has a GSH $T_{1/2}$ = 17 h; on the hand, compound **460** and compound **461** have significantly decreased GSH $T_{1/2}$ = 4 h and 1 h respectively. Further optimization based on compound **460** led to identification of **Adagrasib** (compound **452**). X-ray crystal structure of **Adagrasib** (compound **452**) bound to KRAS G12C revealed that nitrile displaces the Gly10 bound water and forms a hydrogen bond to the backbone NH of Gly10 (**Figure 140**). [4]

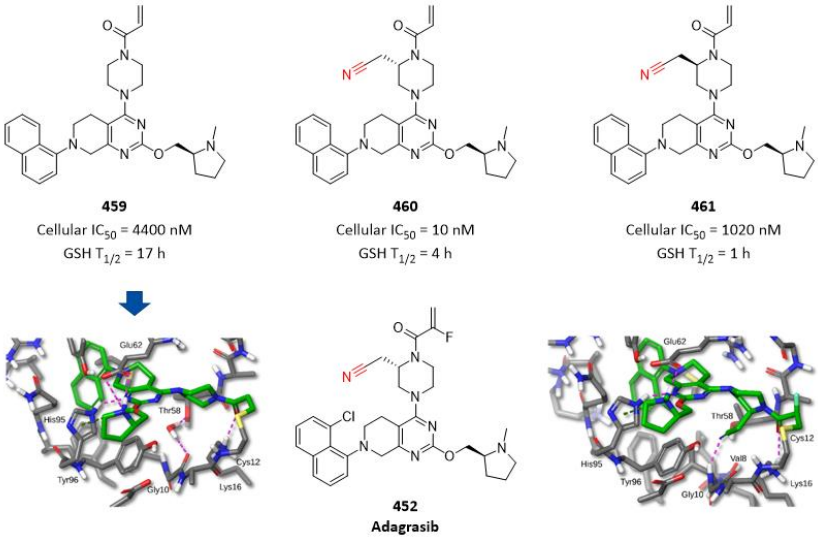

Figure 140. Nitrile displaces water molecule and increased potency. (PDB codes: 6USX, 6UT0)

In the course of discovery of clinical candidate **PF-06826647** (compound **451**) as a selective TYK2 inhibitor, compound **462** was identified as a promising lead compound. X-ray crystal structure of compound **462** bound to TYK2 revealed that the positioning of the alkyl cyano group was shown to be toward the C-terminal lobe in the active site lower lipophilic pocket. The trifluoromethyl azetidine group provided the desired TYK2 potency through engagement of the P-loop, but the overall moderate LipE reflected the high overall lipophilicity of the molecule. In order to improve the modest metabolic stability as judged by human liver microsome turnover, the team attempted to replace trifluoroethylamino group. In addition, replacement of the trifluoroethylamino group

was preferred due to association with testicular toxicity liability for potential metabolites. Unique within this series, the cyanomethyl group of compound **463** recapitulated the potency of compound **462**, and also lowered HLM clearance. Further optimization based on compound **463** led to identification of **PF-06826647** (compound **451**). X-ray crystal structure of **PF-06826647** (compound **451**) bound to TYK2 revealed that the *cis*-cyclobutanecarbonitrile moiety was positioned below and toward the tip of the P-loop. The end of the P-loop contains mainly hydrophobic residues and a generally satisfied hydrogen bond network which may contribute to the calculated lability of this modeled water in the apo structure. This predicted high energy water is displaced by the cyclobutanecarbonitrile group of **PF-06826647** (compound **451**). The electrostatic mapping of this pocket also showed a positive electrostatic potential which could provide a favorable interaction with the cyano group (**Figure 141**). [5]

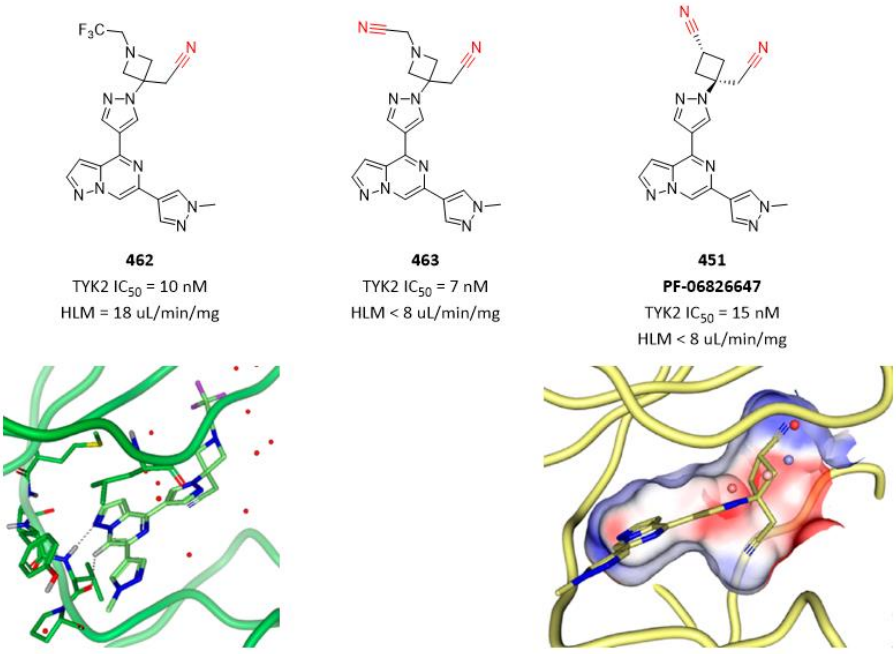

Figure 141. Nitrile replace water molecule and increased metabolic stability. (PDB codes: 6X8F, 6X8G)

Nirmatrelvir inhibits the SARS-CoV-2 main protease, also known as 3C-like protease ($3CL^{pro}$), which plays a crucial role in cleaving the coronavirus polyprotein to form smaller essential proteins required for virus replication and pathogenesis. Nitrile in **Nirmatrelvir** forms a covalent bond with Cys145 of $3CL^{pro}$, which is a critical interaction for high potency. Removing nitrile in compound **464** lost potency completely, while transforming nitrile to amide in compound **465** also lost potency completely, suggesting that an electrophilic warhead is essential for inhibiting 3CL (**Figure 142**). [6] X-ray crystal structure of **Nirmatrelvir** bound to $3CL^{pro}$ revealed that there is a covalent bond between nitrile and Cys145.

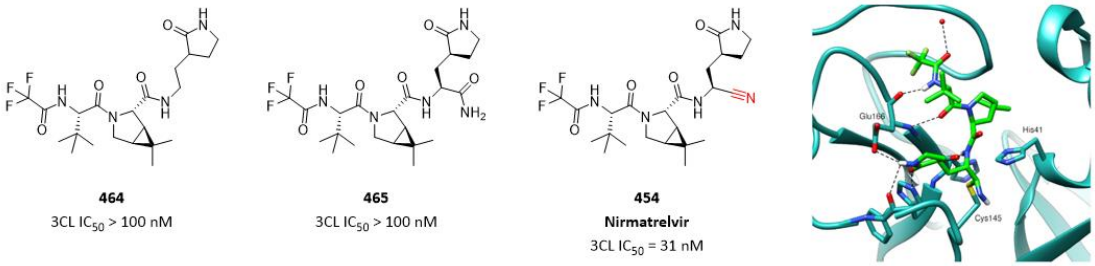

Figure 142. Nitrile forms a covalent bond with Cys145. (PDB code: 7RFW)

Vildagliptin (compound **466**) and **Saxagliptin** (compound **467**), which are DDP-4 inhibitors, can form a reversible covalent bond with Ser630. Their binding modes were characterized by the crystal structure of these inhibitors bound to the enzyme in the covalent state (**Figure 143**). [2]

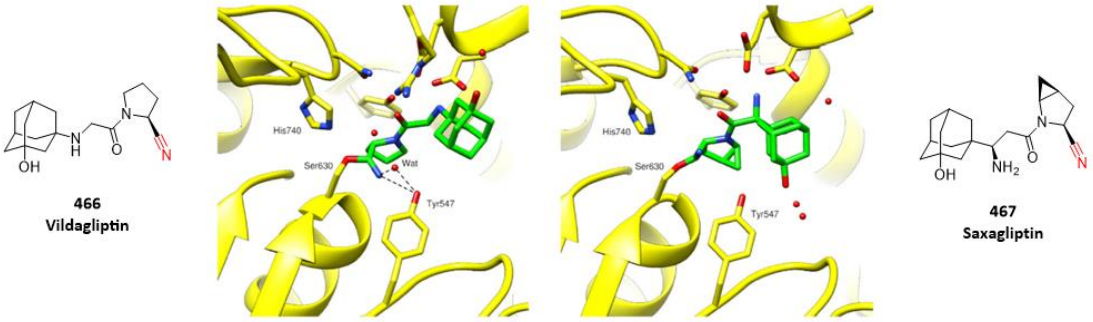

Figure 143. Nitrile in DDP-4 inhibitors can form covalent bond with Ser630. (PDB codes: 6B1E, 3BJM)

As described in above examples, aliphatic building blocks containing nitrile are of great value for discovery of covalent inhibitors (**Figure 144**).

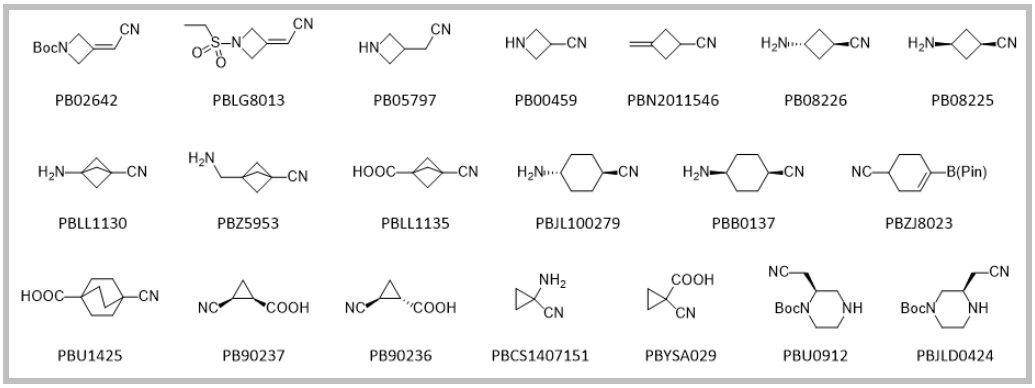

Figure 144. Aliphatic building blocks containing nitrile

It was found that 4-anilinoquinoline-3-carbonitrile **468** is an effective inhibitor of EGFR with activity comparable to 4-anilinoquinazoline **469**. A new homology model of EGFR was constructed based on the X-ray structures of Hck and FGF receptor-1 kinase. The model suggests that with the quinazoline-based inhibitor, the N3 atom is hydrogen bonded to a water molecule which, in turn, interacts with Thr830. It is proposed that the quinolone-3-carbonitrile bind in a similar manner where the water molecule is displaced by the cyano group which interacts with the same Thr830 residue (**Figure 145**). [7]

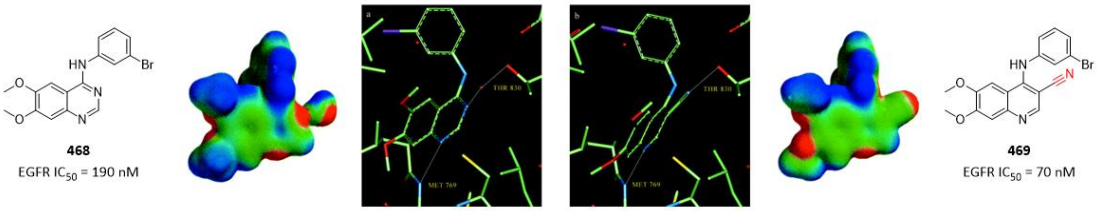

Figure 145. Nitrile displace water molecule, and forms hydrogen bond directly with Thr830.

Based on above findings, several EGFR inhibitors were discovered and approved. One of them is **Neratinib**, a covalent EGFR inhibitor with nitrile forming a hydrogen bond with protein directly (**Figure 146**). [8]

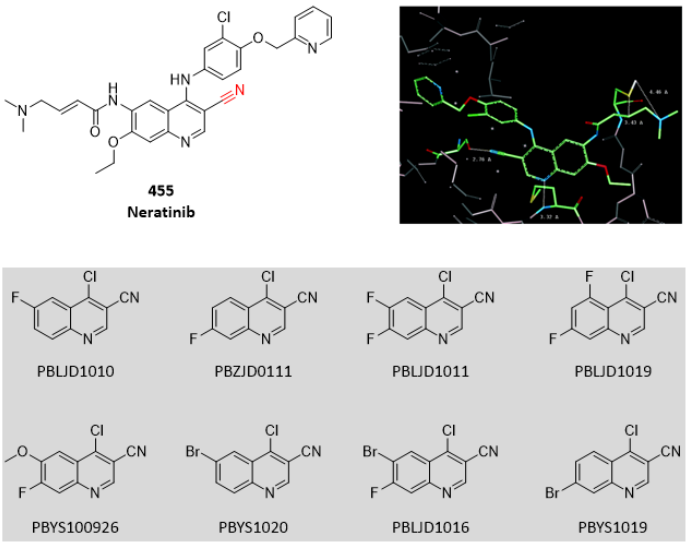

Figure 146. Nitrile in **Neratinib** forms a hydrogen bond with protein directly.

Replication of SARS-CoV-2 depends on the viral RNA-dependent RNA polymerase (RdRp), which is the target of the **Remdesivir** (compound **453**), a pro-drug of compound **473**. **Remdesivir** shows broad-spectrum antiviral activity against RNA viruses, and previous studies with RdRps from Ebola virus and Middle East respiratory syndrome coronavirus (MERS-CoV) have revealed that delayed chain termination is **Remdesivir**'s mechanism of action. [9] Comparing compound **470**, compound **471**, compound **472** and compound **473**, these data established that 1'-CN group was optimal among several 1'-modifications on the adenine C-nucleoside for RSV potency. [10] Structural studies demonstrated that 1'-CN of **Remdesivir** sits in a pocket formed by residues Thr-687 and Ala-688 at the beginning of chain prolongation. At i+4, 1'-CN moiety encounters a steric clash with Ser-861, and prevents RdRp from advancing into i+4, resulting in chain termination (**Figure 147**).

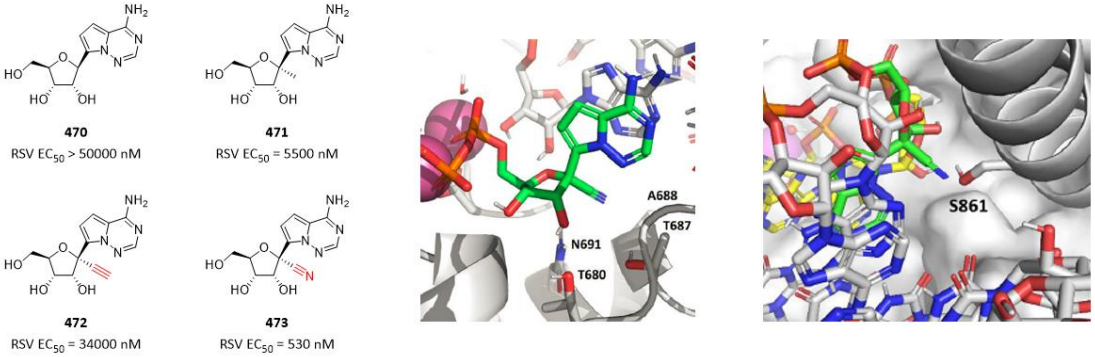

Figure 147. Critical role of 1'-CN and mechanism of action of Remdesivir

Based on compound **474**, addition of a Br in compound **475** increased biochemical potency, but did not increased cellular potency proportionally. It was surprisingly that addition of a cyano in compound **476** increased both biochemical potency and cellular potency significantly. Docking model revealed that the nitrogen atom of nitrile of compound **476** forms a hydrogen bond with Lys590 of protein (**Figure 148**). [12]

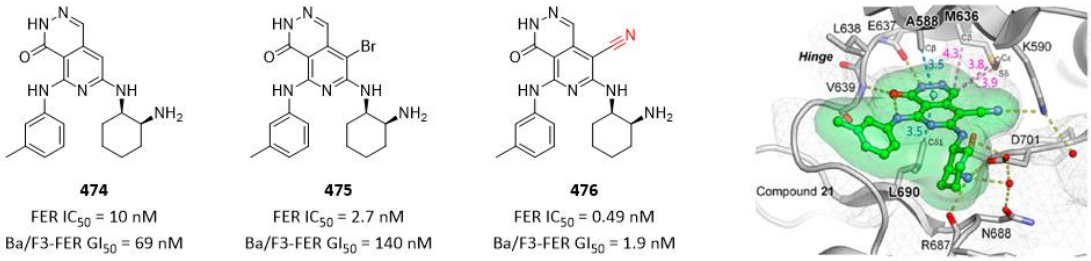

Figure 148. Nitrile increased potency by forming a hydrogen bond with protein.

In the course of discovery **Lorlatinib** (compound **456**) as a selective ALK inhibitor, to increase selectivity of compound **477** against TrkB and other kinases, the team employed the residue difference between ALK (Leu1198) and TrkB (Tyr635). The pyrazole cyano moiety in **Lorlatinib** (compound **456**) was efficient for obtaining selectivity because the cyano contains only one more heavy atom than the unselective methyl analogue **477** and gains at least 35-fold selectivity. It is hypothesized that the nitrile makes an unfavorable contact with the CE atom of the Tyr635 in TrkB, closer to the midpoint of the side chain rather than at the terminus. Unfavorable desolvation penalties or electrostatics due to the proximity of the electron-rich nitrile nitrogen atom and tyrosine may further enhance selectivity (**Figure 149**). [13]

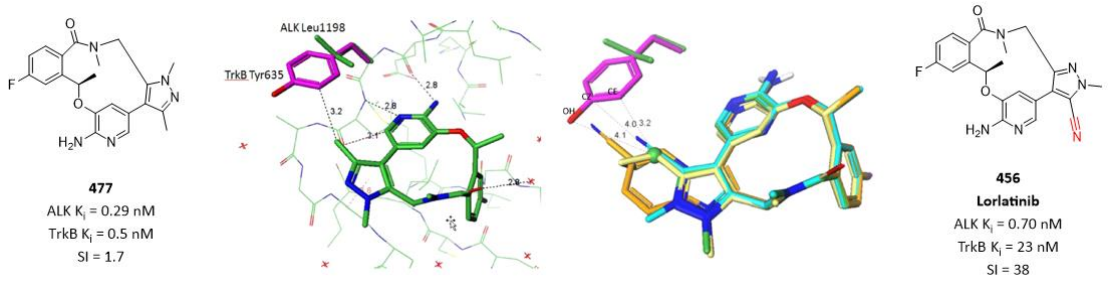

Figure 149. Nitrile increased selectivity. (PBD codes: 4CMU, 4AT3, 4CLI)

A HSQC-based screening of 13,000 fragments revealed 20 fragments hits that displayed chemical shift perturbation patterns of KRAS G12V different than those observed with compounds that bind to switch I/II. Among these compounds was a cluster that included both aminocyanothiophenes and aminothiazoles. NMR titration of the hits using the modified KRAS construct revealed that fragment hit **478** bound to the modified protein with an affinity of 116 uM. Aminothiazole fragment hit **479** showed reduced affinity compared to fragment hit **478**. Using a combination of targeted commercial purchasing and discrete compound synthesis, the cyano group is shown to be important based on complete loss of affinity observed for compound **480**. X-ray crystal structure of fragment hit **478** bound to GDP-KRAS G12V revealed that nitrile interacts with both the amide NH of Glu63 as well as nearby bound water. This network of interactions readily explains the rigid requirement for nitrile for the best affinity (**Figure 150**). [14]

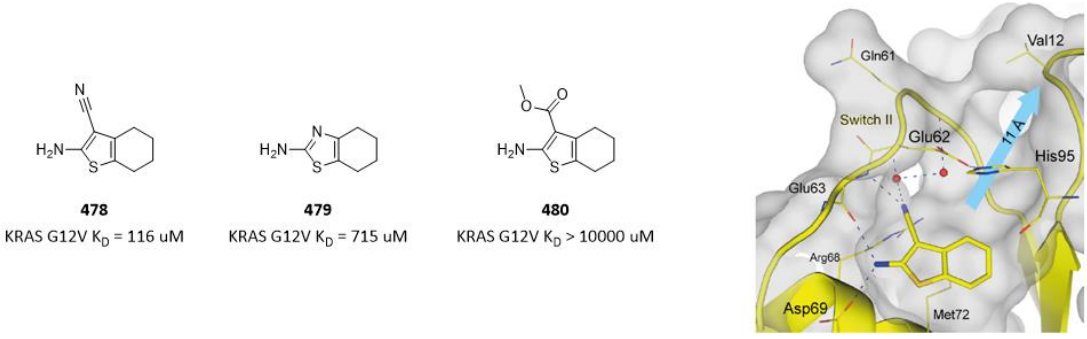

Figure 150. Nitrile interacts with both NH of backbone and nearby bound water. (PDB code: 7U8H)

The above described cases displayed great value of aromatic nitrile building blocks for quick exploration of SAR and SRP (**Figure 151**).

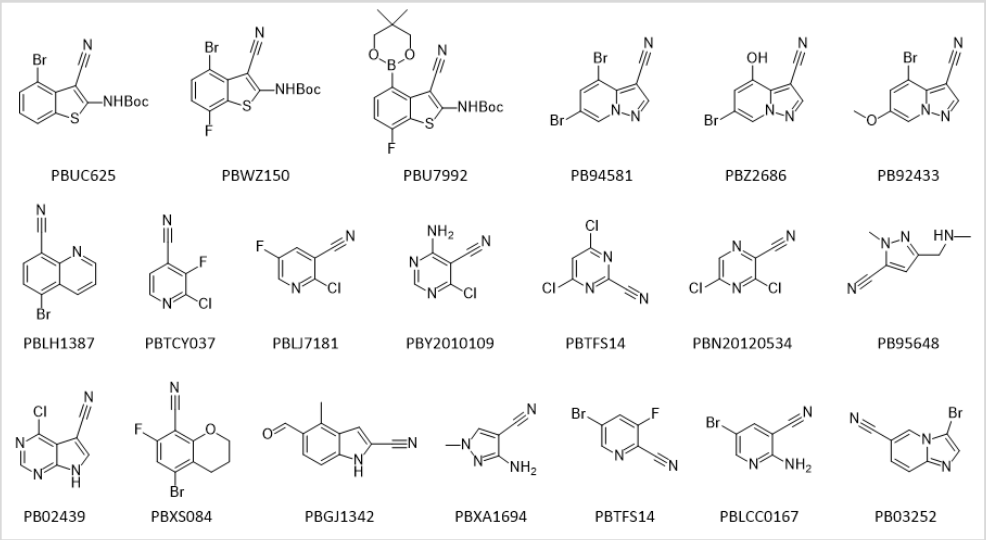

Figure 151. Aromatic nitrile building blocks

References

[1] Xi Wang; *et al.* Nitrile-containing pharmaceuticals: target, mechanism of action, and their SAR studies. *RSC Med. Chem.* **2021**, *12*, 1650-1671.
[2] Vinicius Bonatto; *et al.* Nitriles: an attractive approach to the development of covalent inhibitors. *RSC Med. Chem.* **2023**, *14*, 201-217.
[3] Fraser F. Fleming; *et al.* Nitrile-containing pharmaceuticals: efficacious roles of the nitrile pharmacophore. *J. Med. Chem.* **2010**, *53*, 7902-7917.
[4] Jay B. Fell; *et al.* Identification of the clinical development candidate MRTX849, a covalent KRAS G12C inhibitor for the treatment of cancer. *J. Med. Chem.* **2020**, *63*, 6679-6693.
[5] Brian S. Gerstenberger; *et al.* Discovery of tyrosine kinase 2 (TYK2) inhibitor (PF-06826647) for the treatment of autoimmune diseases. *J. Med. Chem.* **2020**, *63*, 13561-13577.
[6] Subramanyam Vankadara; *et al.* A warhead substitution study on the Coronavirus Main Protease inhibitor Nirmatrelvir. *ACS Med. Chem. Lett.* **2022**, *13*, 1345-1350.
[7] Allan Wissner; *et al.* 4-Anilino-6,7-dialkoxyquinoline-3-carbonitrile inhibitors of epidermal growth factor receptor kinase and their bioisosteric relationship to the 4-anilino-6,7-dialkoxyquinazoline inhibitors. *J. Med. Chem.* **2000**, *43*, 3244-3256.
[8] Hwei-Ru Tsou; *et al.* Optimization of 6,7-disubstituted-4-(arylamino)quinolone-3-carbonitriles as orally active, irreversible inhibitors of human epidermal growth factor receptor-2 kinase activity. *J. Med. Chem.* **2005**, *48*, 1107-1131.
[9] Calvin J. Gordon; *et al.* Remdesivir is a direct-acting antiviral that inhibits RNA-dependent RNA polymerase from severe acute respiratory syndrome coronavirus 2 with high potency. *J. Biol. Chem.* **2020**, *295*, 6785-6797.
[10] Richard L. Mackman; *et al.* Prodrugs of a 1'-CN-4-aza-7,9-dideazaadenosine C-nucleoside leading to the discovery of Remdesivir (GS-5734) as a potent inhibitor of respiratory syncytial virus with efficacy in the African green monkey model of RSV. *J. Med. Chem.* **2021**, *64*, 5001-5017.

[11] Jun Liang; *et al.* Lead optimization of 4-aminopyridine benzamide scaffold to identify potent, selective, and orally bioavailable TYK2 inhibitors. *J. Med. Chem.* **2013**, *56*, 4521-4536.
[12] Toru Taniguchi; *et al.* Discovery of novel pyrido-pyridazinone derivatives as FER tyrosine kinase inhibitors with antitumor activity. *ACS Med. Chem. Lett.* **2019**, *10*, 737-742.
[13] Ted W. Johnson; *et al.* Discovery of (10R)-7-Amino-12-fluoro-2,10,16-trimethyl-15-oxo-10,15,16,17-tetrahydro-2H-8,4-(metheno)pyrazolo[4,3-h][2,5,11]-benzoxadiazacyclotetradecine-3-carbonitrile (PF-06463922), a macrocyclic inhibitor of anaplastic lymphoma kinase (ALK) and c-ros oncogene 1 (ROS1) with preclinical brain exposure and broad-spectrum potency against ALK-resistant mutations. *J. Med. Chem.* **2014**, *57*, 4720-4744.
[14] Joachim Broker; *et al.* Fragment optimization of reversible binding to the switch II pocket on KRAS leads to a potent, in vivo active KRAS G12C inhibitor. *J. Med. Chem.* **2022**, *65*, 14614-14629.

Sulfone in Medicinal Chemistry

The sulfone moiety has been frequently used in medicinal chemistry to optimize potency and physicochemical properties. There are several examples of approved drugs and clinical candidates containing sulfone moiety (**Figure 152**). The sulfone moiety has been found to function as important pharmacophore responsible for a range of biological activities in many therapeutic areas. Its ability to confer conformational constraint, serve as hydrogen bond acceptor, and influence proximal functionality by virtue of its electron-withdrawing property has been exploited to maximize interactions with proteins in order to optimize affinity or potency. Besides, sulfone moiety can be used as one of ketone isosteres that offers increased polarity while avoiding the potential for ketone reduction, and as one of carboxylic acid isosteres that is devoid of the burden of the charge of the carboxylate. In addition, sulfone moiety is very polar that can lower the overall lipophilicity and improve aqueous solubility and metabolic stability of a molecule, which can lead to an overall improvement of ADMET. [1]

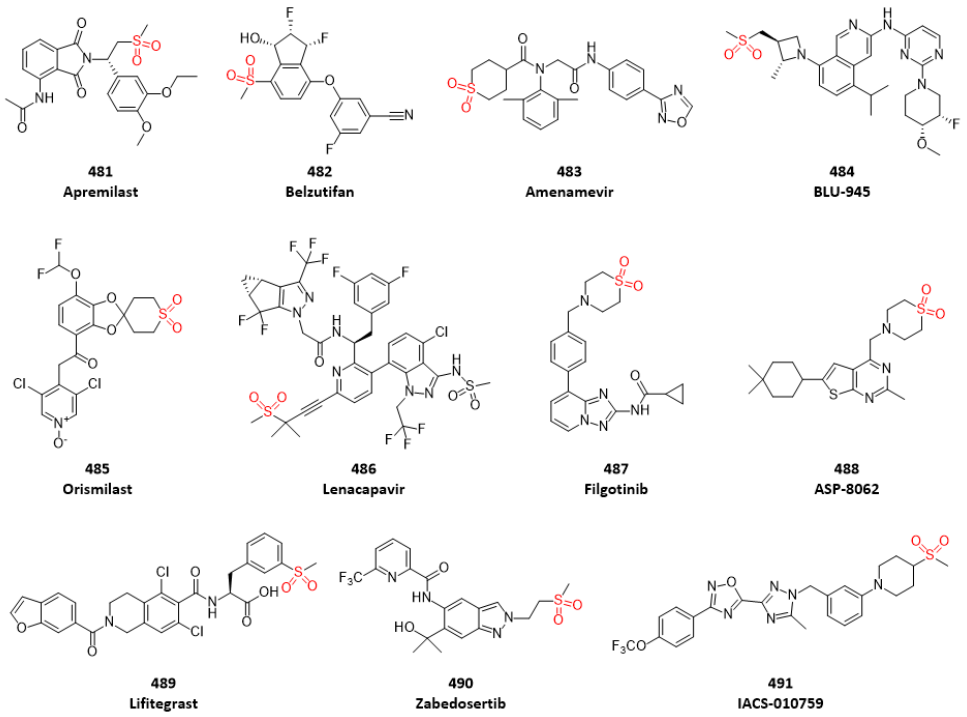

Figure 152. Approved drug and clinical candidate molecules containing sulfone

In the course of discovery of **BLU-945** (compound **484**), a reversible, potent, and wild-type sparing next generation EGFR mutant inhibitor for the treatment-resistant non-small cell lung cancer, compound **492** was identified as a potent and selective lead compound. However, compound **492** suffered a low metabolic stability in human microsome. To address this problem, it was identified that 3-position of the azetidine ring was a vector to explore the addition of polar substituents to tune properties. Among of substituents explored by the team, sulfone-containing compound **493** was distinctly superior, with excellent stability in human microsome and increased potency compared to compound **492**. In order to explain observed potency increasing, X-ray crystal structure of compound **493** bound to EGFR LR/TM revealed that this improvement could be attributed to two hydrogen bonds between sulfone moiety and two Lys716 and Lys728 in the front pocket of protein (**Figure 153**). [2] Further optimization based on compound 493 led to discovery of **BLU-945** (compound **484**).

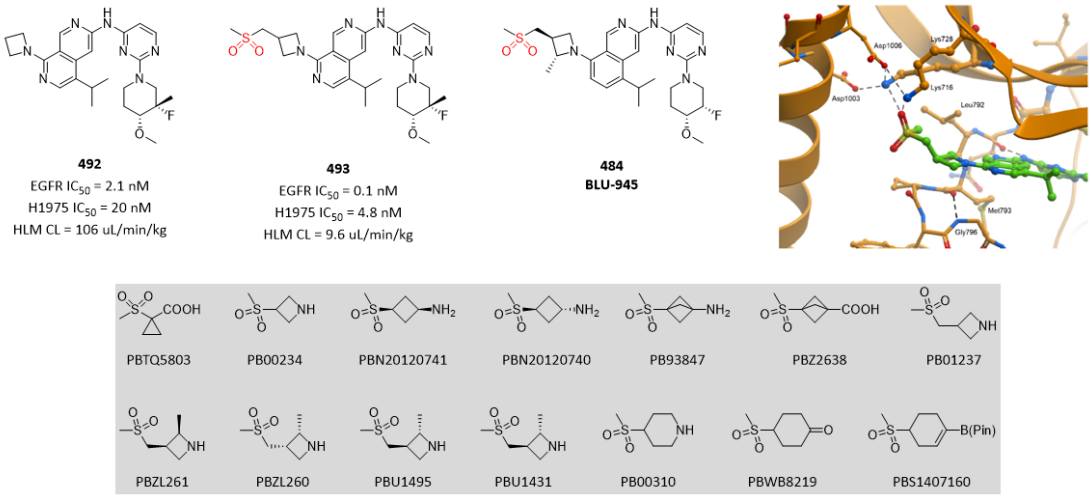

Figure 153. Sulfone moiety increased both metabolic stability and potency. (PDB code: 8D76)

In order to increase ATAD2 potency and selectivity against BRD4 of hit compound **494**, several analogues with increased polarity were synthesized and evaluated. The most promising compound **496** containing sulfone moiety achieved this goal. To better understand the interactions made by the cyclic sulfone, X-ray crystal structure of compound **496** bound to ATAD2 was obtained. There are two polar interactions made by the two sulfone oxygen atoms, each of which accepts hydrogen bonds from the guanidinium group of Arg1077 (**Figure 154**). [3]

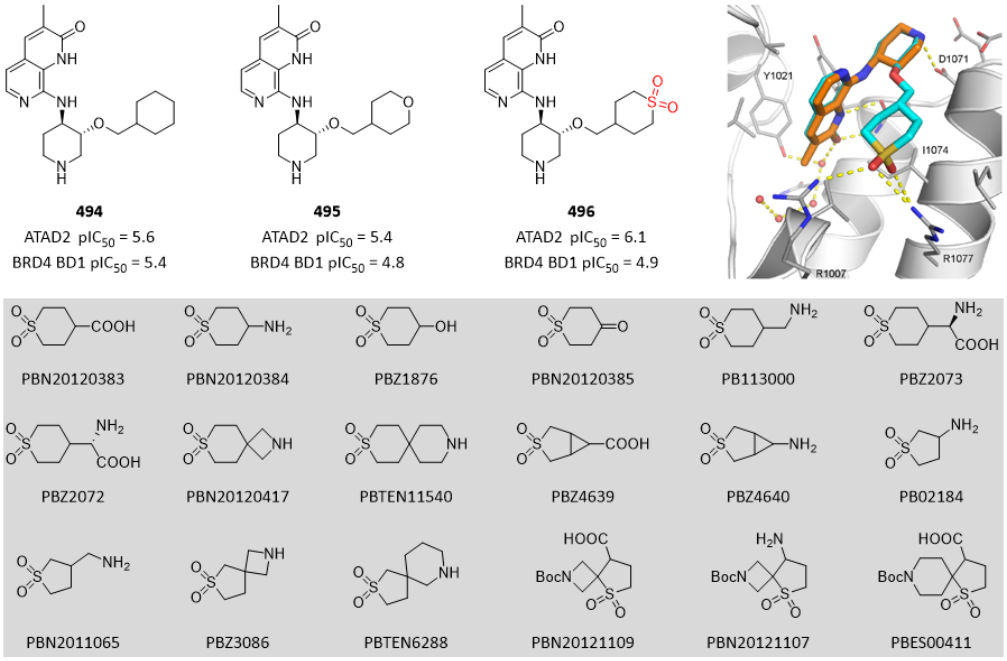

Figure 154. Sulfone moiety increased both potency and selectivity. (PDB code: 5A82)

The enhanced selectivity over BRD4 of compound **496** relative to compound **494** is due to both increased ATAD2 potency and decreased BRD4 activity. The ATAD2 potency gain arises from the new direct hydrogen bonds to the arginines and the displacement of the weakly bound water molecules. The reduction of BRD4 activity presumably results from placing polar sulfone oxygen atoms in an unfavorable lipophilic location. The tetrahydropyran compound **495** is intermediate in polarity between the compound **494** and compound **496**, and shows intermediate selectivity.

Compound **497** was identified as a novel, potent V1b antagonist. However, this compound suffered a high *in vivo* clearance. To address this critical issue, several polar moieties were introduced into

molecules, as exemplified by compound **498** and compound **499** (**Figure 155**). The in vivo clearance was well consistent with polarity of oxygen atom and sulfone moiety. [4]

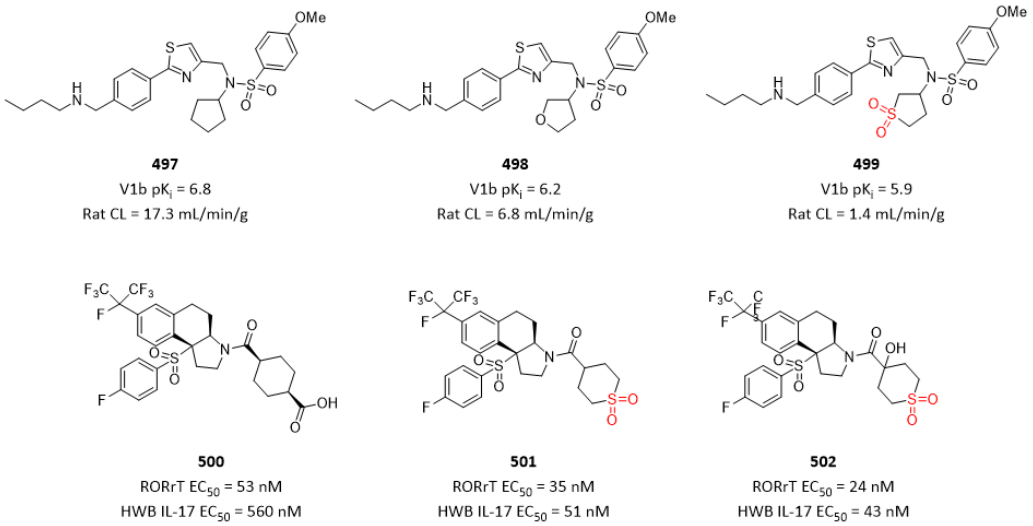

Figure 155. Sulfone moiety improved physicochemical properties of molecules due its high polarity.

Comparing compound **500** and compound **501**, as RORgammaT antagonists, sulfone moiety increased human whole blood potency by at least 10-fold, although both compounds have similar enzymatic RORrT potency. This is probably due to poor permeability of carboxylic acid in compound **500**. Therefore, cyclic six-membered sulfone can be used as one excellent surrogate for carboxylic acid (**Figure 155**). [5]

Piperidine ring often causes hERG inhibition due to basicity of nitrogen. To address this problem, electron-withdrawing atom(s) are introduced, as exemplified by difluoropiperidine, morpholine, etc. Due to the most electron-withdrawing property of sulfone, thiomorpholine dioxide is less basic than morpholine and difluoropiperidine. Therefore, thiomorpholine dioxide is often used when reduction of basicity is desired and specially when avoiding hERG inhibition liability (**Figure 156**).

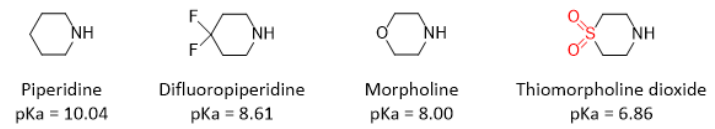

Figure 156. Comparison of pKa values (calculated by ChemDraw software)

Compound **503** was a potent, selective CB2 receptor agonist. However, this compound inhibits hERG with 88% inhibition at 100 uM. As described above, hERG ion channel is well known for its preference of ligands with a basic amine group. To address this issue, general strategies were employed to reduce basicity of nitrogen of piperidine by introducing a fluorine atom in compound **504**, introducing two fluorine atoms in compound **505**, replacing piperidine with morpholine in compound **506** and replacing piperidine with thiomorpholine dioxide in compound **507**. The extent of decreasing hERG inhibition is consistent with the ability of reducing basicity of nitrogen atom (**Figure 157**). [6]

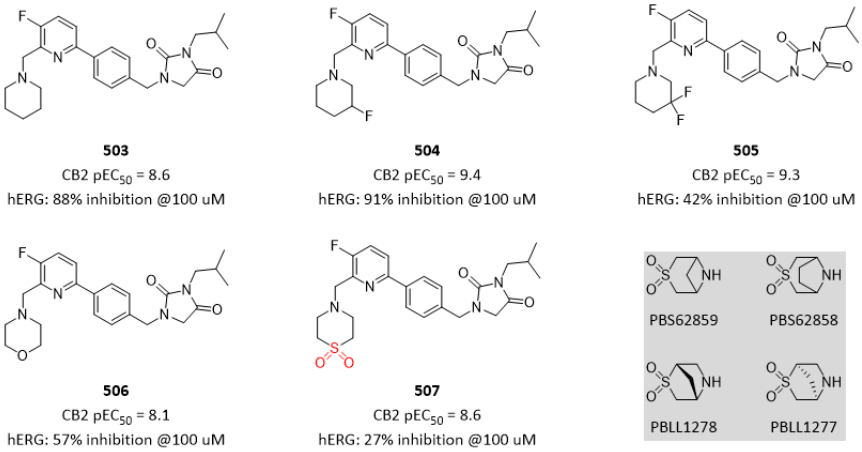

Figure 157. Sulfone moiety in thiomorpholine dioxide decreased hERG inhibition.

In the course of discovery of **Filgotinib** (compound **487**) as a JAK1 selective inhibitor, it was found that replacing morpholine in compound **508** with N-methyl piperazine in compound **509** lost potency completely, while sulfone moiety in **Filgotinib** (compound **487**) increased both potency and metabolic stability in rat liver microsome. X-ray crystal structure of **Filgotinib** (compound **487**) bound to JAK2 revealed that the terminal thiomorpholine dioxide group packs against the glycine rich loop, forming polar interactions with main chain atoms of this flexible loop (Gly861, Ser862), the side chain of Val863, and the catalytic Lys882 and Asp994 of the DFG segment (**Figure 158**). [7]

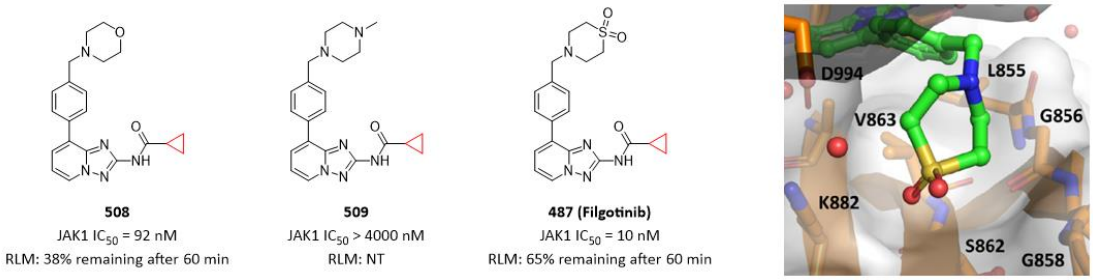

Figure 158. Sulfone moiety increased both potency and metabolic stability. (PDB code: 4P7E)

References

[1] Alicia Regueiro-Ren. Cyclic sulfoxides and sulfones in drug design. *Advances in Heterocyclic Chemistry* **2021**, *134*, 1-30.
[2] Meredith S. Eno; *et al.* Discovery of BLU-945, a reversible, potent, and wild-type-sparing next-generation EGFR mutant inhibitor for treatment-resistant non-small-cell lung cancer. *J. Med. Chem.* **2022**, *65*, 9662-9677.
[3] Paul Bamborough; *et al.* Structure-based optimization of naphthyridones into potent ATAD2 bromodomain inhibitors. *J. Med. Chem.* **2015**, *58*, 6151-6178.
[4] Chris A. Smethurst; *et al.* The characterization of a novel V1b antagonist lead series. *Bioorg. Med. Chem. Lett.* **2011**, *21*, 92-96.
[5] David Marcoux; *et al.* Rationally designed, conformationally constrained inverse agonists of RORrT-identification of a potent, selective series with biologic-like in vivo efficacy. *J. Med. Chem.* **2019**, *62*, 9931-9946.

[6] Mario van der Stelt; *et al.* Discovery and optimization of 1-(4-(pyridine-2-yl)benzyl)-imidazolidine-2,4-dione derivatives as a novel class of selective cannabinoid CB2 receptor agonists. *J. Med. Chem.* **2011**, *54*, 7350-7362.
[7] Christel J. Menet; *et al.* Triazolopyridines as selective JAK1 inhibitors: from hit identification to GLP0634. *J. Med. Chem.* **2014**, *57*, 9323-9342.